

RESEARCH REPORT SERIES no. 7-2013

# CHARD JUNCTION QUARRY, DORSET OPTICAL STIMULATION LUMINESCENCE DATING OF THE PROTO-AXE

SCIENTIFIC DATING REPORT

Phil Toms, Tony Brown, Laura Basell, Geoff Duller, and Jean-Luc Schwenninger



INTERVENTION  
AND ANALYSIS



ENGLISH HERITAGE

*This report has been prepared for use on the internet and the images within it have been down-sampled to optimise downloading and printing speeds.*

*Please note that as a result of this down-sampling the images are not of the highest quality and some of the fine detail may be lost. Any person wishing to obtain a high resolution copy of this report should refer to the ordering information on the following page.*

## CHARD JUNCTION QUARRY DORSET

### OPTICAL STIMULATION LUMINESCENCE DATING OF THE PROTO-AXE

Phil Tomes, Tony Brown, Laura Bassell, Geoff Duller, and Jean-Luc Schwenninger

NGR: ST 35036 04736

© English Heritage

ISSN 2046-9799 (Print)

ISSN 2046-9802 (Online)

The Research Report Series incorporates reports by the expert teams within the Investigation & Analysis Division of the Heritage Protection Department of English Heritage, alongside contributions from other parts of the organisation. It replaces the former Centre for Archaeology Reports Series, the Archaeological Investigation Report Series, the Architectural Investigation Report Series, and the Research Department Report Series.

Many of the Research Reports are of an interim nature and serve to make available the results of specialist investigations in advance of full publication. They are not usually subject to external refereeing, and their conclusions may sometimes have to be modified in the light of information not available at the time of the investigation. Where no final project report is available, readers must consult the author before citing these reports in any publication. Opinions expressed in Research Reports are those of the author(s) and are not necessarily those of English Heritage.

Requests for further hard copies, after the initial print run, can be made by emailing:

Resreports@english-heritage.org.uk

or by writing to:

English Heritage, Fort Cumberland, Fort Cumberland Road, Eastney, Portsmouth PO4 9LD

Please note that a charge will be made to cover printing and postage.

## SUMMARY

The deposits of the proto-Axe at Chard Junction Quarry potentially contain evidence of the earliest human occupation of south west Britain and, along with Broom and Kilmington represent some of the longest terrestrial records of Palaeolithic occupation in Britain. The aim of this report is to summarise and assess the reliability of the optical chronology of the sediment sequence within the Hodge Ditch excavations. The analytical properties of the age estimates are evaluated, with intrinsic measures and a tri-laboratory inter-comparison conducted to assess reliability. The new optical chronology is refined substantially by rejection of those age estimates accompanied by analytical outliers, given principally by poor recycling ratios in the high, saturating region of dose response. One of two inter-laboratory samples produced a significantly different age by one laboratory, which may be caused by the different laboratory thermal treatment. The reliability of D<sub>e</sub> D<sub>r</sub> plots may improve with increasing numbers of samples from equivalent stratigraphic units of divergent dosimetry, but having only two samples may lead to erroneous conclusions. Rapid sedimentation and deposition of artefacts between c 15.2m and 4.5m appears centred on a geometric mean age of 259 ± 10ka (MIS 7). There then followed relatively rapid sedimentation until 8.5ka (MIS 5a) beyond which the deposits were incised to form the current course of the River Axe.

## CONTRIBUTORS

Phil Tomes, Tony Brown, Laura Bassell, Geoff Duller and Jean-Luc Schwenninger

## ACKNOWLEDGEMENTS

The authors thank Tony Pearson, site manager at Chard Junction Quarry and all employees of Bardon Aggregates (Aggregate Industries Ltd) who have offered unparalleled assistance with the excavations. The authors also thank Forde Abbey Estate for their assistance. This research has been funded through the English Heritage Historic Environment Enabling Programme (EH Project Number 5695), building on the earlier work of the ALSF-funded Palaeolithic Rivers of south west Britain project (EH project number: 3847MAN).

## ARCHIVE LOCATION

Environment, Dorset County Council, County Hall, Colliton Park, Dorchester, Dorset DT1 1XJ

## DATE OF RESEARCH

2009

CONTACT DETAILS

Phil Tomes, Geochronology Laboratories, Department of Natural & Social Sciences,  
University of Gloucestershire, Swindon Road, Cheltenham GL50 4AZ  
Tel: 01242 714708

Tony Brown, School of Geography, University of Southampton, Highfield, Southampton  
SO 17 1BJ

Laura Bassell, School of Geography, University of Southampton, Highfield, Southampton  
SO 17 1BJ

Geoff Duller, Institute of Geography & Earth Sciences, Aberystwyth University, Penglais  
Campus, Aberystwyth SY23 3DB

Jean-Luc Schwenninger, Research Laboratory for Archaeology and the History of Art,  
Dyson Perrins Building, South Parks Road, Oxford OX1 3QY

# CONTENTS

1.0 Introduction .....	1
2.0 Mechanisms and principals.....	1
3.0 Sample collection and preparation.....	2
3.1 Sample collection.....	2
3.2 Sample preparation.....	2
4.0 Acquisition and accuracy of $D_e$ value .....	3
4.1 Laboratory factors.....	4
4.1.1 Feldspar contamination.....	4
4.1.2 Preheating.....	4
4.1.3 Irradiation .....	5
4.1.4 Internal consistency.....	5
4.2 Environmental factors.....	6
4.2.1 Incomplete zeroing.....	6
4.2.2 Pedoturbation .....	6
5.0 Acquisition and accuracy of $D_r$ value.....	6
6.0 Estimation of age.....	7
7.0 Analytical uncertainty.....	7
8.0 Discussion.....	9
8.1 Analytical validity.....	9
8.2 $D_e:D_r$ plots.....	9
8.3 Inter-laboratory comparison.....	9
9.0 Synopsis.....	10
10.0 Bibliography.....	12
Tables .....	15
Figures .....	18
Appendix.....	21

## 1.0 INTRODUCTION

The deposits of the proto-Axe at Chard Junction Quarry are potentially of international significance. Optical dating of the upper 7m (out of 16m) of sediments within Hodge Ditch 1, conducted previously under PROSW EB (Tomaset al 2008), demonstrated intervals of deposition spanning 85ka to 402ka (Marine Isotope Stages (MIS) 5a to 11). With the subsequent discovery of two bifaces at a depth of c 15m in Hodge Ditch 1 (Brown and Base 2008), the deposits at Chard Junction may contain the oldest evidence of hominin occupation in at least south west Britain and may represent one of the longest terrestrial sequences of Palaeolithic occupation. As such the lateral extension of aggregate extraction into Hodge Ditch 2 and 3 has been the subject of monitoring and further dating through the English Heritage Environment Enabling Programme (Project Number 5695).

The aim of this report is to summarise and assess the reliability of the optical chronology of the Hodge Ditch sequence. The objectives are two-fold. Firstly, to assess the analytical validity of the optical age estimates. Secondly, to assess the accuracy of age estimates by intrinsic measures and inter-laboratory comparison between the Universities of Aberystwyth, Gloucestershire, and Oxford.

## 2.0 MECHANISMS AND PRINCIPALS

Upon exposure to ionising radiation, electrons within the crystal lattice of insulating minerals are displaced from their atomic orbits. Whilst this displacement is momentary for most electrons, a portion of charge is redistributed to meta-stable sites (traps) within the crystal lattice. In the absence of significant optical and thermal stimulation, this charge can be stored for extensive periods. The quantity of charge recombination and storage relates to the magnitude and period of irradiation. When the lattice is optically or thermally stimulated, charge is evicted from traps and may return to a vacant orbit position (hole). Upon recombination with a hole, an electron's energy can be dissipated in the form of light generating crystal luminescence providing a measure of dose absorption.

Quartz is the most commonly used mineral in luminescence dating. The utility of this mineralogical dosimeter lies in the stability of its datable signal over the mid to late-Quaternary period, predicted through isothermal decay studies (eg Smith et al 1990; retention lifetime 630Ma at 20°C) and evidenced by optical age estimates concordant with independent chronological controls (eg Murray and Oley 2002).

Optical age estimates of sediment (Huntley et al 1985) are premised upon reduction of the mineralogical time-dependent signal (Optically Stimulated Luminescence, OSL) to zero through exposure to sunlight and, once buried, signal reformulation by absorption of litho- and cosmogenic radiation. The signal accumulated post-burial acts as a dosimeter recording total dose absorption, converting to a chronometer by estimating the rate of

dose absorption quantified through the assay of radioactivity in the surrounding lithology and streaming from the cosmos.

$$\text{Age} = \frac{\text{Mean Equivalent Dose (D}_e\text{, Gy)}}{\text{Mean Dose Rate (D}_r\text{, Gy.k}^{-1}\text{)}}$$

Aiken (1998) and Bøtter-Jensen et al (2003) offer a detailed review of optical dating.

## 3.0 SAMPLE COLLECTION AND PREPARATION

### 3.1 Sample collection

A total of 33 sediment samples were extracted from matrix-supported deposits within the Hodge Ditch excavations at Chard Junction Quarry. Triplicate samples of GL10001 and GL10002 were taken for the purposes of inter-laboratory comparison. Contained within opaque plastic tubing (100x45mm) forced into each face, each sample was wrapped in cellophane and parceled in order to preserve moisture content and sample integrity until ready for laboratory preparation. For each sample, an additional c. 100g of sediment was collected for laboratory-based assessment of radioactive disequilibrium.

### 3.2 Sample preparation

To preclude optical erosion of the datable signal prior to measurement, all samples were prepared under controlled laboratory illumination. To isolate that material potentially exposed to daylight during sampling, sediment located within 20mm of each tube-end was removed.

The remaining sample was dried. The triplicates of samples GL10001 and GL10002 were then mixed at Gloucestershire and aqua-hashed at Aberystwyth and Oxford on light-tight parafilm. Quartz within the fine sand (125–180 or 180–250µm) or fine silt (5–15µm) fraction was then segregated (Table 1). Samples were subjected to acid and alkaline digestion (10% HCl, 15% H<sub>2</sub>O<sub>2</sub>) to attain removal of carbonate and organic components respectively.

For fine sand fractions, after acid digestion in HF (40%, 60mins) was used to etch the outer 10–15µm layer affected by  $\alpha$  radiation and degrade each sample's feldspar content. During HF treatment, continuous magnetic stirring was used to effect isotropic etching of grains. 10% HCl was then added to remove acid soluble fluorides. Each sample was dried, reserved, and quartz isolated from the remaining heavy mineral fraction using a sodium polytungstate density separation at 2.68gcm<sup>-3</sup>. Multi-grain aliquots (c. 3–6mg) of quartz from each sample were then mounted on aluminium discs for diagnostics and determination of D<sub>e</sub> values.



Fine silt-sized quartz, along with other mineral grains of varying density and size, was extracted by sample sedimentation in acetone (< 15µm in 2m in 20s, > 5µm in 21mins at 20 °C). Feldspars and amorphous silicates were removed from this fraction through acid digestion (35% H<sub>2</sub>SO<sub>4</sub> for 2 weeks, Jackson et al 1976; Berger et al 1980). Following addition of 10% HCl to remove acid soluble fluorides, degraded to < 5µm as a result of acid treatment were removed by acetone sedimentation. Multi-grain aliquots (c. 1.5mg) were then mounted on aluminium discs for diagnostics and D<sub>e</sub> evaluation.

All drying was conducted at 40°C to prevent thermal erosion of the signal. Alkalies and alkalis were analysed. All dilutions were made in distilled water to prevent signal contamination by extraneous particles.

#### 4.0 ACQUISITION AND ACCURACY OF D<sub>e</sub> VALUE

All mineral standards were marked inter-sample variability in luminescence per unit dose (sensitivity). Therefore, the estimation of D<sub>e</sub> acquired since burial requires calibration of the natural signal using known amounts of laboratory dose. D<sub>e</sub> values were quantified using a single-aliquot regenerative-dose (SAR) protocol (Murray and Wintle 2000; 2003), facilitated by a Risø TL-DA-15 irradiation-stimulation-detection system (Markey et al 1997; Bøtter-Jensen et al 1999) and standardised for inter-laboratory comparison. Within this apparatus and for the majority of samples, optical stimulation was provided by a 150W tungsten halogen lamp, filtered to a broad blue-green light, 420–560nm (2.21–2.95 eV) conveying 16mW cm<sup>-2</sup>, using three 2m Schott GG 420 and a broadband interference filter. For the inter-laboratory comparison, optical stimulation was conducted by an assembly of blue diodes (5 packs of 6 Nichia SPB500S), filtered to 470±80nm conveying 15mW cm<sup>-2</sup> using a 3m Schott GG 420 positioned in front of each diode pack. Infrared stimulation provided by 13 IR diodes (Telefunken TSHA 6203) stimulating at 875±80nm delivering ~5mW cm<sup>-2</sup>, was used to indicate the presence of contaminant feldspars (Hütt et al 1988). Stimulated photon emissions from quartz aliquots are in the ultraviolet (UV) range and were filtered from stimulating photons by 7.5mm HOYA U-340 glass and detected by an EM I9235Q A photomultiplier fitted with a blue-green sensitive alkaline cathode. The input irradiation was conducted using calibrated 1.48GBq <sup>90</sup>Sr/<sup>90</sup>Y β sources.

SAR by definition evaluates D<sub>e</sub> through measuring the natural signal (Appendices 1–27, Fig 1) of a single aliquot and then regenerating that aliquot's signal by using known laboratory doses to enable calibration. For each aliquot, up to 5 different regenerative-doses were administered so as to image dose response. D<sub>e</sub> values for each aliquot were then interpolated, and associated counting and fitting errors calculated, by way of exponential plus linear regression (Appendices 27, Fig 1) using Analyst v3.24 (Duller 2007). Weighted (geometric) mean D<sub>e</sub> values were calculated from 12 aliquots using the central age model outlined by Gaborath et al (1999) and are quoted at 1σ confidence. Owing to limited sample mass, only 6 aliquots of GL09120 were used for D<sub>e</sub> measurement. The

accuracy with which  $D_e$  equates to total absorbed dose and that dose absorbed since burial was assessed. The former can be considered a function of laboratory factors, the latter, one of environmental issues. Diagnostics were deployed to estimate the influence of these factors and criteria instituted to optimise the accuracy of  $D_e$  values.

## 4.1 Laboratory factors

### 4.1.1 Feldspar contamination

The propensity of feldspar signals to fade and underestimate age (Wintle 1973), coupled with their higher sensitivity relative to quartz makes it imperative to quantify feldspar contamination. At room temperature, feldspars generate a signal (RSL) upon exposure to R whereas quartz does not. The signal from feldspars contributing to OSL can be depleted by prior exposure to R. For all aliquots the contribution of any remaining feldspar was estimated from the OSL/R depletion ratio (Duller 2003). If the addition to OSL by feldspars is insignificant, then the repeat dose ratio of OSL to post-R OSL should be statistically consistent with unity (Appendices – 27 Figures and v). Significant feldspar contamination was noted for only one sample, GL06012.

### 4.1.2 Preheating

Preheating is required between irradiation and optical stimulation necessary to ensure comparability between natural and laboratory-induced signals. However, the multiple irradiation and preheating steps that are required to define single aliquot regenerative-dose response leads to signal sensitisation, rendering calibration of the natural signal inaccurate. The SAR protocol (Murray and Wintle 2000; 2003) enables this sensitisation to be monitored and corrected using a test dose, set in this study at c 5Gy, to track signal sensitivity between irradiation-preheat steps. However, the accuracy of sensitisation correction for both natural and laboratory signals can be preheat dependent. Two diagnostics were used to assess the optimal preheat temperature for accurate correction and calibration.

$D_e$  preheat dependence quantifies the combined effects of thermal transfer and sensitisation on the natural signal. Insignificant adjustment in  $D_e$  values in response to differing preheats may reflect limited influence of these effects. Samples generating  $D_e$  values < 10Gy and exhibiting a systematic, statistically significant adjustment in  $D_e$  value with increasing preheat temperature may indicate the presence of significant thermal transfer, such instances over temperature (>20°C) preheats provide the opposite measure of  $D_e$ . A total of 18 aliquots were divided into sets of 3; each set was assigned a 10s preheat between 180°C and 280°C and the  $D_e$  value from each aliquot was then assessed.

The Dose Recovery test (Appendices 1–27, Fig ii) attempts to replicate the above diagnostic, yet provide improved resolution of thermal effects through removal of variability induced by heterogeneous dose absorption in the environment, using a precise laboratory dose to simulate natural dose. The ratio between the applied dose and recovered  $D_e$  value should be statistically concordant with unity. For this diagnostic, a further 6 aliquots were each assigned a 10s preheat between 180°C and 280°C. In the case of the inter-laboratory comparison, this test used 18 aliquots divided into sets of 3; each set was assigned a 10s preheat between 180°C and 280°C.

Measurements of  $D_e$  preheat dependence were used exclusively within Hodge Ditch 1 early in the site's study by Tomaset al (2008). There were limited instances where  $D_e$  thermal dependence occurred. When observed the dose recovery test also demonstrated thermal dependence for sample L09030 the effect of preheating was monitored by this test only. That preheat treatment fulfilling the criteria of accuracy for thermal diagnostics was selected to refine the final  $D_e$  value from 12 aliquots.

Further thermal treatments, prescribed by Murray and White (2000;2003), were applied to optimise accuracy and precision. Optical stimulation occurred at 125°C in order to minimise self-associated photo-transferred thermoluminescence and maximise signal to noise ratios. Inter-cycle optical stimulation was conducted at 280°C to minimise recuperation.

#### 4.1.3 Irradiation

For all samples having  $D_e$  values in excess of 100Gy, matters of signal saturation and laboratory irradiation effects are of concern. With regards the former, the rate of signal accumulation generally adheres to a saturating exponential form and it is this that limits the precision and accuracy of  $D_e$  values for samples having absorbed large doses. For such samples the functional range of  $D_e$  interpolation by SAR has been verified up to 600Gy by Pawley et al (2010). Age estimates based on  $D_e$  values exceeding this value should be accepted tentatively.

#### 4.1.4 Internal consistency

Quasi-radial plots (Appendices 1–27, Figs iii to v; cf Gabraath 1990) are used to illustrate inter-aliquot variability for natural and repeated regeneration of low and high laboratory doses.  $D_e$  values are standardised relative to the central  $D_e$  value for natural signals and applied dose for regenerated signals.  $D_e$  values are described as overdispersed when >5% lie beyond  $\pm 2\sigma$  of the standardising value; resulting from a heterogeneous absorption of burial dose and/or response to the SAR protocol. From multi-grain aliquots, overdispersion from natural signals does not necessarily imply inaccuracy. However, where overdispersion is observed for regenerated signals, the age estimate from that sample should be accepted tentatively. The majority of sensitivity corrected signals from repeated

regeneration does appear overdispersed. This measure of SAR protocol success at Gloucestershire is more stringent than that prescribed by Murray and White (2000; 2003). They suggest repeat dose ratios (Table 1) should be concordant with the range 0.9–1.1; this filter has been applied in this study (Table 2).

## 4.2 Environmental factors

### 4.2.1 Incomplete zeroing

Post-burial signals of pre-burial absorption are rare where pre-burial sunlight exposures limit intensity and/or period, leading to age overestimation. This effect is particularly acute for material eroded and redeposited sub-aqueously (Ollley et al 1998, 1999; Wallinga 2002) and exposed to a burial dose of < 20 Gy (eg Oley et al 2004). It has some influence in sub-aerial contexts but is rarely of consequence where aerial transport has occurred. Given the  $D_e$  values recorded for the Hodge Ditch sequence (Table 1), partial bleaching is unlikely to impact on age estimates but was nevertheless evaluated for each sample by signal analysis (Appendices 1–27, Fig vi; Bailey et al 2003). Systematic increase in  $D_e(t)$ , testifying to partial bleaching, was observed only for sample, GL09029.

### 4.2.2 Pedoturbation

The accuracy of sediment ages is further controlled by post-burial trans-stratigraphic movement forced by pedo- or cryoturbation (Berger 2003; Singhvi et al 2001; Bateman et al 2003). Within the Hodge Ditch sequences there is no evidence of in situ paleosols. Cryoturbation was observed in a number of locations; inaccuracy created by such forces may be bidirectional, moving material upwards or drawing younger material downwards into the level to be dated. Areas of cryogenic deformation of matrix-supported material were avoided.

## 5.0 ACQUISITION AND ACCURACY OF $D_r$ VALUE

Lithogenic  $D_r$  values were defined through measurement of U, Th, and K radionuclide concentration and conversion of these quantities into  $\beta$  and  $\gamma D_r$  values (Table 1).  $\beta$  contributions were estimated from sub-samples at Gloucestershire by laboratory-based  $\gamma$  spectrometry using an Ortec GEM-S high purity Ge coaxial detector system, calibrated using certified reference materials supplied by CANMET. For the inter-laboratory samples, each laboratory used their standard approach ( $\beta$  counting at Aberystwyth and CPMS at Oxford; Table 3).  $\gamma$  dose rates were estimated from  $^{137}\text{Cs}$  gamma spectrometry using an EG&G  $\mu$ nomad portable NaI gamma spectrometer (calibrated using the block standard LLAHA); this reduces uncertainty relating to potential heterogeneity in the  $\gamma$  dose field surrounding each sample. For the inter-laboratory samples, each laboratory

measured the same position with their portable spectrometer (Table 3). The level of U disequilibrium was estimated by laboratory-based Ge  $\gamma$  spectrometry. Estimates of radionuclide concentration were converted into  $D_r$  values (Adamiec and Aiken 1998), accounting for  $D_r$  modulation forced by grain size (Mejdahl 1979), and present moisture content (Zimmernan 1971). Cosmogenic  $D_r$  values were calculated on the basis of sample depth, geographical position, and matrix density (Prescott and Hutton 1994).

The spatio-temporal validity of  $D_r$  values can be considered as four variables. Firstly, disequilibrium can force temporal instability in U and Th emissions. The impact of this infrequent phenomenon (Olley et al 1996) upon age estimation is usually insignificant given their associated margins of error. However, for samples where this effect is pronounced (>50% disequilibrium between  $^{238}\text{U}$  and  $^{226}\text{Ra}$ ; Appendices 1–27, Fig vii), the resulting age estimates should be accepted tentatively. Secondly, pedogenically-induced variations in matrix composition of B and C horizons, such as radionuclide and/or mineral remobilisation, may alter the rate of energy emission and/or absorption. Thirdly, spatio-temporal attractions of present moisture content are difficult to assess directly, requiring knowledge of the magnitude and timing of differing contents. However, the maximum influence of moisture content variations can be delimited by recalculating  $D_r$  for minimum (zero) and maximum (saturation) content. Finally, temporal alteration in the thickness of overburden alters cosmogenic  $D_r$  values. Cosmogenic  $D_r$  often form a negligible portion of total  $D_r$ . It is possible to quantify the maximum influence of overburden flux by recalculating  $D_r$  from minimum (zero) and maximum (surface sample) cosmogenic  $D_r$ .

## 6.0 ESTIMATION OF AGE

The ages reported in Table 1 provide an estimate of sediment burial period based on mean  $D_e$  and  $D_r$  values and their associated analytical uncertainties. Uncertainty in age estimation is reported as a product of systematic and experimental errors, with the magnitude of experimental errors shown in parenthesis (Table 1). Probability distribution in this case is the inter-annual variability (Appendices 1–27, Figs iii and viii). The maximum influence of temporal variations forced by minimum maximum variation in moisture content and overburden thickness is illustrated in Appendices 1–27 Figure viii. Where uncertainty in these parameters exists this age range may prove instructive, although the combined extremes represented should not be construed as preferred age estimates. The analytical validity of each sample is presented in Table 2.

## 7.0 ANALYTICAL UNCERTAINTY

All errors are based upon analytical uncertainty and quoted at 1 $\sigma$  confidence. Error calculations account for the propagation of systematic and/or experimental (random) errors associated with  $D_e$  and  $D_r$  values.

For  $D_e$  values, systematic errors are confined to laboratory  $\beta$  source calibration. Uncertainty in this respect is combined from the delivery of the calibrating dose

(1.2 NPL personnel), the conversion of this dose to  $S_i$  using the respective mass energy-absorption coefficient (ICRU Hubbell 1982), and experimental error, totalling 3.5%. Mass attenuation and bremsstrahlung losses during  $\gamma$  dose delivery are considered negligible. Experimental errors relate to  $D_e$  interpolation using sensitisation corrected dose response. Natural and regenerated sensitisation corrected dose point ( $S_i$ ) are quantified by,

$$S_i = (D_i - xL_i) / (d_i - xL_i) \quad \text{Eq 1}$$

where  $D_i$  = Natural or regenerated OSL, initial 0.2s  
 $L_i$  = Background natural or regenerated OSL, final 5s  
 $d_i$  = Test dose OSL, initial 0.2s  
 $x$  = Scaling factor, 0.08

The error on each signal parameter is based on counting statistics, reflected by the square-root of measured values. The propagation of these errors within Eq. 1 generating  $\sigma S_i$  follows the general formula given in Eq. 2.  $\sigma S_i$  are then used to define fitting and interpolation errors within exponential plus linear regressions performed by Analyst 3.24 (Duller 2007).

For  $D_x$  values, systematic errors accommodate uncertainty in radionuclide conversion factors (5%),  $\beta$  attenuation coefficients (5%),  $\alpha$ -value (4%; derived from a systematic  $\alpha$  source uncertainty of 3.5% and experimental error), matrix density ( $0.20 \text{ g cm}^{-3}$ ), vertical thickness of sample section (specific to sample collection site), saturation moisture content (3%), moisture content attenuation (2%), burial moisture content (25% relative, unless direct evidence exists of the magnitude and period of differing content), and NaI gamma spectrometer calibration (3%). Experimental errors are associated with radionuclide identification for each sample by NaI and Ge gamma spectrometry.

The propagation of these errors through to age calculation is quantified using the expression,

$$\sigma_y (\delta y / \delta x) = \left( \sum (\delta y / \delta x_n) \sigma_{x_n} \right)^{1/2} \quad \text{Eq 2}$$

where  $y$  is a value equivalent to that function comprising terms  $x_n$  and where  $\sigma_y$  and  $\sigma_{x_n}$  are associated uncertainties.

Errors on age estimates are presented as combined systematic and experimental errors and experimental errors alone. The former (combined) error should be considered when comparing luminescence ages herein with independent chronometric controls. The latter assumes systematic errors are common to luminescence age estimates generated by means equal to those detailed herein and enable direct comparison with those estimates.

## 8.0 DISCUSSION

Taking the youngest and oldest age estimates (samples GL06011 and GL08047); the raw optical chronology for Hodge Ditch spans 86 to 544ka (MS 5a to 15; Table 1 and Fig.1). There is a broad increase in age with depth to 274ka (MS 7) at c.45m. Beyond this level, there is an age plateau that appears to broaden with depth (169 to 544ka at c.15m). The overall age-depth sequence is incompatible with Bayesian analysis, precluding a whole-site quantitative assessment of age consistency with relative stratigraphic position. In the absence of independent chronological or other intrinsic measures of reliability are the sole means by which to evaluate the accuracy of the age estimates.

### 8.1 Analytical validity

A total of 23 samples failed one or more diagnostic elements; Table 2 outlines the analytical caveats by sample. Five samples failed the Dose Recovery test (see 4.1.2), five samples exhibited varying levels of U disequilibrium (see 5.0), four samples produced  $D_e > 600$ Gy (see 4.1.3), one sample produced insufficient datable mass, and one proved to have significant feldspar contamination. However, the most common failure, in 13 samples, was in the repeat dose ratio assessed as part of the  $D_e$  measurement (Murray and Wintle 2000; 2003; see 4.1.4). Data within Table 1 indicates there is 70% more variation in the ratio for high doses (17%) than low (10%). The majority of samples yield  $D_e$  values in the high, saturating region of dose response. As such, estimates of  $D_e$  in this region are particularly sensitive to inaccuracies in the form of dose response forced by inaccurate correction of sensitivity change. Figure 1 highlights those samples with analytical caveats.

### 8.2 $D_e:D_r$ plots

Samples obtained from the same or equivalent stratigraphic units whose ages converge but are based on divergent  $D_r$  values offer a powerful, though resource-intensive intrinsic assessment of reliability (Tom s et al 2005). Figure 2 summarises the  $D_e:D_r$  plots for multiple age estimates obtained within stratigraphic units or between those at an equivalent stratigraphic level. Of the intra-unit assessments, samples GL10015/GL10016 and GL08043/GL08044 show convergent age estimates from statistically distinct  $D_r$  values (Fig 2c and 2d). At c.13m (Fig 2e), this pattern is broadly true of the age estimates from units of equivalent depth within the sequence. However, this contrasts with those at c.15m (Fig 2f) where there is a marked variation in age. The concern evolved here is that the apparent convergence or divergence of age estimates may be dependent on the number of samples dated; Figure 2f indicates at least two distinct age bands within which at least two samples with distinct  $D_r$  values appear to plot.

### 8.3 Inter-laboratory comparison

Luminescence dating requires calibration, maintenance, and monitoring of equipment involved in  $D_e$  and  $D_r$  evaluation. Though a rigorous methodology may be employed by a laboratory in the absence of independent chronological controls in a large study such as this inter-laboratory comparison, it is advisable to corroborate age estimates and thereby verify the accuracy of equipment calibration and function. In this study, the comparability of three procedural elements as well as age estimates was assessed from three Luminescence laboratories for two samples, GL10001 and GL10002 (Table 3; Fig 3; Appendix 5-18).

Figure 3a shows the outcome of the Dose recovery test for GL10001. Laboratory A recorded a strong thermal dependence, Laboratory C slight and Laboratory B none. The origin of this variable response remains to be determined, but critically this decision-making process led to differences in preheat selection between laboratories. For GL10002, Laboratory B and C elected a preheat temperature based on extrapolation from their respective Dose Recovery tests on GL10001. Laboratory A conducted a separate Dose Recovery test on GL10002. Extrapolation of preheat temperature using Dose Recovery tests conducted on a sub-set of samples is not uncommon in Luminescence Dating. Figures 3b and 3c illustrate the outcome of  $\beta$  and  $\gamma$   $D_r$  assessment. Inter-laboratory difference in  $\gamma$   $D_r$  is a maximum of  $12 \pm 7\%$ , whilst for  $\beta$   $D_r$  this climbs to  $34 \pm 12\%$ . The greater variation in  $\beta$   $D_r$  may arise from differences in technology between laboratories. Figure 3d shows the age envelope of each sample based on the inter-laboratory range. The maximum difference in age is  $29 \pm 18\%$  for sample GL10001 between Laboratories B and C, and  $39 \pm 21\%$  for GL10002 between Laboratories A and C. The principal driver behind these differences is  $D_e$  ( $43 \pm 18\%$ , GL10001;  $29 \pm 17\%$ , GL10002), with Laboratory C systematically lower than A and B. The divergence between laboratory natural  $D_e$  value was further investigated by giving a precise dose to three sets of three aliquots of bleached GL10001. Each laboratory then adopted the same measurement sequence and preheat temperature to estimate the dose applied. Figure 3e shows that the lower natural  $D_e$  value reported by Laboratory C is not rooted in source calibration, with statistically concordant doses recovered between laboratories. It is possible here that the inter-laboratory discrepancy in natural  $D_e$  originates from the choice of preheat temperature. For sample GL10002, where Laboratory A and B selected the same preheat temperature the natural  $D_e$  values are indistinguishable. Sources of differential thermal dependence of inter-laboratory dose recovery tests should form the focus of future work. It is possible that application of this test to some, rather than all, samples from a site may affect the choice of preheat temperature.

## 9.0 SYNOPSIS

Excluding those samples with analytical caveats reduces the variability of the chronological sequence. The youngest unit of the site at 2.5m in Hodge Ditch 1 (GL06011) suggests a minimum age of 86ka (MS 5a). The current data set suggests relatively slow or pulsed sedimentation back to c 274ka (MS 7; c 4.5m, GL06013). This refined sequence then



suggests rapid sedimentation and deposition of artefacts centred on a geometric mean age of  $259 \pm 10$  ka (MS 7) between c 4.5m and 15.2m .

This study highlights areas for consideration in future application of luminescence dating. Firstly, for late and middle Pleistocene samples, it is important to assess the success of correction for sensitivity change in the high dose region by repeat regenerative-dose ratio tests. Secondly, inter-laboratory methodological differences can lead to significant differences in  $\beta D_r$ , whereas the standard approach to measurement of  $\gamma D_r$  produces equivalent values. Moreover and thirdly, a standardised approach to  $D_e$  acquisition can produce significant differences in this value between laboratories that may be caused by the choice of preheat temperature. Finally, targeting areas of divergent dosimetry in equivalent stratigraphic units and measuring the convergence of age estimates is not an infallible measure of reliability. The quality of this metric improves with increasing numbers of samples from each unit. It is apparent that two samples per unit may lead to an erroneous conclusion on their reliability.

## 10.0 BIBLIOGRAPHY

- Adamiec, G, and Aitken, M J, 1998 Dose-rate conversion factors: new data, *Ancient TL*, **16**, 37–50
- Aitken, M J, 1998 *An Introduction to Optical Dating: the Dating of Quaternary Sediments by the Use of Photon-Stimulated Luminescence*, Oxford University Press
- Bailey, R M, Singarayer, JS, Ward, S, and Stokes, S, 2003 Identification of partial resetting using  $D_e$  as a function of illumination time, *Radiat Measurement*, **37**, 511–8
- Bateman, M D, Frederick, C D, Jaiswal, M K, Singhvi, A K, 2003 Investigations into the potential effects of pedoturbation on luminescence dating, *Quat Sci Rev*, **22**, 1169–76
- Bergge, W, 2003 Luminescence chronology of late Pleistocene loess-paleosol and tephra sequences near Fairbanks, Alaska, *Quat Res*, **60**, 70–83
- Berger, G W, Muehlen, P J, and Huntley, D J, 1980 Isolation of silt-sized quartz from sediment, *Ancient TL*, **11**, 147–52
- Bøtter-Jensen, L, Mejdahl, V, and Murray, A S, 1999 New light on OSL, *Quat Sci Rev*, **18**, 303–10
- Bøtter-Jensen, L, McKeever, S W S, and Wintle, A G, 2003 *Optically Stimulated Luminescence Dosimetry*, Amsterdam (Elsevier)
- Brown, A G, and Basell, L S, 2008 New Lower Palaeolithic Finds from the Axe Valley, Dorset, *PAST*, **60**, 1–4
- Duller, G A T, 2003 Distinguishing quartz and feldspar in single grain luminescence measurements, *Radiat Measurement*, **37**, 161–5
- Duller, G A T, 2007 *Luminescence Analyst*, Aberystwyth University
- Gabraith, R F, 1990 The radioplot: graphical assessment of spread in ages, *Nuclear Tracks and Radiation Measurements*, **17**, 207–14
- Gabraith, R F, Roberts, R G, Laslett, G M, Yoshida, H, and O'Leary, J M, 1999 Optical dating of single and multiple grains of quartz from a rock shelter (northern Australia): Part I, Experimental design and statistical models, *Archaeometry*, **41**, 339–64
- Hubbell, J H, 1982 Photon mass attenuation and energy-absorption coefficients from 1 keV to 20 MeV, *International Journal of Applied Radiotopes*, **33**, 1269–90

Huntley, D. J., Godfrey-Smith, D. I., and Thewalt, M. L. W., 1985 Optical dating of sediments, *Nature*, **313**, 105–7

Hütt, G., Jäek, I., and Tchonka, J., 1988 Optical dating: K-feldspars optical response stimulation spectra, *Quat Sci Rev*, **7**, 381–6

Jackson, M. L., Sayin, M., and Clayton, R. N., 1976 Hexafluorosilicic acid reagent modification for quartz isolation, *Soil Science Society of America Journal*, **40**, 958–60

Markey, B. G., Bøtter-Jensen, L., and Duller, G. A. T., 1997 A new flexible system for measuring thermally and optically stimulated luminescence, *Radiation Measurements*, **27**, 83–9

Mejdahl, V., 1979 Thermoluminescence dating: beta-dose attenuation in quartz grains, *Archaeometry*, **21**, 61–72

Murray, A. S., and Oley, J. M., 2002 Precision and accuracy in the optically stimulated luminescence dating of sedimentary quartz: a status review, *Geochronometry*, **21**, 1–16

Murray, A. S., and Wintle, A. G., 2000 Luminescence dating of quartz using an improved single-aliquot regenerative-dose protocol, *Radiation Measurements*, **32**, 57–73

Murray, A. S., and Wintle, A. G., 2003 The single aliquot regenerative dose protocol: potential for improvements in reliability, *Radiation Measurements*, **37**, 377–81

Oley, J. M., Murray, A. S., and Roberts, R. G., 1996 The effects of disequilibria in the Uranium and Thorium decay chains on burial dose rates in fluvial sediments, *Quat Sci Rev*, **15**, 751–60

Oley, J. M., Catcheen, G. G., and Murray, A. S., 1998 The distribution of apparent dose as determined by optical stimulation luminescence in small aliquots of fluvial quartz: implications for dating young sediments, *Quat Sci Rev*, **17**, 1033–40

Oley, J. M., Catcheen, G. G., and Roberts, R. G., 1999 The origin of dose distributions in fluvial sediments, and the prospect of dating single grains from fluvial deposits using optically stimulated luminescence, *Radiation Measurements*, **30**, 207–17

Oley, J. M., Pietsch, T., and Roberts, R. G., 2004 Optical dating of Holocene sediments from a variety of geomorphic settings using single grains of quartz, *Geomorphology*, **60**, 337–58

Pawley, M., Tomes, P. S., Armistead, S. J., and Rose, J., 2010 Quartz luminescence dating of Anglian Stage fluvial sediments: Comparison of SAR age estimates to the terrace chronology of the Middle Thames valley, UK, *Quaternary Geochronology*, **5**, 569–82

Prescott, JR, and Hutton, JT, 1994 Cosmic ray contributions to dose rates for luminescence and ESR dating: large depths and long-term time variations, *Radiation Measurements*, **23**, 497–500

Singhvi, O K, Bluszcz, A, Bateman, M D, Someshwar Rao, M, 2001 Luminescence dating of loess-paleosol sequences and coversands: methodological aspects and paleoclimatic implications, *Earth Sci Rev*, **54**, 193–211

Smith, B W, Rhodes, E J, Stokes, S and Spooner, N A 1990 The optical dating of sediments using quartz, *Radiation Protection Dosimetry*, **34**, 75–8

Toms, P S, Brown, A G, Bassett, L S, and Hosfield, R T, 2008 Paleolithic Rivers of south-west Britain: optical stimulated luminescence dating of residual deposits of the proto-Axe, Exe, Otter and Doniford, *English Heritage Res Dep Rep Ser*, **2-2008**

Toms, P S, Hosfield, R T, Chambers, J C, Green, C P, and Marshall, P, 2005 Optical dating of the Broom Paleolithic sites, Devon and Dorset, *English Heritage Centre for Archaeol Rep* **16/2005**

Wallinga, J 2002 Optically stimulated luminescence dating of fluvial deposits: a review, *Boreas*, **31**, 303–22

Wintle, A G, 1973 Anomalous fading of thermoluminescence in mineral samples, *Nature*, **245**, 143–4

Zimmerman, D W, 1971 Thermoluminescent dating using fine grains from pottery, *Archaeometry*, **13**, 29–52



Table 2: Analytical validity of sample suite age estimates and caveats for consideration

Field Code	Lab Code	Sample specific considerations
CHAR01	GL06010	
CHAR02	GL06011	
CHAR03	GL06012	Significant feldspar contamination Failed dose recovery test
CHAR04	GL06013	
CHAR05	GL06057	
CHAR06	GL06058	
CHAR07	GL08043	Failed repeat dose ratio test
CHAR08	GL08044	
CHAR09	GL08045	Failed repeat dose ratio test
CHAR10	GL08046	
CHAR11	GL08047	$D_e$ exceeds 600Gy Failed repeat dose ratio test
CHAR12	GL09029	Potential partial bleaching
CHAR13	GL09030	Failed repeat dose ratio test
CHAR14	GL09031	Failed repeat dose ratio test
CHAR15	GL09117	$D_e$ exceeds 600Gy Minor to moderate U disequilibrium
CHAR16	GL09118	$D_e$ exceeds 600Gy Minor to moderate U disequilibrium
CHAR17	GL09119	
CHAR18	GL09120	Limited sample mass
CHAR19	GL10013	Failed repeat dose ratio test
CHAR20	GL10014	Failed dose recovery test
CHAR21	GL10015	Failed dose recovery test Minor U disequilibrium
CHAR22	GL10016	
CHAR23	GL10001	Failed dose recovery test Minor U disequilibrium
CHAR24	GL10002	
CHAR25	GL10019	Failed repeat dose ratio test
CHAR26	GL10020	Failed dose recovery test Failed repeat dose ratio test
CHAR27	GL10055	Failed dose recovery test
CHAR28	GL10063	Failed repeat dose ratio test
CHAR29	GL10064	Failed repeat dose ratio test
CHAR30	GL10065	Failed repeat dose ratio test
CHAR31	GL10066	Significant feldspar contamination $D_e$ exceeds 600Gy Minor U disequilibrium
CHAR32	GL10067	Failed repeat dose ratio test
CHAR33	GL10084	Significant feldspar contamination

Table 3: Anonymised inter-laboratory results for samples GL10001 and GL10002.  $\gamma D_r$  acquired by each laboratory's NaI  $\gamma$  spectrometer.  $\beta D_r$  determined by each laboratories standard method. Preheat selected by each laboratory based on their dose recover tests

Sample	Laboratory	$\gamma D_r$ (Gyka <sup>-1</sup> )	$\beta D_r$ (Gyka <sup>-1</sup> )	Total $D_r$ (Gyka <sup>-1</sup> )	Preheat (°C for 10s)	$D_e$ (Gy)	Age (ka)
GL10001	A	0.46 ± 0.02	0.57 ± 0.04	1.17 ± 0.05	280	164.9 ± 15.6	141 ± 14
	B	0.48 ± 0.02	0.66 ± 0.04	1.24 ± 0.05	240	195.4 ± 15.5	158 ± 14
	C	0.44 ± 0.02	0.49 ± 0.03	1.12 ± 0.06	260	136.6 ± 13.4	122 ± 14
GL10002	A	0.31 ± 0.02	0.51 ± 0.05	0.86 ± 0.05	240	229.4 ± 16.2	268 ± 25
	B	0.34 ± 0.02	0.58 ± 0.04	0.92 ± 0.04	240	212.2 ± 15.4	231 ± 20
	C	0.30 ± 0.01	0.54 ± 0.04	0.92 ± 0.05	260	177.7 ± 19.8	193 ± 24

# FIGURES

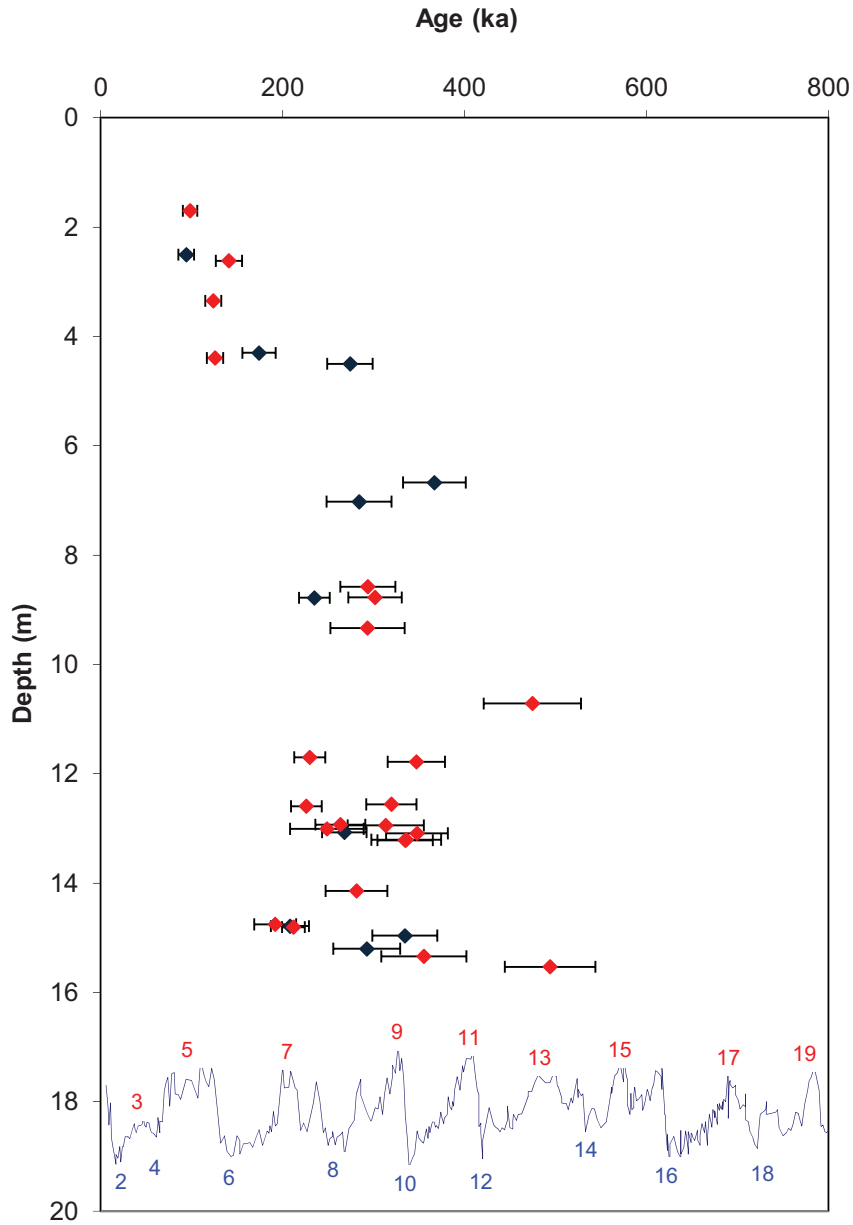


Figure 1: Age-depth plot for Chard Junction Quarry optical dating samples analysed at Gloucestershire. Red fill indicates those samples with analytical caveats. The blue line shows the oxygen isotope curve from ODP 677 along with temperate (red numbered) and cool (blue numbered) MIS



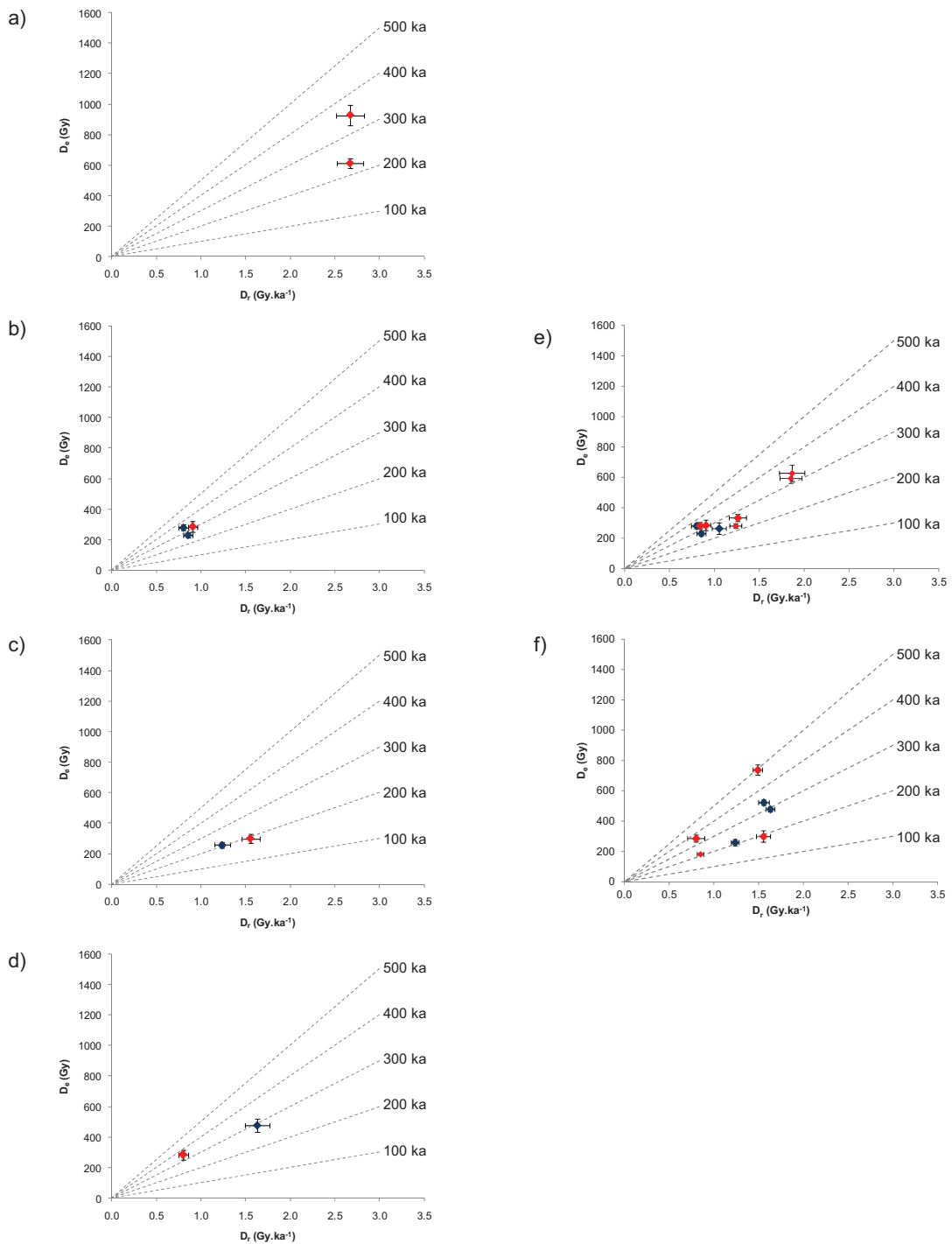


Figure 2:  $D_e:D_r$  plots for samples within the same unit; a) GL09117 and GL09118 (11.7m depth), b) GL10002, GL10013, GL10014 (13m depth), c) GL10015 and GL10016 (14.7m depth), d) GL08043 and GL08044 (15.2m depth) and from units at equivalent depth within the sequence; e) GL08045, GL10002, GL10013, GL10014, GL10019, GL10055, GL10063, GL10065, GL10066 (13m depth) and f) GL08043, GL08044, GL08046, GL08047, GL10015, GL10016, GL10064 (15m depth). Red fill indicates samples with analytical caveats. The gradient of dashed lines represents age, which increases with slope

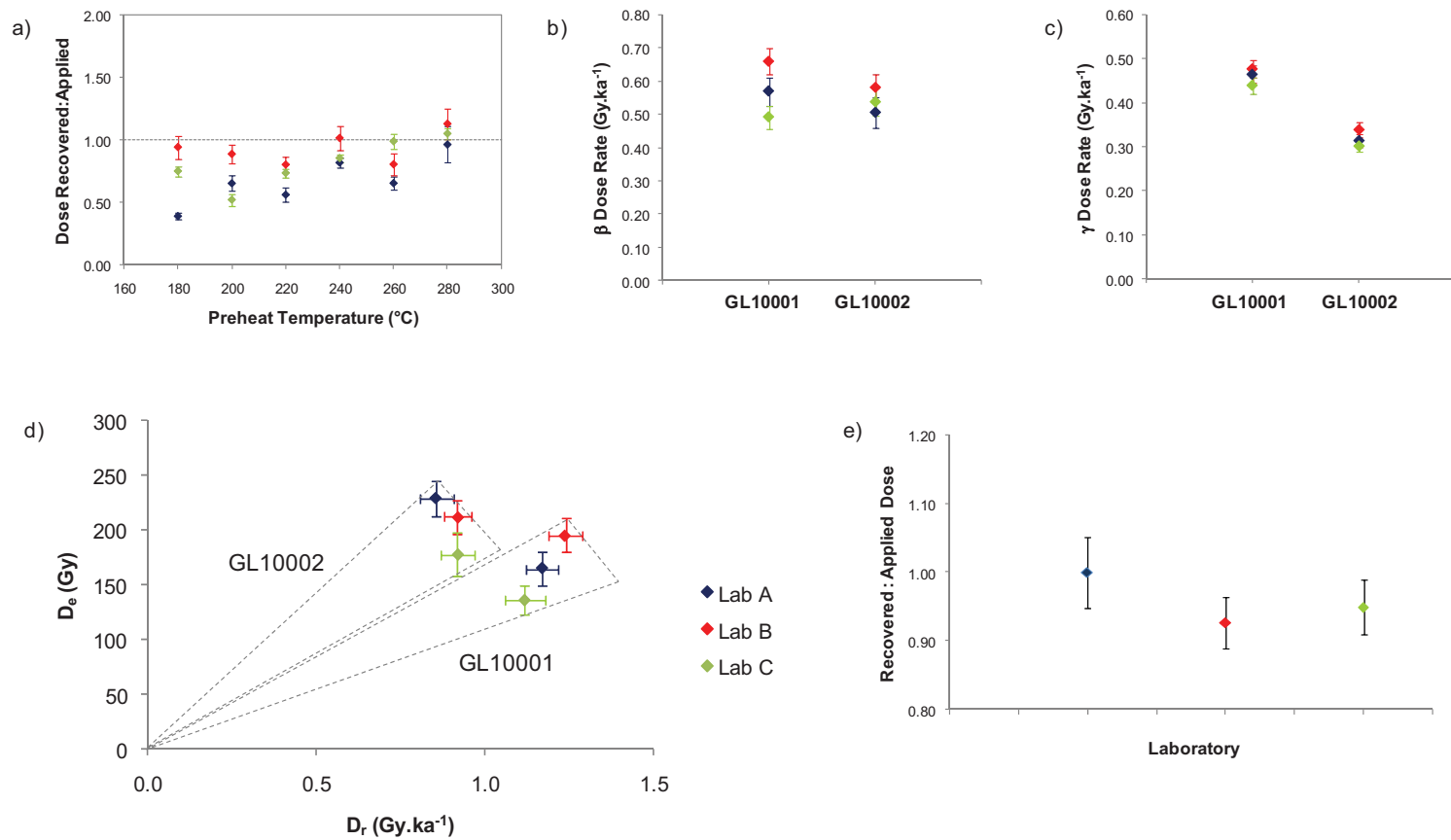
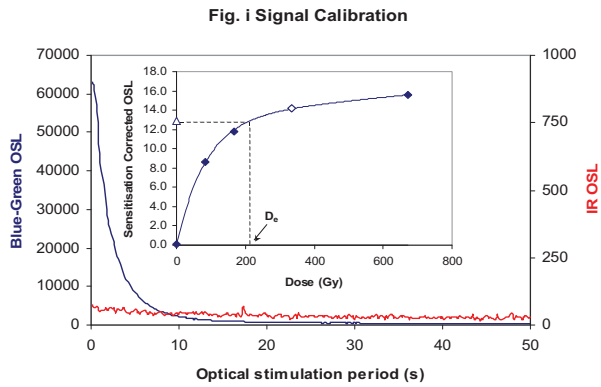


Figure 3: Summary of inter-comparison for samples GL10001 and GL10002 between Laboratory A, B and C in blue, red and green fill respectively; a) dose recovery test, b)  $\beta$   $D_r$  assessment, c)  $\gamma$   $D_r$  assessment, d) age envelopes and e) dose recovery test of source calibration centred on that dose recovered from Laboratory A

## APPENDIX

(excluding data reported in Tom s et al 2008)



**Fig. i Signal Calibration** Natural blue and laboratory-induced infrared (IR) OSL signals. Detectable IR signal decays are diagnostic of feldspar contamination. Inset, the natural blue OSL signal (open triangle) of each aliquot is calibrated against known laboratory doses to yield equivalent dose ( $D_0$ ) values. Repeats of low and high doses (open diamonds) illustrate the success of sensitivity correction.

**Fig. ii Dose Recovery** The acquisition of  $D_0$  values is necessarily predicated upon thermal treatment of aliquots succeeding environmental and laboratory irradiation. The Dose Recovery test quantifies the combined effects of thermal transfer and sensitisation on the natural signal using a precise lab dose to simulate natural dose. Based on this an appropriate thermal treatment is selected to generate the final  $D_0$  value.

**Fig. iii Inter-aliquot  $D_0$  distribution** Provides a measure of inter-aliquot statistical concordance in  $D_0$  values derived from natural irradiation. Discordant data (those points lying beyond  $\pm 2$  standardised  $\ln D_0$ ) reflects heterogeneous dose absorption and/or inaccuracies in calibration.

**Fig. iv Low and High Repeat Regenerative-dose Ratio** Measures the statistical concordance of signals from repeated low and high regenerative-doses. Discordant data (those points lying beyond  $\pm 2$  standardised  $\ln D_0$ ) indicate inaccurate sensitivity correction.

**Fig. v OSL to Post-IR OSL Ratio** Measures the statistical concordance of OSL and post-IR OSL responses to the same regenerative-dose. Discordant, underestimating data (those points lying below  $-2$  standardised  $\ln D_0$ ) highlight the presence of significant feldspar contamination.

**Fig. vi Signal Analysis** Statistically significant increase in natural  $D_0$  value with signal stimulation period is indicative of a partially-bleached signal, provided a significant increase in  $D_0$  results from simulated partial bleaching followed by insignificant adjustment in  $D_0$  for simulated zero and full bleach conditions. Ages from such samples are considered maximum estimates. In the absence of a significant rise in  $D_0$  with stimulation time, simulated partial bleaching and zero/full bleach tests are not assessed.

**Fig. vii U Activity** Statistical concordance (equilibrium) in the activities of the daughter radioisotope  $^{226}\text{Ra}$  with its parent  $^{238}\text{U}$  may signify the temporal stability of  $D_0$  emissions from these chains. Significant differences (disequilibrium;  $>50\%$ ) in activity indicate addition or removal of isotopes creating a time-dependent shift in  $D_0$  values and increased uncertainty in the accuracy of age estimates. A 20% disequilibrium marker is also shown.

**Fig. viii Age Range** The mean age range provides an estimate of sediment burial period based on mean  $D_0$  and  $D_e$  values with associated analytical uncertainties. The probability distribution indicates the inter-aliquot variability in age. The maximum influence of temporal variations in  $D_0$  forced by minima-maxima variation in moisture content and overburden thickness may prove instructive where there is uncertainty in these parameters, however the combined extremes represented should not be construed as preferred age estimates.

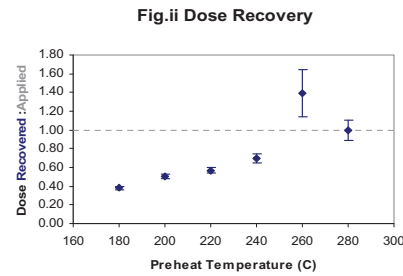


**Fig. iii and iv (combined) Inter-aliquot  $D_0$  distribution**

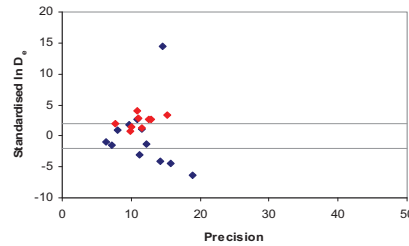


**Fig. v OSL to Post-IR OSL Ratio**

Not available

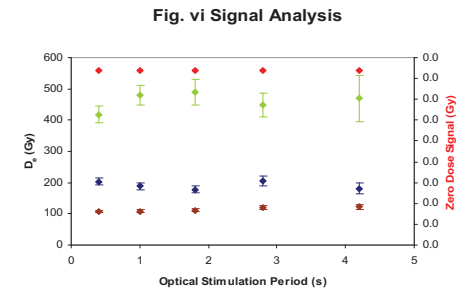


**Fig. vii U Decay Activity**

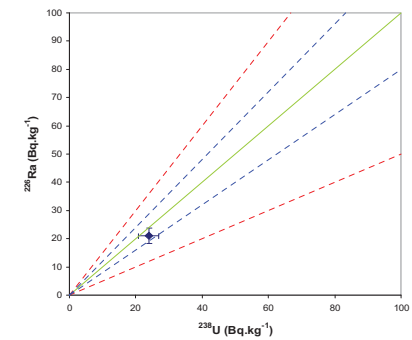
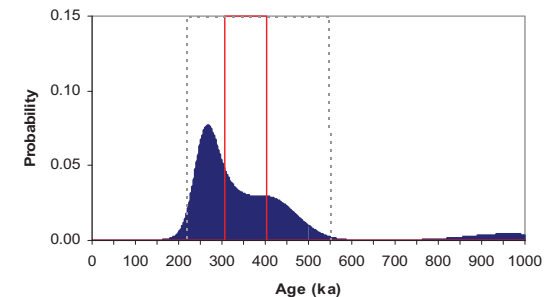


**Fig. viii Age Range**



## Appendix 1 Sample: GL08043

**Fig. i Signal Calibration**

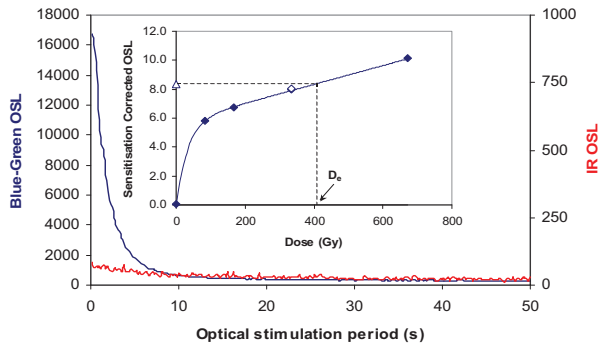


**Fig. i Signal Calibration** Natural blue and laboratory-induced infrared (IR) OSL signals. Detectable IR signal decays are diagnostic of feldspar contamination. Inset, the natural blue OSL signal (open triangle) of each aliquot is calibrated against known laboratory doses to yield equivalent dose ( $D_e$ ) values. Repeats of low and high doses (open diamonds) illustrate the success of sensitivity correction.

**Fig. ii Dose Recovery** The acquisition of  $D_e$  values is necessarily predicated upon thermal treatment of aliquots succeeding environmental and laboratory irradiation. The Dose Recovery test quantifies the combined effects of thermal transfer and sensitisation on the natural signal using a precise lab dose to simulate natural dose. Based on this an appropriate thermal treatment is selected to generate the final  $D_e$  value.

**Fig. iii Inter-aliquot  $D_e$  distribution** Provides a measure of inter-aliquot statistical concordance in  $D_e$  values derived from natural irradiation. Discordant data (those points lying beyond  $\pm 2$  standardised in  $D_e$ ) reflects heterogeneous dose absorption and/or inaccuracies in calibration.

**Fig. iv Low and High Repeat Regenerative-dose Ratio** Measures the statistical concordance of signals from repeated low and high regenerative-doses. Discordant data (those points lying beyond  $\pm 2$  standardised in  $D_e$ ) indicate inaccurate sensitivity correction.

**Fig. v OSL to Post-IR OSL Ratio** Measures the statistical concordance of OSL and post-IR OSL responses to the same regenerative-dose. Discordant, underestimating data (those points lying below  $-2$  standardised in  $D_e$ ) highlight the presence of significant feldspar contamination.

**Fig.vi Signal Analysis** Statistically significant increase in natural  $D_e$  value with signal stimulation period is indicative of a partially-bleached signal, provided a significant increase in  $D_e$  results from simulated partial bleaching followed by insignificant adjustment in  $D_e$  for simulated zero and full bleach conditions. Ages from such samples are considered maximum estimates. In the absence of a significant rise in  $D_e$  with stimulation time, simulated partial bleaching and zero/full bleach tests are not assessed.

**Fig. vii U Activity** Statistical concordance (equilibrium) in the activities of the daughter radioisotope  $^{226}\text{Ra}$  with its parent  $^{238}\text{U}$  may signify the temporal stability of  $D_e$  emissions from these chains. Significant differences (disequilibrium;  $>50\%$ ) in activity indicate addition or removal of isotopes creating a time-dependent shift in  $D_e$  values and increased uncertainty in the accuracy of age estimates. A 20% disequilibrium marker is also shown.

**Fig. viii Age Range** The mean age range provides an estimate of sediment burial period based on mean  $D_e$  and  $D_e$  values with associated analytical uncertainties. The probability distribution indicates the inter-aliquot variability in age. The maximum influence of temporal variations in  $D_e$  forced by minima-maxima variation in moisture content and overburden thickness may prove instructive where there is uncertainty in these parameters, however the combined extremes represented should not be construed as preferred age estimates.

**Fig.ii Dose Recovery**

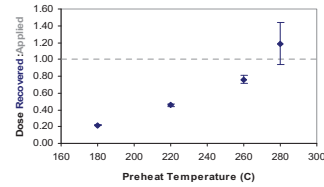


**Fig. iii and iv (combined) Inter-aliquot  $D_e$  distribution**

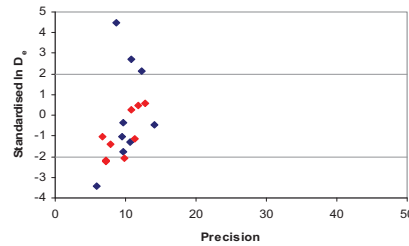


**Fig. v OSL to Post-IR OSL Ratio**

Not available

**Fig. vi Signal Analysis**

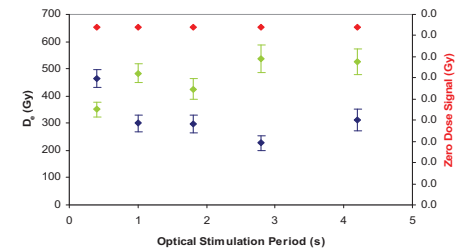


**Fig. vii U Decay Activity**

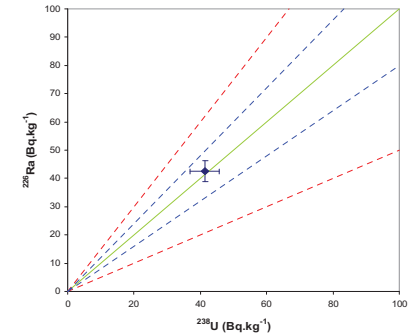
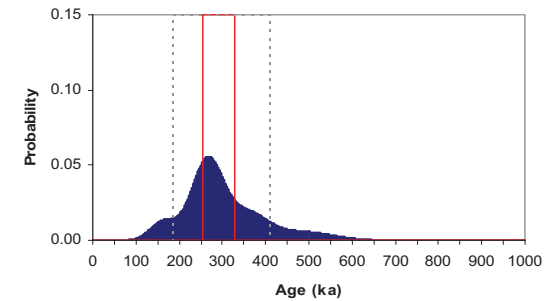


**Fig. viii Age Range**



**Appendix 2  
Sample: GL08044**

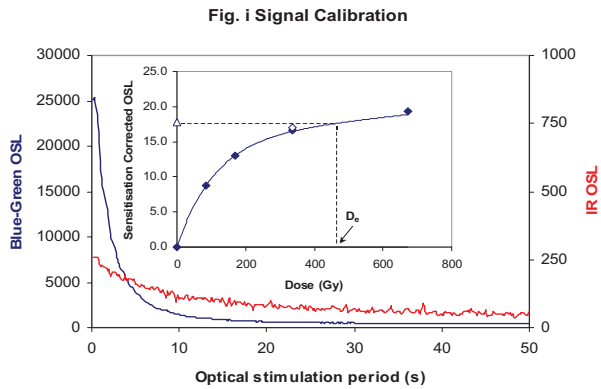


**Fig. i Signal Calibration** Natural blue and laboratory-induced infrared (IR) OSL signals. Detectable IR signal decays are diagnostic of feldspar contamination. Inset, the natural blue OSL signal (open triangle) of each aliquot is calibrated against known laboratory doses to yield equivalent dose ( $D_0$ ) values. Repeats of low and high doses (open diamonds) illustrate the success of sensitivity correction.

**Fig. ii Dose Recovery** The acquisition of  $D_0$  values is necessarily predicated upon thermal treatment of aliquots succeeding environmental and laboratory irradiation. The Dose Recovery test quantifies the combined effects of thermal transfer and sensitisation on the natural signal using a precise lab dose to simulate natural dose. Based on this an appropriate thermal treatment is selected to generate the final  $D_0$  value.

**Fig. iii Inter-aliquot  $D_0$  distribution** Provides a measure of inter-aliquot statistical concordance in  $D_0$  values derived from natural irradiation. Discordant data (those points lying beyond  $\pm 2$  standardised  $\ln D_0$ ) reflects heterogeneous dose absorption and/or inaccuracies in calibration.

**Fig. iv Low and High Repeat Regenerative-dose Ratio** Measures the statistical concordance of signals from repeated low and high regenerative-doses. Discordant data (those points lying beyond  $\pm 2$  standardised  $\ln D_0$ ) indicate inaccurate sensitivity correction.

**Fig. v OSL to Post-IR OSL Ratio** Measures the statistical concordance of OSL and post-IR OSL responses to the same regenerative-dose. Discordant, underestimating data (those points lying below  $-2$  standardised  $\ln D_0$ ) highlight the presence of significant feldspar contamination.

**Fig.vi Signal Analysis** Statistically significant increase in natural  $D_0$  value with signal stimulation period is indicative of a partially-bleached signal, provided a significant increase in  $D_0$  results from simulated partial bleaching followed by insignificant adjustment in  $D_0$  for simulated zero and full bleach conditions. Ages from such samples are considered maximum estimates. In the absence of a significant rise in  $D_0$  with stimulation time, simulated partial bleaching and zero/full bleach tests are not assessed.

**Fig. vii U Activity** Statistical concordance (equilibrium) in the activities of the daughter radioisotope  $^{226}\text{Ra}$  with its parent  $^{238}\text{U}$  may signify the temporal stability of  $D_0$  emissions from these chains. Significant differences (disequilibrium;  $>50\%$ ) in activity indicate addition or removal of isotopes creating a time-dependent shift in  $D_0$  values and increased uncertainty in the accuracy of age estimates. A 20% disequilibrium marker is also shown.

**Fig. viii Age Range** The mean age range provides an estimate of sediment burial period based on mean  $D_0$  and  $D_0$  values with associated analytical uncertainties. The probability distribution indicates the inter-aliquot variability in age. The maximum influence of temporal variations in  $D_0$  forced by minima-maxima variation in moisture content and overburden thickness may prove instructive where there is uncertainty in these parameters, however the combined extremes represented should not be construed as preferred age estimates.

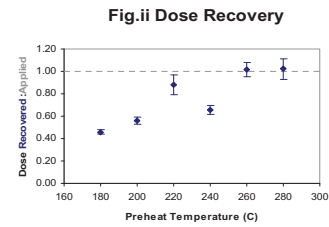


**Fig. iii and iv (combined) Inter-aliquot  $D_0$  distribution**

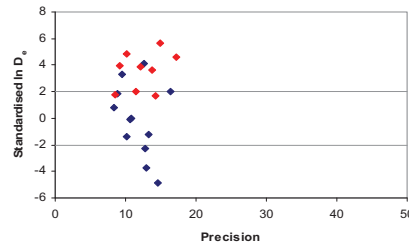


**Fig. v OSL to Post-IR OSL Ratio**

Not available

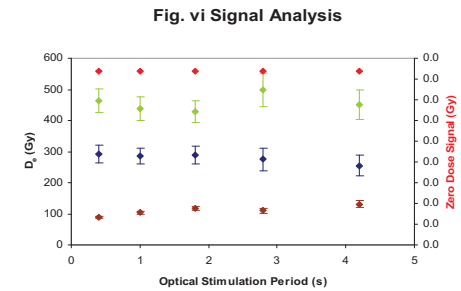


**Fig. vii U Decay Activity**

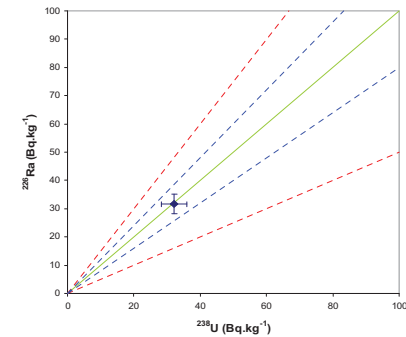
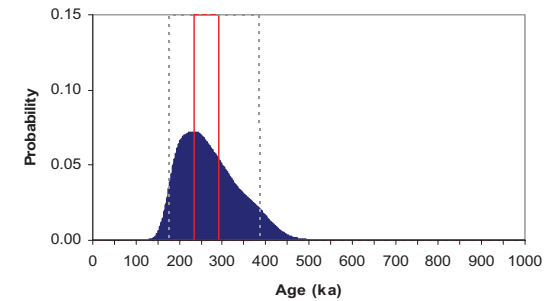


**Fig. viii Age Range**



### Appendix 3 Sample: GL08045

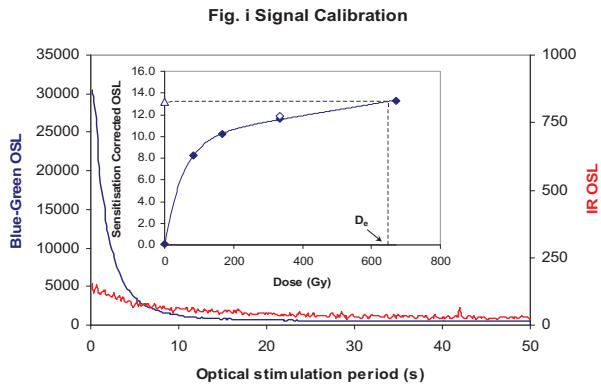


**Fig. i Signal Calibration** Natural blue and laboratory-induced infrared (IR) OSL signals. Detectable IR signal decays are diagnostic of feldspar contamination. Inset, the natural blue OSL signal (open triangle) of each aliquot is calibrated against known laboratory doses to yield equivalent dose ( $D_e$ ) values. Repeats of low and high doses (open diamonds) illustrate the success of sensitivity correction.

**Fig. ii Dose Recovery** The acquisition of  $D_e$  values is necessarily predicated upon thermal treatment of aliquots succeeding environmental and laboratory irradiation. The Dose Recovery test quantifies the combined effects of thermal transfer and sensitisation on the natural signal using a precise lab dose to simulate natural dose. Based on this an appropriate thermal treatment is selected to generate the final  $D_e$  value.

**Fig. iii Inter-aliquot  $D_e$  distribution** Provides a measure of inter-aliquot statistical concordance in  $D_e$  values derived from natural irradiation. Discordant data (those points lying beyond  $\pm 2$  standardised in  $D_e$ ) reflects heterogeneous dose absorption and/or inaccuracies in calibration.

**Fig. iv Low and High Repeat Regenerative-dose Ratio** Measures the statistical concordance of signals from repeated low and high regenerative-doses. Discordant data (those points lying beyond  $\pm 2$  standardised in  $D_e$ ) indicate inaccurate sensitivity correction.

**Fig. v OSL to Post-IR OSL Ratio** Measures the statistical concordance of OSL and post-IR OSL responses to the same regenerative-dose. Discordant, underestimating data (those points lying below  $-2$  standardised in  $D_e$ ) highlight the presence of significant feldspar contamination.

**Fig. vi Signal Analysis** Statistically significant increase in natural  $D_e$  value with signal stimulation period is indicative of a partially-bleached signal, provided a significant increase in  $D_e$  results from simulated zero and full bleach conditions. Ages from such samples are considered maximum estimates. In the absence of a significant rise in  $D_e$  with stimulation time, simulated partial bleaching and zero/full bleach tests are not assessed.

**Fig. vii U Activity** Statistical concordance (equilibrium) in the activities of the daughter radioisotope  $^{226}\text{Ra}$  with its parent  $^{238}\text{U}$  may signify the temporal stability of  $D_e$  emissions from these chains. Significant differences (disequilibrium;  $>50\%$ ) in activity indicate addition or removal of isotopes creating a time-dependent shift in  $D_e$  values and increased uncertainty in the accuracy of age estimates. A 20% disequilibrium marker is also shown.

**Fig. viii Age Range** The mean age range provides an estimate of sediment burial period based on mean  $D_e$  and  $D_e$  values with associated analytical uncertainties. The probability distribution indicates the inter-aliquot variability in age. The maximum influence of temporal variations in  $D_e$  forced by minima-maxima variation in moisture content and overburden thickness may prove instructive where there is uncertainty in these parameters, however the combined extremes represented should not be construed as preferred age estimates.

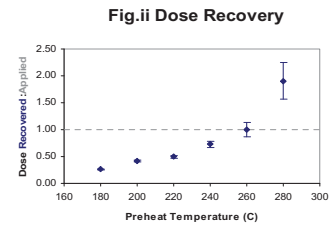


**Fig. iii and iv (combined) Inter-aliquot  $D_e$  distribution**

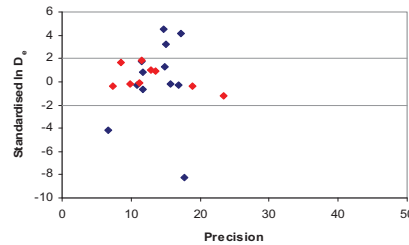


**Fig. v OSL to Post-IR OSL Ratio**

Not available

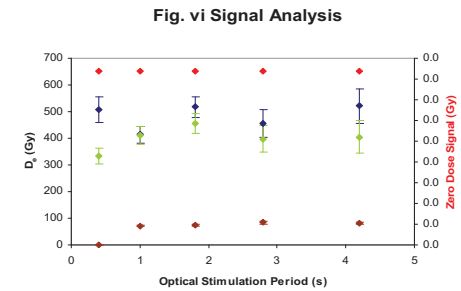


**Fig. vii U Decay Activity**

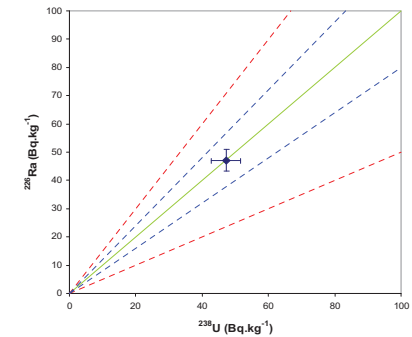
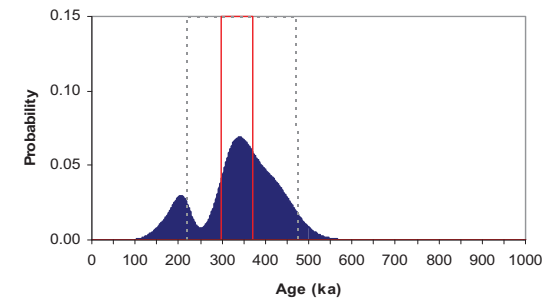


**Fig. viii Age Range**



## Appendix 4 Sample: GL08046

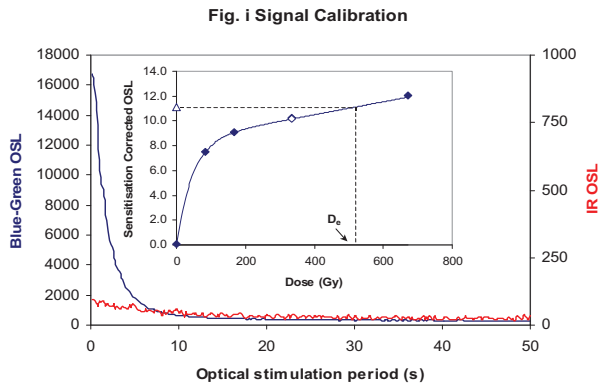


**Fig. i Signal Calibration** Natural blue and laboratory-induced infrared (IR) OSL signals. Detectable IR signal decays are diagnostic of feldspar contamination. Inset, the natural blue OSL signal (open triangle) of each aliquot is calibrated against known laboratory doses to yield equivalent dose ( $D_e$ ) values. Repeats of low and high doses (open diamonds) illustrate the success of sensitivity correction.

**Fig. ii Dose Recovery** The acquisition of  $D_e$  values is necessarily predicated upon thermal treatment of aliquots succeeding environmental and laboratory irradiation. The Dose Recovery test quantifies the combined effects of thermal transfer and sensitisation on the natural signal using a precise lab dose to simulate natural dose. Based on this an appropriate thermal treatment is selected to generate the final  $D_e$  value.

**Fig. iii Inter-aliquot  $D_e$  distribution** Provides a measure of inter-aliquot statistical concordance in  $D_e$  values derived from natural irradiation. Discordant data (those points lying beyond  $\pm 2$  standardised  $\ln D_e$ ) reflects heterogeneous dose absorption and/or inaccuracies in calibration.

**Fig. iv Low and High Repeat Regenerative-dose Ratio** Measures the statistical concordance of signals from repeated low and high regenerative-doses. Discordant data (those points lying beyond  $\pm 2$  standardised  $\ln D_e$ ) indicate inaccurate sensitivity correction.

**Fig. v OSL to Post-IR OSL Ratio** Measures the statistical concordance of OSL and post-IR OSL responses to the same regenerative-dose. Discordant, underestimating data (those points lying below  $-2$  standardised  $\ln D_e$ ) highlight the presence of significant feldspar contamination.

**Fig. vi Signal Analysis** Statistically significant increase in natural  $D_e$  value with signal stimulation period is indicative of a partially-bleached signal, provided a significant increase in  $D_e$  results from simulated partial bleaching followed by insignificant adjustment in  $D_e$  for simulated zero and full bleach conditions. Ages from such samples are considered maximum estimates. In the absence of a significant rise in  $D_e$  with stimulation time, simulated partial bleaching and zero/full bleach tests are not assessed.

**Fig. vii U Activity** Statistical concordance (equilibrium) in the activities of the daughter radioisotope  $^{226}\text{Ra}$  with its parent  $^{238}\text{U}$  may signify the temporal stability of  $D_e$  emissions from these chains. Significant differences (disequilibrium;  $>50\%$ ) in activity indicate addition or removal of isotopes creating a time-dependent shift in  $D_e$  values and increased uncertainty in the accuracy of age estimates. A 20% disequilibrium marker is also shown.

**Fig. viii Age Range** The mean age range provides an estimate of sediment burial period based on mean  $D_e$  and  $D_e$  values with associated analytical uncertainties. The probability distribution indicates the inter-aliquot variability in age. The maximum influence of temporal variations in  $D_e$  forced by minima-maxima variation in moisture content and overburden thickness may prove instructive where there is uncertainty in these parameters, however the combined extremes represented should not be construed as preferred age estimates.

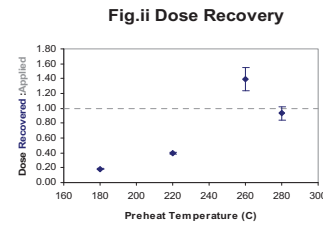


**Fig. iii and iv (combined) Inter-aliquot  $D_e$  distribution**

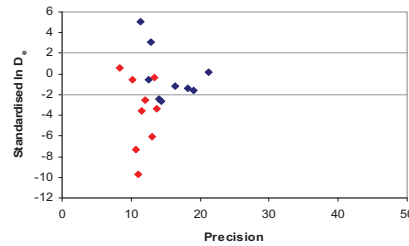


**Fig. v OSL to Post-IR OSL Ratio**

Not available

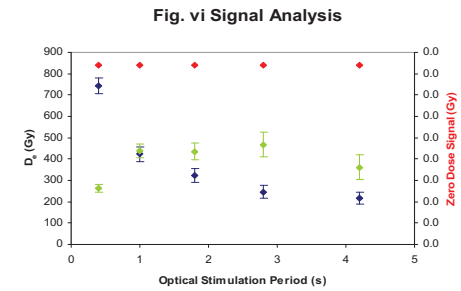


**Fig. vii U Decay Activity**

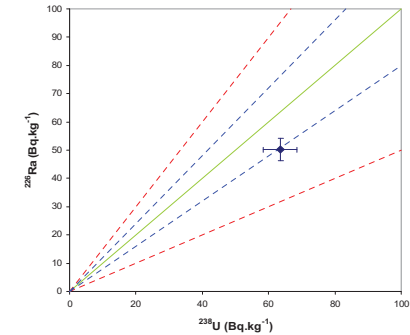
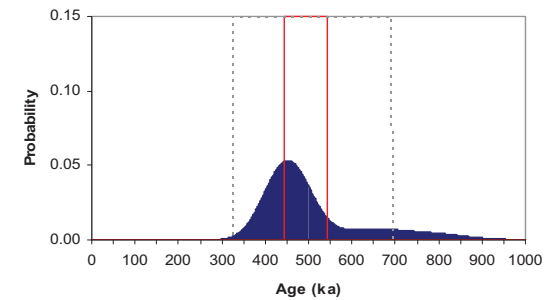


**Fig. viii Age Range**



## Appendix 5 Sample: GL08047



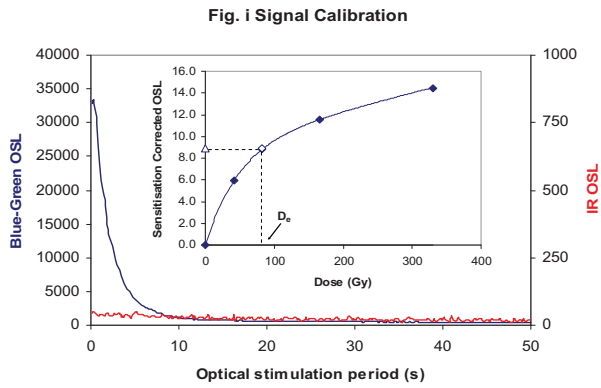


**Fig. i Signal Calibration** Natural blue and laboratory-induced infrared (IR) OSL signals. Detectable IR signal decays are diagnostic of feldspar contamination. Inset, the natural blue OSL signal (open triangle) of each aliquot is calibrated against known laboratory doses to yield equivalent dose ( $D_0$ ) values. Repeats of low and high doses (open diamonds) illustrate the success of sensitivity correction.

**Fig. ii Dose Recovery** The acquisition of  $D_0$  values is necessarily predicated upon thermal treatment of aliquots succeeding environmental and laboratory irradiation. The Dose Recovery test quantifies the combined effects of thermal transfer and sensitisation on the natural signal using a precise lab dose to simulate natural dose. Based on this an appropriate thermal treatment is selected to generate the final  $D_0$  value.

**Fig. iii Inter-aliquot  $D_0$  distribution** Provides a measure of inter-aliquot statistical concordance in  $D_0$  values derived from natural irradiation. Discordant data (those points lying beyond  $\pm 2$  standardised in  $D_0$ ) reflects heterogeneous dose absorption and/or inaccuracies in calibration.

**Fig. iv Low and High Repeat Regenerative-dose Ratio** Measures the statistical concordance of signals from repeated low and high regenerative-doses. Discordant data (those points lying beyond  $\pm 2$  standardised in  $D_0$ ) indicate inaccurate sensitivity correction.

**Fig. v OSL to Post-IR OSL Ratio** Measures the statistical concordance of OSL and post-IR OSL responses to the same regenerative-dose. Discordant, underestimating data (those points lying below  $-2$  standardised in  $D_0$ ) highlight the presence of significant feldspar contamination.

**Fig.vi Signal Analysis** Statistically significant increase in natural  $D_0$  value with signal stimulation period is indicative of a partially-bleached signal, provided a significant increase in  $D_0$  results from simulated zero and full bleach conditions. Ages from such samples are considered maximum estimates. In the absence of a significant rise in  $D_0$  with stimulation time, simulated partial bleaching and zero/full bleach tests are not assessed.

**Fig. vii U Activity** Statistical concordance (equilibrium) in the activities of the daughter radioisotope  $^{226}\text{Ra}$  with its parent  $^{238}\text{U}$  may signify the temporal stability of  $D_0$  emissions from these chains. Significant differences (disequilibrium;  $>50\%$ ) in activity indicate addition or removal of isotopes creating a time-dependent shift in  $D_0$  values and increased uncertainty in the accuracy of age estimates. A 20% disequilibrium marker is also shown.

**Fig. viii Age Range** The mean age range provides an estimate of sediment burial period based on mean  $D_0$  and  $D_1$  values with associated analytical uncertainties. The probability distribution indicates the inter-aliquot variability in age. The maximum influence of temporal variations in  $D_0$  forced by minima-maxima variation in moisture content and overburden thickness may prove instructive where there is uncertainty in these parameters, however the combined extremes represented should not be construed as preferred age estimates.

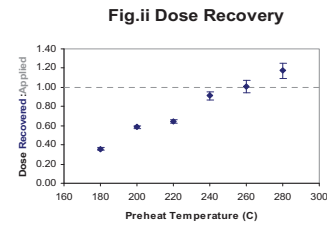


**Fig. iii and iv (combined) Inter-aliquot  $D_0$  distribution**

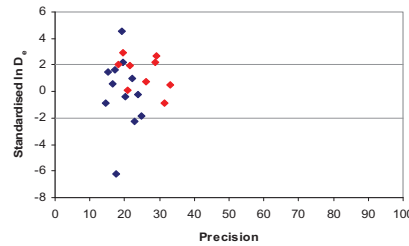


**Fig. v OSL to Post-IR OSL Ratio**

Not available

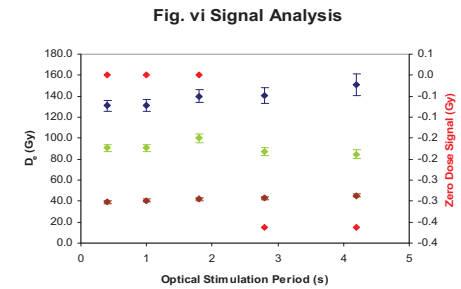


**Fig. vii U Decay Activity**

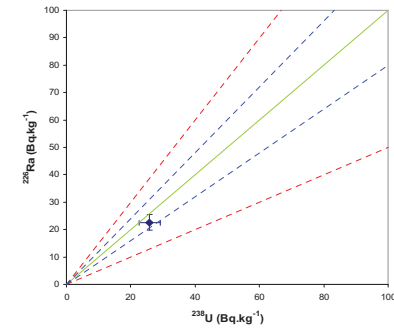
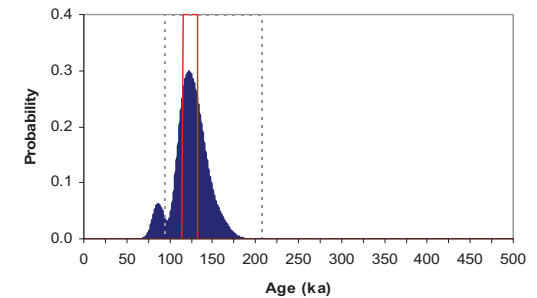


**Fig. viii Age Range**



## Appendix 6 Sample: GL09029

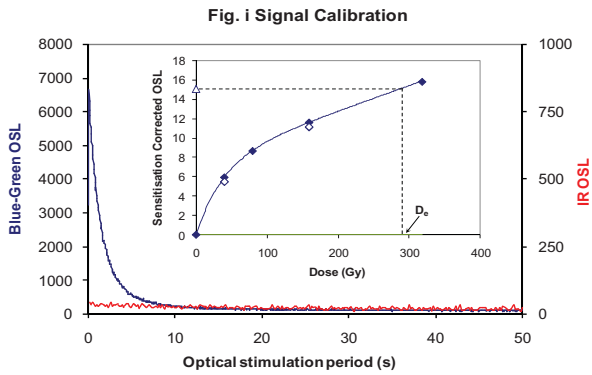


**Fig. i Signal Calibration** Natural blue and laboratory-induced infrared (IR) OSL signals. Detectable IR signal decays are diagnostic of feldspar contamination. Inset, the natural blue OSL signal (open triangle) of each aliquot is calibrated against known laboratory doses to yield equivalent dose ( $D_e$ ) values. Repeats of low and high doses (open diamonds) illustrate the success of sensitivity correction.

**Fig. ii Dose Recovery** The acquisition of  $D_e$  values is necessarily predicated upon thermal treatment of aliquots succeeding environmental and laboratory irradiation. The Dose Recovery test quantifies the combined effects of thermal transfer and sensitisation on the natural signal using a precise lab dose to simulate natural dose. Based on this an appropriate thermal treatment is selected to generate the final  $D_e$  value.

**Fig. iii Inter-aliquot  $D_e$  distribution** Provides a measure of inter-aliquot statistical concordance in  $D_e$  values derived from natural irradiation. Discordant data (those points lying beyond  $\pm 2$  standardised  $\ln D_e$ ) reflects heterogeneous dose absorption and/or inaccuracies in calibration.

**Fig. iv Low and High Repeat Regenerative-dose Ratio** Measures the statistical concordance of signals from repeated low and high regenerative-doses. Discordant data (those points lying beyond  $\pm 2$  standardised  $\ln D_e$ ) indicate inaccurate sensitivity correction.

**Fig. v OSL to Post-IR OSL Ratio** Measures the statistical concordance of OSL and post-IR OSL responses to the same regenerative-dose. Discordant, underestimating data (those points lying below -2 standardised  $\ln D_e$ ) highlight the presence of significant feldspar contamination.

**Fig. vi Signal Analysis** Statistically significant increase in natural  $D_e$  value with signal stimulation period is indicative of a partially-bleached signal, provided a significant increase in  $D_e$  results from simulated partial bleaching followed by insignificant adjustment in  $D_e$  for simulated zero and full bleach conditions. Ages from such samples are considered maximum estimates. In the absence of a significant rise in  $D_e$  with stimulation time, simulated partial bleaching and zero/full bleach tests are not assessed.

**Fig. vii U Activity** Statistical concordance (equilibrium) in the activities of the daughter radioisotope  $^{226}\text{Ra}$  with its parent  $^{238}\text{U}$  may signify the temporal stability of  $D_e$  emissions from these chains. Significant differences (disequilibrium;  $>50\%$ ) in activity indicate addition or removal of isotopes creating a time-dependent shift in  $D_e$  values and increased uncertainty in the accuracy of age estimates. A 20% disequilibrium marker is also shown.

**Fig. viii Age Range** The mean age range provides an estimate of sediment burial period based on mean  $D_e$  and  $D_e$  values with associated analytical uncertainties. The probability distribution indicates the inter-aliquot variability in age. The maximum influence of temporal variations in  $D_e$  forced by minima-maxima variation in moisture content and overburden thickness may prove instructive where there is uncertainty in these parameters, however the combined extremes represented should not be construed as preferred age estimates.

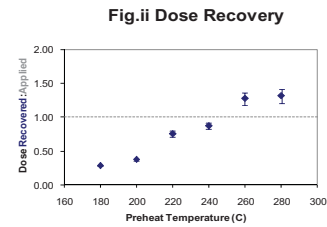


**Fig. iii Inter-aliquot  $D_e$  distribution**

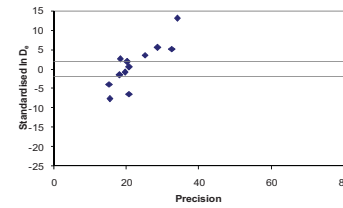


**Fig. iv Low and High Repeat Regenerative-dose Ratio**

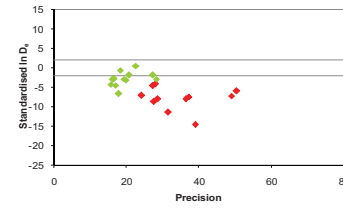


**Fig. v OSL to Post-IR OSL Ratio**

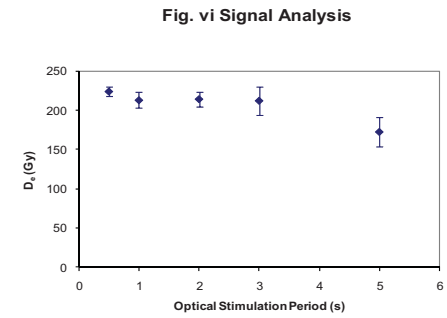
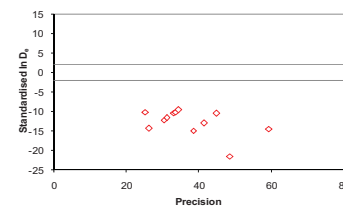


**Fig. vii U Decay Activity**

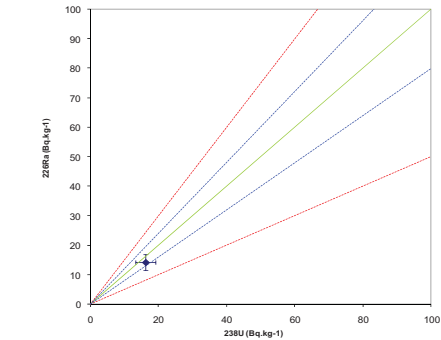
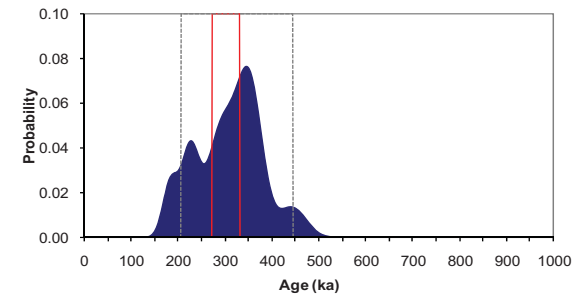


**Fig. viii Age Range**



## Appendix 7 Sample: GL09030

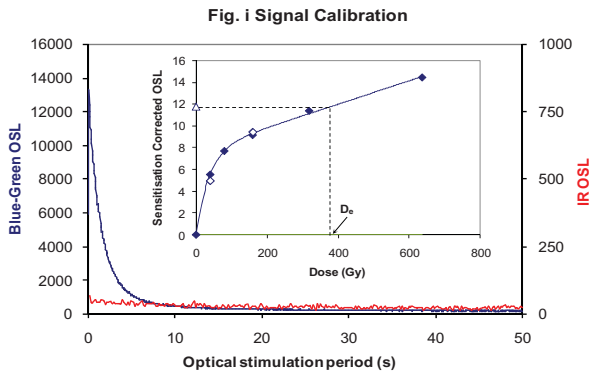


**Fig. i Signal Calibration** Natural blue and laboratory-induced infrared (IR) OSL signals. Detectable IR signal decays are diagnostic of feldspar contamination. Inset, the natural blue OSL signal (open triangle) of each aliquot is calibrated against known laboratory doses to yield equivalent dose ( $D_e$ ) values. Repeats of low and high doses (open diamonds) illustrate the success of sensitivity correction.

**Fig. ii Dose Recovery** The acquisition of  $D_e$  values is necessarily predicated upon thermal treatment of aliquots succeeding environmental and laboratory irradiation. The Dose Recovery test quantifies the combined effects of thermal transfer and sensitisation on the natural signal using a precise lab dose to simulate natural dose. Based on this an appropriate thermal treatment is selected to generate the final  $D_e$  value.

**Fig. iii Inter-aliquot  $D_e$  distribution** Provides a measure of inter-aliquot statistical concordance in  $D_e$  values derived from natural irradiation. Discordant data (those points lying beyond  $\pm 2$  standardised  $\ln D_e$ ) reflects heterogeneous dose absorption and/or inaccuracies in calibration.

**Fig. iv Low and High Repeat Regenerative-dose Ratio** Measures the statistical concordance of signals from repeated low and high regenerative-doses. Discordant data (those points lying beyond  $\pm 2$  standardised  $\ln D_e$ ) indicate inaccurate sensitivity correction.

**Fig. v OSL to Post-IR OSL Ratio** Measures the statistical concordance of OSL and post-IR OSL responses to the same regenerative-dose. Discordant, underestimating data (those points lying below -2 standardised  $\ln D_e$ ) highlight the presence of significant feldspar contamination.

**Fig. vi Signal Analysis** Statistically significant increase in natural  $D_e$  value with signal stimulation period is indicative of a partially-bleached signal, provided a significant increase in  $D_e$  results from simulated partial bleaching followed by insignificant adjustment in  $D_e$  for simulated zero and full bleach conditions. Ages from such samples are considered maximum estimates. In the absence of a significant rise in  $D_e$  with stimulation time, simulated partial bleaching and zero/full bleach tests are not assessed.

**Fig. vii U Activity** Statistical concordance (equilibrium) in the activities of the daughter radioisotope  $^{226}\text{Ra}$  with its parent  $^{238}\text{U}$  may signify the temporal stability of  $D_e$  emissions from these chains. Significant differences (disequilibrium;  $>50\%$ ) in activity indicate addition or removal of isotopes creating a time-dependent shift in  $D_e$  values and increased uncertainty in the accuracy of age estimates. A 20% disequilibrium marker is also shown.

**Fig. viii Age Range** The mean age range provides an estimate of sediment burial period based on mean  $D_e$  and  $D_e$  values with associated analytical uncertainties. The probability distribution indicates the inter-aliquot variability in age. The maximum influence of temporal variations in  $D_e$  forced by minima-maxima variation in moisture content and overburden thickness may prove instructive where there is uncertainty in these parameters, however the combined extremes represented should not be construed as preferred age estimates.

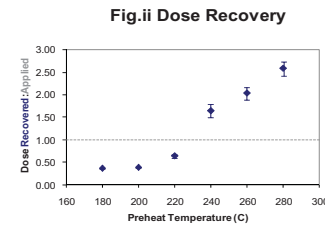


**Fig. ii Dose Recovery**

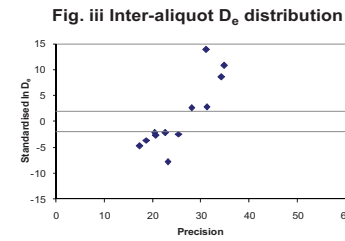


**Fig. iii Inter-aliquot  $D_e$  distribution**

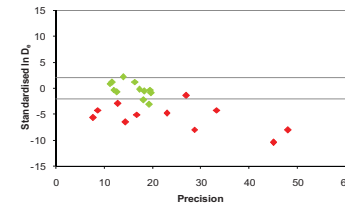


**Fig. iv Low and High Repeat Regenerative-dose Ratio**

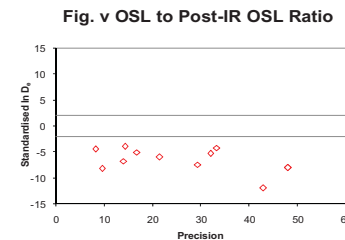


**Fig. v OSL to Post-IR OSL Ratio**

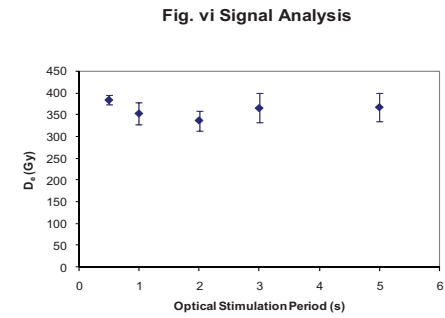


**Fig. vi Signal Analysis**

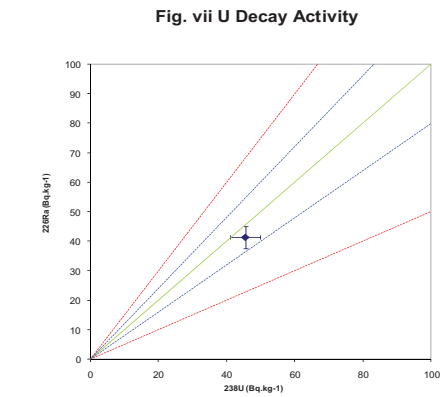


**Fig. vii U Decay Activity**

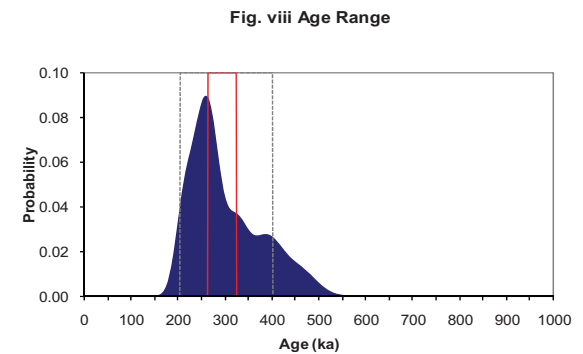


**Fig. viii Age Range**

## Appendix 8 Sample: GL09031

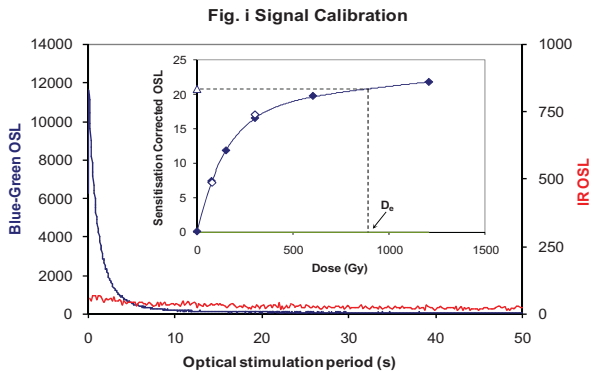


**Fig. i Signal Calibration** Natural blue and laboratory-induced infrared (IR) OSL signals. Detectable IR signal decays are diagnostic of feldspar contamination. Inset, the natural blue OSL signal (open triangle) of each aliquot is calibrated against known laboratory doses to yield equivalent dose ( $D_e$ ) values. Repeats of low and high doses (open diamonds) illustrate the success of sensitivity correction.

**Fig. ii Dose Recovery** The acquisition of  $D_e$  values is necessarily predicated upon thermal treatment of aliquots succeeding environmental and laboratory irradiation. The Dose Recovery test quantifies the combined effects of thermal transfer and significant increase on the natural signal using a precise lab dose to simulate natural dose. Based on this an appropriate thermal treatment is selected to generate the final  $D_e$  value.

**Fig. iii Inter-aliquot  $D_e$  distribution** Provides a measure of inter-aliquot statistical concordance in  $D_e$  values derived from natural irradiation. Discordant data (those points lying beyond  $\pm 2$  standardised  $\ln D_e$ ) reflects heterogeneous dose absorption and/or inaccuracies in calibration.

**Fig. iv Low and High Repeat Regenerative-dose Ratio** Measures the statistical concordance of signals from repeated low and high regenerative-doses. Discordant data (those points lying beyond  $\pm 2$  standardised  $\ln D_e$ ) indicate inaccurate sensitivity correction.

**Fig. v OSL to Post-IR OSL Ratio** Measures the statistical concordance of OSL and post-IR OSL responses to the same regenerative-dose. Discordant, underestimating data (those points lying below -2 standardised  $\ln D_e$ ) highlight the presence of significant feldspar contamination.

**Fig. vi Signal Analysis** Statistically significant increase in natural  $D_e$  value with signal stimulation period is indicative of a partially-bleached signal, provided a significant increase in  $D_e$  results from simulated partial bleaching followed by insignificant adjustment in  $D_e$  for simulated zero and full bleach conditions. Ages from such samples are considered maximum estimates. In the absence of a significant rise in  $D_e$  with stimulation time, simulated partial bleaching and zero/full bleach tests are not assessed.

**Fig. vii U Activity** Statistical concordance (equilibrium) in the activities of the daughter radioisotope  $^{226}\text{Ra}$  with its parent  $^{238}\text{U}$  may signify the temporal stability of  $D_e$  emissions from these chains. Significant differences (disequilibrium;  $>50\%$ ) in activity indicate addition or removal of isotopes creating a time-dependent shift in  $D_e$  values and increased uncertainty in the accuracy of age estimates. A 20% disequilibrium marker is also shown.

**Fig. viii Age Range** The mean age range provides an estimate of sediment burial period based on mean  $D_e$  and  $D_e$  values with associated analytical uncertainties. The probability distribution indicates the inter-aliquot variability in age. The maximum influence of temporal variations in  $D_e$  forced by minima-maxima variation in moisture content and overburden thickness may prove instructive where there is uncertainty in these parameters, however the combined extremes represented should not be construed as preferred age estimates.

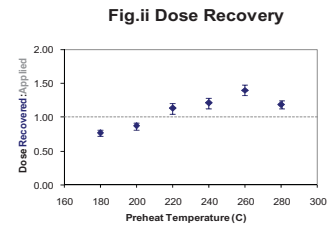


**Fig. ii Dose Recovery**

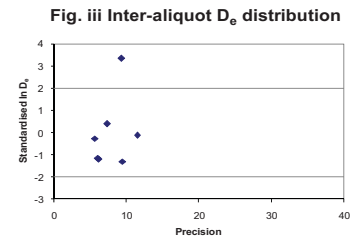


**Fig. iii Inter-aliquot  $D_e$  distribution**

**Fig. iv Low and High Repeat Regenerative-dose Ratio**

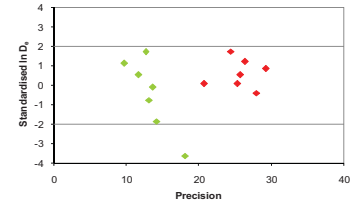


**Fig. v OSL to Post-IR OSL Ratio**

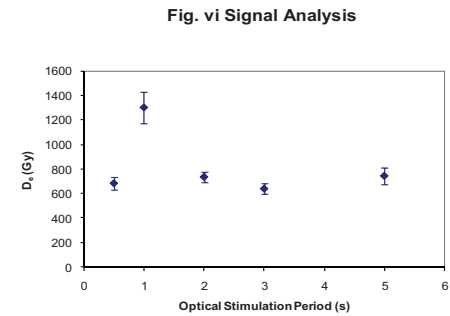
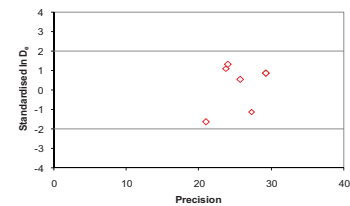


**Fig. vi Signal Analysis**

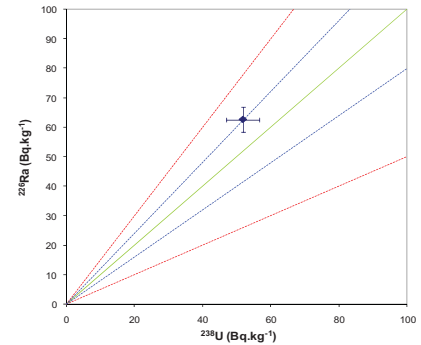


**Fig. vii U Decay Activity**

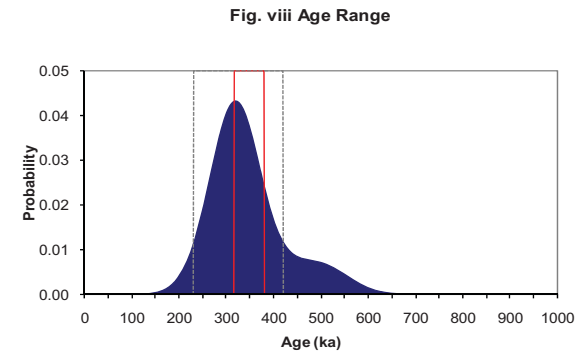


**Fig. viii Age Range**

## Appendix 9 Sample: GL09117

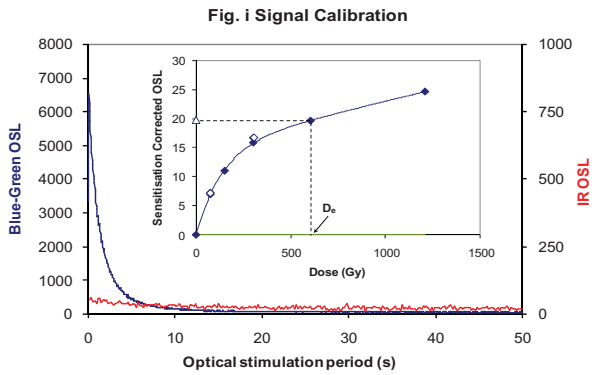


**Fig. i Signal Calibration** Natural blue and laboratory-induced infrared (IR) OSL signals. Detectable IR signal decays are diagnostic of feldspar contamination. Inset, the natural blue OSL signal (open triangle) of each aliquot is calibrated against known laboratory doses to yield equivalent dose ( $D_e$ ) values. Repeats of low and high doses (open diamonds) illustrate the success of sensitivity correction.

**Fig. ii Dose Recovery** The acquisition of  $D_e$  values is necessarily predicated upon thermal treatment of aliquots succeeding environmental and laboratory irradiation. The Dose Recovery test quantifies the combined effects of thermal transfer and sensitisation on the natural signal using a precise lab dose to simulate natural dose. Based on this an appropriate thermal treatment is selected to generate the final  $D_e$  value.

**Fig. iii Inter-aliquot  $D_e$  distribution** Provides a measure of inter-aliquot statistical concordance in  $D_e$  values derived from natural irradiation. Discordant data (those points lying beyond  $\pm 2$  standardised  $\ln D_e$ ) reflects heterogeneous dose absorption and/or inaccuracies in calibration.

**Fig. iv Low and High Repeat Regenerative-dose Ratio** Measures the statistical concordance of signals from repeated low and high regenerative-doses. Discordant data (those points lying beyond  $\pm 2$  standardised  $\ln D_e$ ) indicate inaccurate sensitivity correction.

**Fig. v OSL to Post-IR OSL Ratio** Measures the statistical concordance of OSL and post-IR OSL responses to the same regenerative-dose. Discordant, underestimating data (those points lying below -2 standardised  $\ln D_e$ ) highlight the presence of significant feldspar contamination.

**Fig. vi Signal Analysis** Statistically significant increase in natural  $D_e$  value with signal stimulation period is indicative of a partially-bleached signal, provided a significant increase in  $D_e$  results from simulated partial bleaching followed by insignificant adjustment in  $D_e$  for simulated zero and full bleach conditions. Ages from such samples are considered maximum estimates. In the absence of a significant rise in  $D_e$  with stimulation time, simulated partial bleaching and zero/full bleach tests are not assessed.

**Fig. vii U Activity** Statistical concordance (equilibrium) in the activities of the daughter radioisotope  $^{226}\text{Ra}$  with its parent  $^{238}\text{U}$  may signify the temporal stability of  $D_e$  emissions from these chains. Significant differences (disequilibrium;  $>50\%$ ) in activity indicate addition or removal of isotopes creating a time-dependent shift in  $D_e$  values and increased uncertainty in the accuracy of age estimates. A 20% disequilibrium marker is also shown.

**Fig. viii Age Range** The mean age range provides an estimate of sediment burial period based on mean  $D_e$  and  $D_e$  values with associated analytical uncertainties. The probability distribution indicates the inter-aliquot variability in age. The maximum influence of temporal variations in  $D_e$  forced by minima-maxima variation in moisture content and overburden thickness may prove instructive where there is uncertainty in these parameters, however the combined extremes represented should not be construed as preferred age estimates.

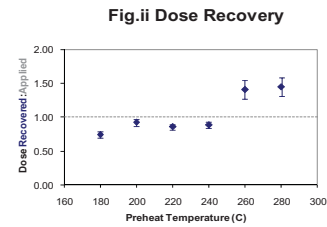


**Fig. iii Inter-aliquot  $D_e$  distribution**

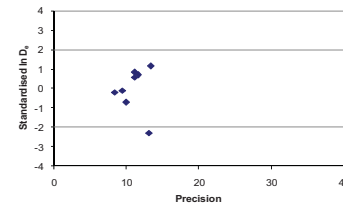


**Fig. iv Low and High Repeat Regenerative-dose Ratio**

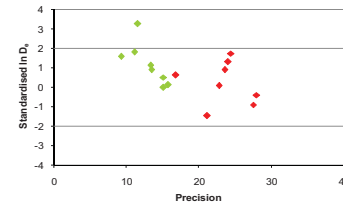


**Fig. v OSL to Post-IR OSL Ratio**

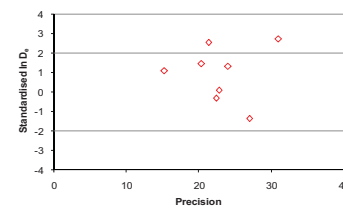


**Fig. vi Signal Analysis**

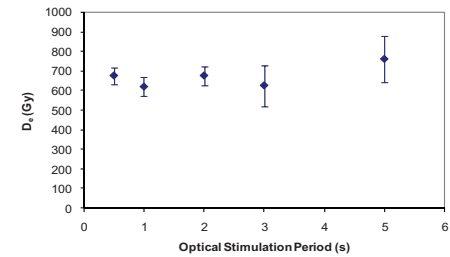


**Fig. vii U Decay Activity**

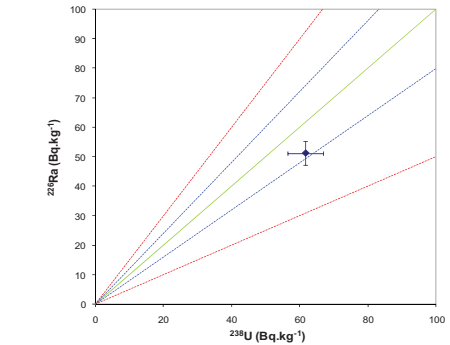
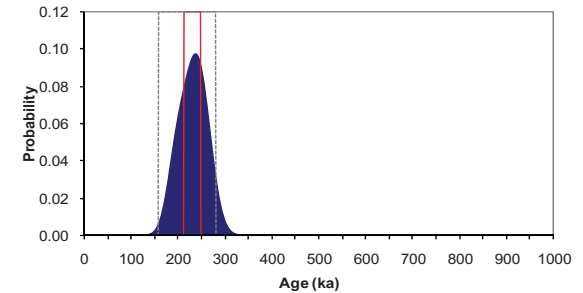


**Fig. viii Age Range**



## Appendix 10 Sample: GL09118

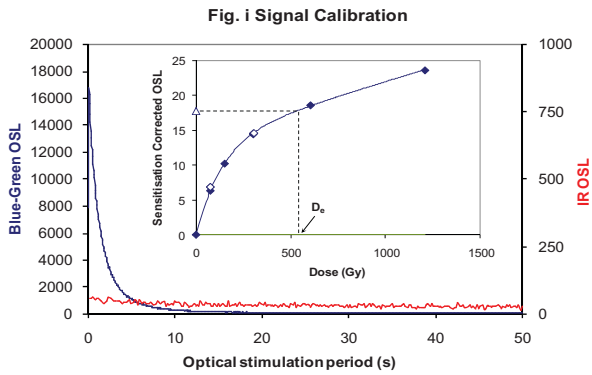


**Fig. i Signal Calibration** Natural blue and laboratory-induced infrared (IR) OSL signals. Detectable IR signal decays are diagnostic of feldspar contamination. Inset, the natural blue OSL signal (open triangle) of each aliquot is calibrated against known laboratory doses to yield equivalent dose ( $D_e$ ) values. Repeats of low and high doses (open diamonds) illustrate the success of sensitivity correction.

**Fig. ii Dose Recovery** The acquisition of  $D_e$  values is necessarily predicated upon thermal treatment of aliquots succeeding environmental and laboratory irradiation. The Dose Recovery test quantifies the combined effects of thermal transfer and sensitisation on the natural signal using a precise lab dose to simulate natural dose. Based on this an appropriate thermal treatment is selected to generate the final  $D_e$  value.

**Fig. iii Inter-aliquot  $D_e$  distribution** Provides a measure of inter-aliquot statistical concordance in  $D_e$  values derived from natural irradiation. Discordant data (those points lying beyond  $\pm 2$  standardised  $\ln D_e$ ) reflects heterogeneous dose absorption and/or inaccuracies in calibration.

**Fig. iv Low and High Repeat Regenerative-dose Ratio** Measures the statistical concordance of signals from repeated low and high regenerative-doses. Discordant data (those points lying beyond  $\pm 2$  standardised  $\ln D_e$ ) indicate inaccurate sensitivity correction.

**Fig. v OSL to Post-IR OSL Ratio** Measures the statistical concordance of OSL and post-IR OSL responses to the same regenerative-dose. Discordant, underestimating data (those points lying below -2 standardised  $\ln D_e$ ) highlight the presence of significant feldspar contamination.

**Fig. vi Signal Analysis** Statistically significant increase in natural  $D_e$  value with signal stimulation period is indicative of a partially-bleached signal, provided a significant increase in  $D_e$  results from simulated partial bleaching followed by insignificant adjustment in  $D_e$  for simulated zero and full bleach conditions. Ages from such samples are considered maximum estimates. In the absence of a significant rise in  $D_e$  with stimulation time, simulated partial bleaching and zero/full bleach tests are not assessed.

**Fig. vii U Activity** Statistical concordance (equilibrium) in the activities of the daughter radioisotope  $^{226}\text{Ra}$  with its parent  $^{238}\text{U}$  may signify the temporal stability of  $D_e$  emissions from these chains. Significant differences (disequilibrium;  $>50\%$ ) in activity indicate addition or removal of isotopes creating a time-dependent shift in  $D_e$  values and increased uncertainty in the accuracy of age estimates. A 20% disequilibrium marker is also shown.

**Fig. viii Age Range** The mean age range provides an estimate of sediment burial period based on mean  $D_e$  and  $D_e$  values with associated analytical uncertainties. The probability distribution indicates the inter-aliquot variability in age. The maximum influence of temporal variations in  $D_e$  forced by minima-maxima variation in moisture content and overburden thickness may prove instructive where there is uncertainty in these parameters, however the combined extremes represented should not be construed as preferred age estimates.

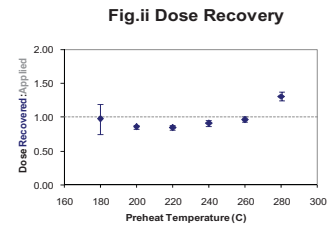


**Fig. iii Inter-aliquot  $D_e$  distribution**

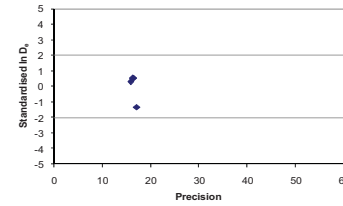


**Fig. iv Low and High Repeat Regenerative-dose Ratio**

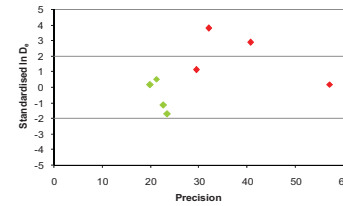


**Fig. v OSL to Post-IR OSL Ratio**

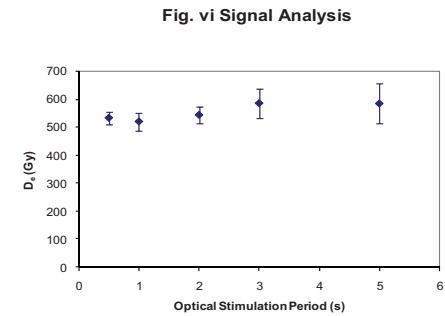
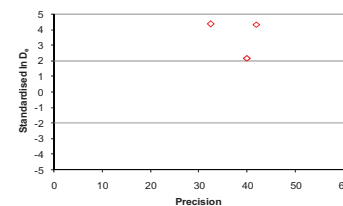


**Fig. vii U Decay Activity**

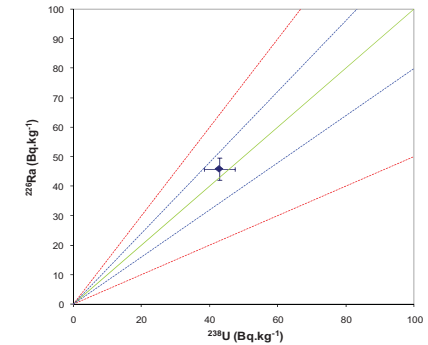
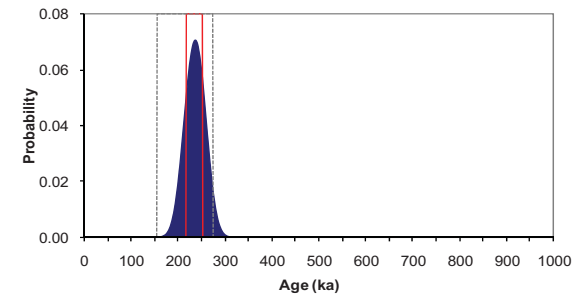


**Fig. viii Age Range**



## Appendix 11 Sample: GL09119

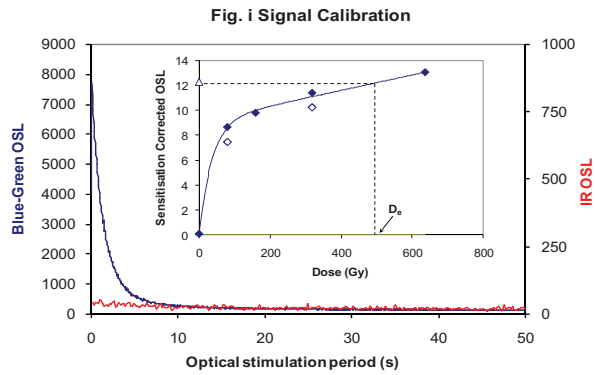


**Fig. i Signal Calibration** Natural blue and laboratory-induced infrared (IR) OSL signals. Detectable IR signal decays are diagnostic of feldspar contamination. Inset, the natural blue OSL signal (open triangle) of each aliquot is calibrated against known laboratory doses to yield equivalent dose ( $D_e$ ) values. Repeats of low and high doses (open diamonds) illustrate the success of sensitivity correction.

**Fig. ii Dose Recovery** The acquisition of  $D_e$  values is necessarily predicated upon thermal treatment of aliquots succeeding environmental and laboratory irradiation. The Dose Recovery test quantifies the combined effects of thermal transfer and sensitisation on the natural signal using a precise lab dose to simulate natural dose. Based on this an appropriate thermal treatment is selected to generate the final  $D_e$  value.

**Fig. iii Inter-aliquot  $D_e$  distribution** Provides a measure of inter-aliquot statistical concordance in  $D_e$  values derived from natural irradiation. Discordant data (those points lying beyond  $\pm 2$  standardised  $\ln D_e$ ) reflects heterogeneous dose absorption and/or inaccuracies in calibration.

**Fig. iv Low and High Repeat Regenerative-dose Ratio** Measures the statistical concordance of signals from repeated low and high regenerative-doses. Discordant data (those points lying beyond  $\pm 2$  standardised  $\ln D_e$ ) indicate inaccurate sensitivity correction.

**Fig. v OSL to Post-IR OSL Ratio** Measures the statistical concordance of OSL and post-IR OSL responses to the same regenerative-dose. Discordant, underestimating data (those points lying below -2 standardised  $\ln D_e$ ) highlight the presence of significant feldspar contamination.

**Fig. vi Signal Analysis** Statistically significant increase in natural  $D_e$  value with signal stimulation period is indicative of a partially-bleached signal, provided a significant increase in  $D_e$  results from simulated partial bleaching followed by insignificant adjustment in  $D_e$  for simulated zero and full bleach conditions. Ages from such samples are considered maximum estimates. In the absence of a significant rise in  $D_e$  with stimulation time, simulated partial bleaching and zero/full bleach tests are not assessed.

**Fig. vii U Activity** Statistical concordance (equilibrium) in the activities of the daughter radioisotope  $^{226}\text{Ra}$  with its parent  $^{238}\text{U}$  may signify the temporal stability of  $D_e$  emissions from these chains. Significant differences (disequilibrium;  $>50\%$ ) in activity indicate addition or removal of isotopes creating a time-dependent shift in  $D_e$  values and increased uncertainty in the accuracy of age estimates. A 20% disequilibrium marker is also shown.

**Fig. viii Age Range** The mean age range provides an estimate of sediment burial period based on mean  $D_e$  and  $D_e$  values with associated analytical uncertainties. The probability distribution indicates the inter-aliquot variability in age. The maximum influence of temporal variations in  $D_e$  forced by minima-maxima variation in moisture content and overburden thickness may prove instructive where there is uncertainty in these parameters, however the combined extremes represented should not be construed as preferred age estimates.

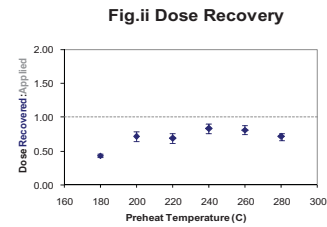


**Fig. ii Dose Recovery**

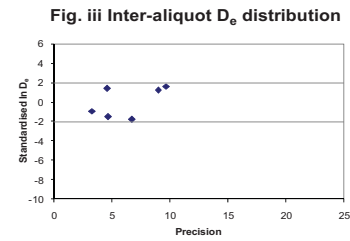


**Fig. iii Inter-aliquot  $D_e$  distribution**

**Fig. iv Low and High Repeat Regenerative-dose Ratio**

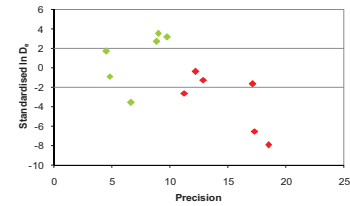


**Fig. v OSL to Post-IR OSL Ratio**

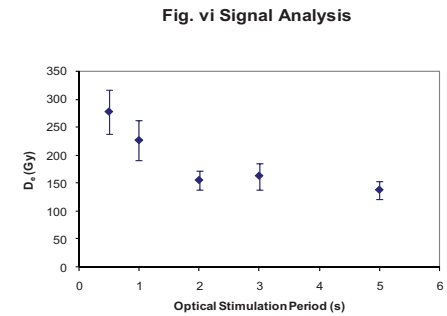
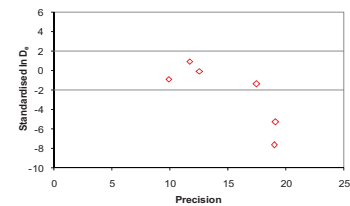


**Fig. vi Signal Analysis**

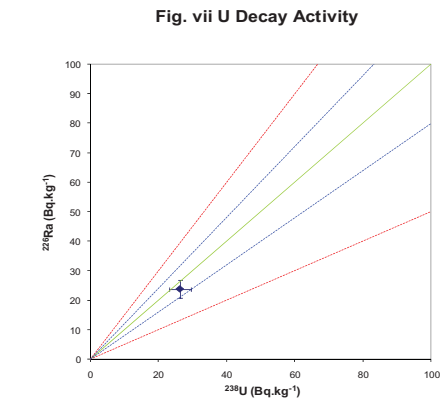


**Fig. vii U Decay Activity**

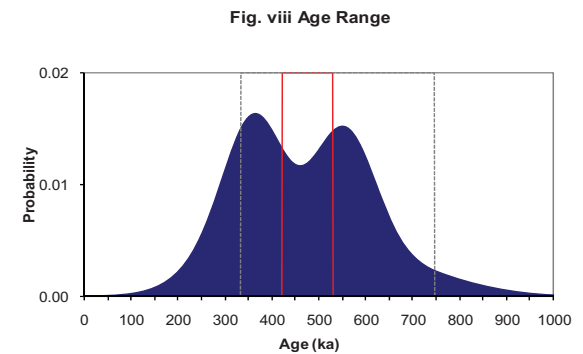


**Fig. viii Age Range**

## Appendix 12 Sample: GL09120

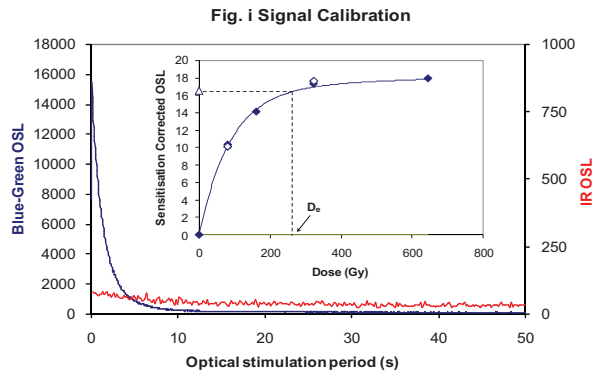


**Fig. i Signal Calibration** Natural blue and laboratory-induced infrared (IR) OSL signals. Detectable IR signal decays are diagnostic of feldspar contamination. Inset, the natural blue OSL signal (open triangle) of each aliquot is calibrated against known laboratory doses to yield equivalent dose ( $D_e$ ) values. Repeats of low and high doses (open diamonds) illustrate the success of sensitivity correction.

**Fig. ii Dose Recovery** The acquisition of  $D_e$  values is necessarily predicated upon thermal treatment of aliquots succeeding environmental and laboratory irradiation. The Dose Recovery test quantifies the combined effects of thermal transfer and sensitisation on the natural signal using a precise lab dose to simulate natural dose. Based on this an appropriate thermal treatment is selected to generate the final  $D_e$  value.

**Fig. iii Inter-aliquot  $D_e$  distribution** Provides a measure of inter-aliquot statistical concordance in  $D_e$  values derived from natural irradiation. Discordant data (those points lying beyond  $\pm 2$  standardised  $\ln D_e$ ) reflects heterogeneous dose absorption and/or inaccuracies in calibration.

**Fig. iv Low and High Repeat Regenerative-dose Ratio** Measures the statistical concordance of signals from repeated low and high regenerative-doses. Discordant data (those points lying beyond  $\pm 2$  standardised  $\ln D_e$ ) indicate inaccurate sensitivity correction.

**Fig. v OSL to Post-IR OSL Ratio** Measures the statistical concordance of OSL and post-IR OSL responses to the same regenerative-dose. Discordant, underestimating data (those points lying below -2 standardised  $\ln D_e$ ) highlight the presence of significant feldspar contamination.

**Fig. vi Signal Analysis** Statistically significant increase in natural  $D_e$  value with signal stimulation period is indicative of a partially-bleached signal, provided a significant increase in  $D_e$  results from simulated partial bleaching followed by insignificant adjustment in  $D_e$  for simulated zero and full bleach conditions. Ages from such samples are considered maximum estimates. In the absence of a significant rise in  $D_e$  with stimulation time, simulated partial bleaching and zero/full bleach tests are not assessed.

**Fig. vii U Activity** Statistical concordance (equilibrium) in the activities of the daughter radioisotope  $^{226}\text{Ra}$  with its parent  $^{238}\text{U}$  may signify the temporal stability of  $D_e$  emissions from these chains. Significant differences (disequilibrium;  $>50\%$ ) in activity indicate addition or removal of isotopes creating a time-dependent shift in  $D_e$  values and increased uncertainty in the accuracy of age estimates. A 20% disequilibrium marker is also shown.

**Fig. viii Age Range** The mean age range provides an estimate of sediment burial period based on mean  $D_e$  and  $D_e$  values with associated analytical uncertainties. The probability distribution indicates the inter-aliquot variability in age. The maximum influence of temporal variations in  $D_e$  forced by minima-maxima variation in moisture content and overburden thickness may prove instructive where there is uncertainty in these parameters, however the combined extremes represented should not be construed as preferred age estimates.

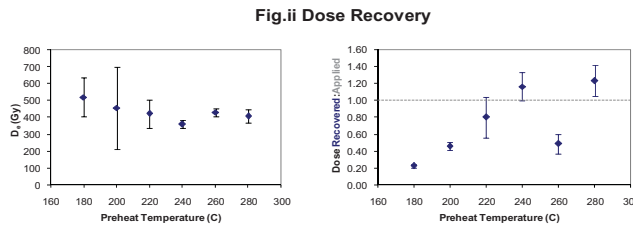


**Fig. ii Dose Recovery**

**Fig. iii Inter-aliquot  $D_e$  distribution**

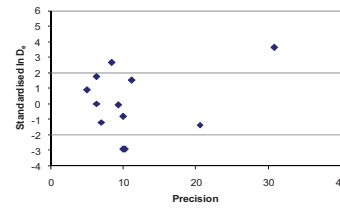


**Fig. iv Low and High Repeat Regenerative-dose Ratio**

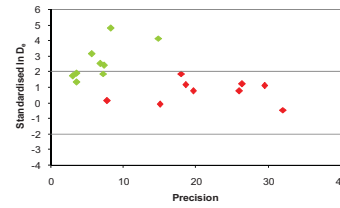


**Fig. v OSL to Post-IR OSL Ratio**

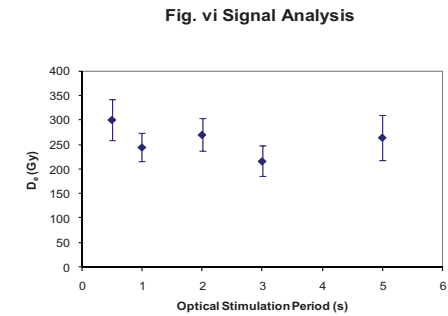
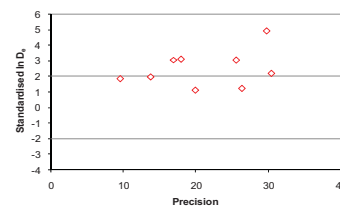


**Fig. vi Signal Analysis**

**Fig. vii U Decay Activity**

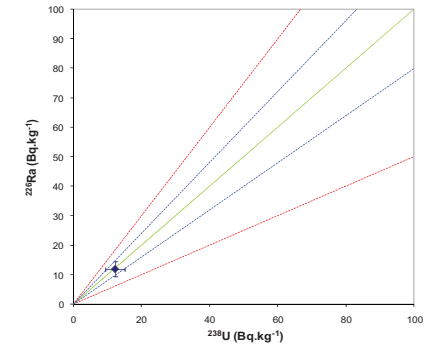
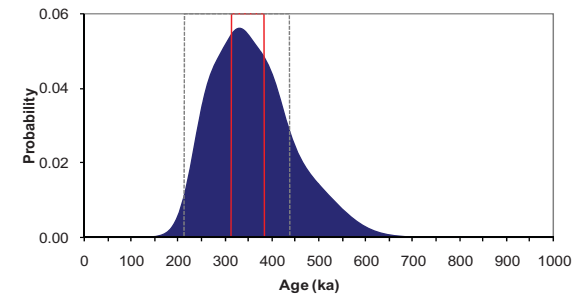


**Fig. viii Age Range**



**Appendix 13  
Sample: GL10013**



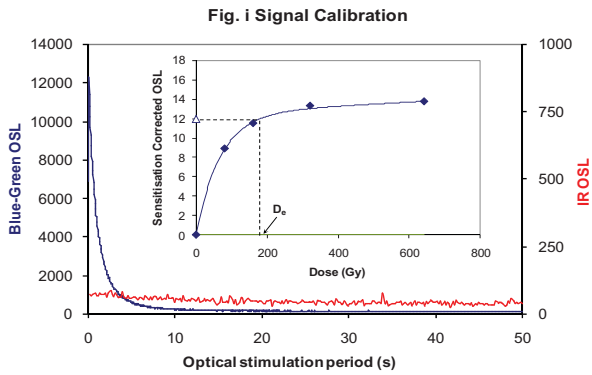


**Fig. i Signal Calibration** Natural blue and laboratory-induced infrared (IR) OSL signals. Detectable IR signal decays are diagnostic of feldspar contamination. Inset, the natural blue OSL signal (open triangle) of each aliquot is calibrated against known laboratory doses to yield equivalent dose ( $D_e$ ) values. Repeats of low and high doses (open diamonds) illustrate the success of sensitivity correction.

**Fig. ii Dose Recovery** The acquisition of  $D_e$  values is necessarily predicated upon thermal treatment of aliquots succeeding environmental and laboratory irradiation. The Dose Recovery test quantifies the combined effects of thermal transfer and sensitisation on the natural signal using a precise lab dose to simulate natural dose. Based on this an appropriate thermal treatment is selected to generate the final  $D_e$  value.

**Fig. iii Inter-aliquot  $D_e$  distribution** Provides a measure of inter-aliquot statistical concordance in  $D_e$  values derived from natural irradiation. Discordant data (those points lying beyond  $\pm 2$  standardised  $\ln D_e$ ) reflects heterogeneous dose absorption and/or inaccuracies in calibration.

**Fig. iv Low and High Repeat Regenerative-dose Ratio** Measures the statistical concordance of signals from repeated low and high regenerative-doses. Discordant data (those points lying beyond  $\pm 2$  standardised  $\ln D_e$ ) indicate inaccurate sensitivity correction.

**Fig. v OSL to Post-IR OSL Ratio** Measures the statistical concordance of OSL and post-IR OSL responses to the same regenerative-dose. Discordant, underestimating data (those points lying below -2 standardised  $\ln D_e$ ) highlight the presence of significant feldspar contamination.

**Fig.vi Signal Analysis** Statistically significant increase in natural  $D_e$  value with signal stimulation period is indicative of a partially-bleached signal, provided a significant increase in  $D_e$  results from simulated partial bleaching followed by insignificant adjustment in  $D_e$  for simulated zero and full bleach conditions. Ages from such samples are considered maximum estimates. In the absence of a significant rise in  $D_e$  with stimulation time, simulated partial bleaching and zero/full bleach tests are not assessed.

**Fig. vii U Activity** Statistical concordance (equilibrium) in the activities of the daughter radioisotope  $^{226}\text{Ra}$  with its parent  $^{238}\text{U}$  may signify the temporal stability of  $D_e$  emissions from these chains. Significant differences (disequilibrium;  $>50\%$ ) in activity indicate addition or removal of isotopes creating a time-dependent shift in  $D_e$  values and increased uncertainty in the accuracy of age estimates. A 20% disequilibrium marker is also shown.

**Fig. viii Age Range** The mean age range provides an estimate of sediment burial period based on mean  $D_e$  and  $D_e$  values with associated analytical uncertainties. The probability distribution indicates the inter-aliquot variability in age. The maximum influence of temporal variations in  $D_e$  forced by minima-maxima variation in moisture content and overburden thickness may prove instructive where there is uncertainty in these parameters, however the combined extremes represented should not be construed as preferred age estimates.

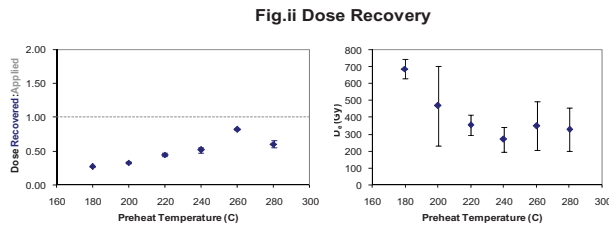


**Fig.ii Dose Recovery**

**Fig. iii Inter-aliquot  $D_e$  distribution**

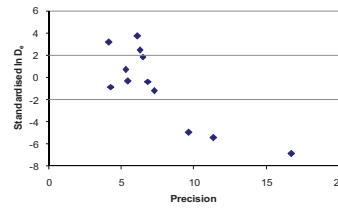


**Fig. iv Low and High Repeat Regenerative-dose Ratio**

Not available

**Fig. v OSL to Post-IR OSL Ratio**

Not available

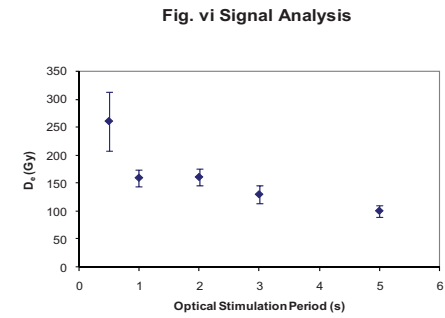


**Fig. vi Signal Analysis**

**Fig. vii U Decay Activity**

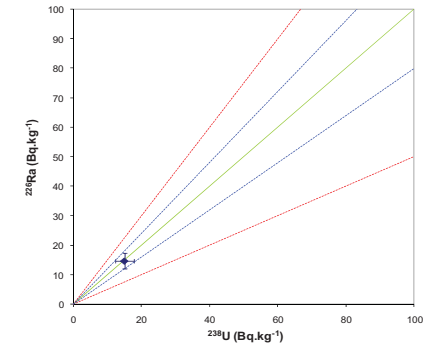
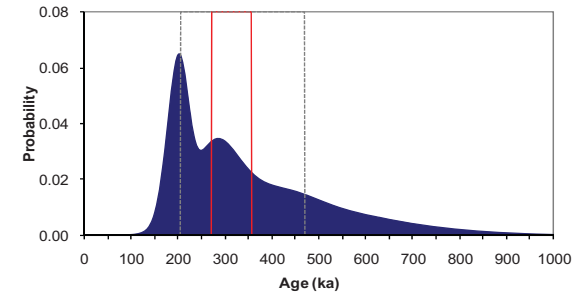


**Fig. viii Age Range**



**Appendix 14  
Sample: GL10014**

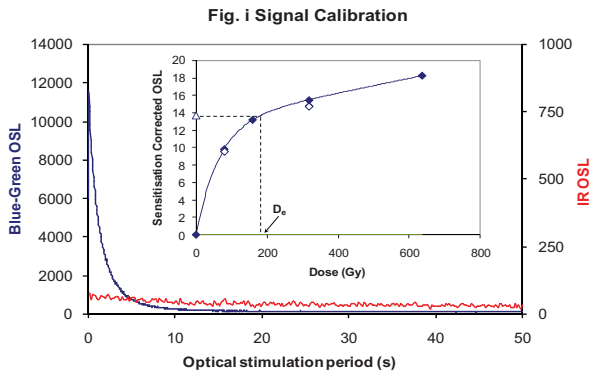


**Fig. i Signal Calibration** Natural blue and laboratory-induced infrared (IR) OSL signals. Detectable IR signal decays are diagnostic of feldspar contamination. Inset, the natural blue OSL signal (open triangle) of each aliquot is calibrated against known laboratory doses to yield equivalent dose ( $D_e$ ) values. Repeats of low and high doses (open diamonds) illustrate the success of sensitivity correction.

**Fig. ii Dose Recovery** The acquisition of  $D_e$  values is necessarily predicated upon thermal treatment of aliquots succeeding environmental and laboratory irradiation. The Dose Recovery test quantifies the combined effects of thermal transfer and significant increase on the natural signal using a precise lab dose to simulate natural dose. Based on this an appropriate thermal treatment is selected to generate the final  $D_e$  value.

**Fig. iii Inter-aliquot  $D_e$  distribution** Provides a measure of inter-aliquot statistical concordance in  $D_e$  values derived from natural irradiation. Discordant data (those points lying beyond  $\pm 2$  standardised  $\ln D_e$ ) reflects heterogeneous dose absorption and/or inaccuracies in calibration.

**Fig. iv Low and High Repeat Regenerative-dose Ratio** Measures the statistical concordance of signals from repeated low and high regenerative-doses. Discordant data (those points lying beyond  $\pm 2$  standardised  $\ln D_e$ ) indicate inaccurate sensitivity correction.

**Fig. v OSL to Post-IR OSL Ratio** Measures the statistical concordance of OSL and post-IR OSL responses to the same regenerative-dose. Discordant, underestimating data (those points lying below -2 standardised  $\ln D_e$ ) highlight the presence of significant feldspar contamination.

**Fig. vi Signal Analysis** Statistically significant increase in natural  $D_e$  value with signal stimulation period is indicative of a partially-bleached signal, provided a significant increase in  $D_e$  results from simulated partial bleaching followed by insignificant adjustment in  $D_e$  for simulated zero and full bleach conditions. Ages from such samples are considered maximum estimates. In the absence of a significant rise in  $D_e$  with stimulation time, simulated partial bleaching and zero/full bleach tests are not assessed.

**Fig. vii U Activity** Statistical concordance (equilibrium) in the activities of the daughter radioisotope  $^{226}\text{Ra}$  with its parent  $^{238}\text{U}$  may signify the temporal stability of  $D_e$  emissions from these chains. Significant differences (disequilibrium;  $>50\%$ ) in activity indicate addition or removal of isotopes creating a time-dependent shift in  $D_e$  values and increased uncertainty in the accuracy of age estimates. A 20% disequilibrium marker is also shown.

**Fig. viii Age Range** The mean age range provides an estimate of sediment burial period based on mean  $D_e$  and  $D_e$  values with associated analytical uncertainties. The probability distribution indicates the inter-aliquot variability in age. The maximum influence of temporal variations in  $D_e$  forced by minima-maxima variation in moisture content and overburden thickness may prove instructive where there is uncertainty in these parameters, however the combined extremes represented should not be construed as preferred age estimates.

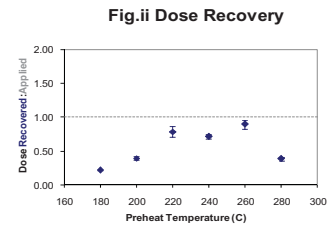


**Fig. ii Dose Recovery**

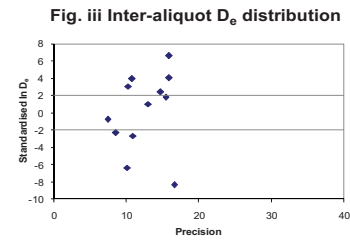


**Fig. iii Inter-aliquot  $D_e$  distribution**

**Fig. iv Low and High Repeat Regenerative-dose Ratio**

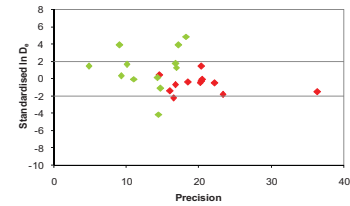


**Fig. v OSL to Post-IR OSL Ratio**

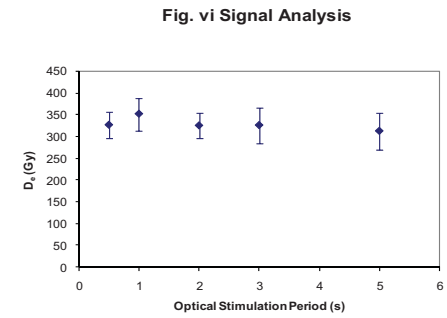
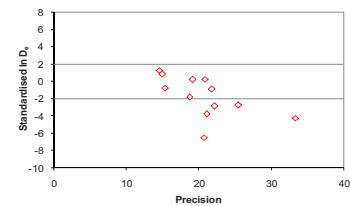


**Fig. vi Signal Analysis**

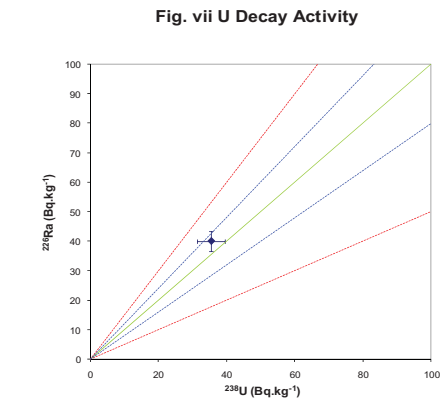


**Fig. vii U Decay Activity**

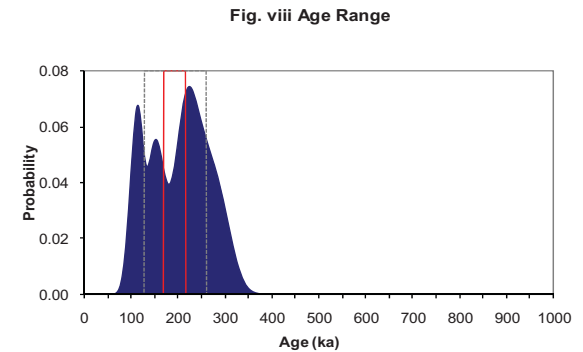


**Fig. viii Age Range**

**Appendix 15  
Sample: GL10015**

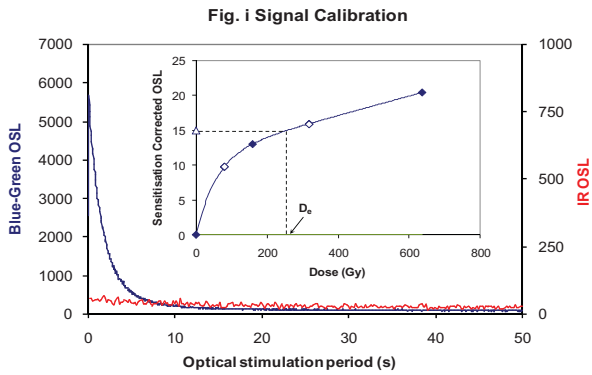


**Fig. i Signal Calibration** Natural blue and laboratory-induced infrared (IR) OSL signals. Detectable IR signal decays are diagnostic of feldspar contamination. Inset, the natural blue OSL signal (open triangle) of each aliquot is calibrated against known laboratory doses to yield equivalent dose ( $D_e$ ) values. Repeats of low and high doses (open diamonds) illustrate the success of sensitivity correction.

**Fig. ii Dose Recovery** The acquisition of  $D_e$  values is necessarily predicated upon thermal treatment of aliquots succeeding environmental and laboratory irradiation. The Dose Recovery test quantifies the combined effects of thermal transfer and sensitisation on the natural signal using a precise lab dose to simulate natural dose. Based on this an appropriate thermal treatment is selected to generate the final  $D_e$  value.

**Fig. iii Inter-aliquot  $D_e$  distribution** Provides a measure of inter-aliquot statistical concordance in  $D_e$  values derived from natural irradiation. Discordant data (those points lying beyond  $\pm 2$  standardised  $\ln D_e$ ) reflects heterogeneous dose absorption and/or inaccuracies in calibration.

**Fig. iv Low and High Repeat Regenerative-dose Ratio** Measures the statistical concordance of signals from repeated low and high regenerative-doses. Discordant data (those points lying beyond  $\pm 2$  standardised  $\ln D_e$ ) indicate inaccurate sensitivity correction.

**Fig. v OSL to Post-IR OSL Ratio** Measures the statistical concordance of OSL and post-IR OSL responses to the same regenerative-dose. Discordant, underestimating data (those points lying below -2 standardised  $\ln D_e$ ) highlight the presence of significant feldspar contamination.

**Fig. vi Signal Analysis** Statistically significant increase in natural  $D_e$  value with signal stimulation period is indicative of a partially-bleached signal, provided a significant increase in  $D_e$  results from simulated partial bleaching followed by insignificant adjustment in  $D_e$  for simulated zero and full bleach conditions. Ages from such samples are considered maximum estimates. In the absence of a significant rise in  $D_e$  with stimulation time, simulated partial bleaching and zero/full bleach tests are not assessed.

**Fig. vii U Activity** Statistical concordance (equilibrium) in the activities of the daughter radioisotope  $^{226}\text{Ra}$  with its parent  $^{238}\text{U}$  may signify the temporal stability of  $D_e$  emissions from these chains. Significant differences (disequilibrium;  $>50\%$ ) in activity indicate addition or removal of isotopes creating a time-dependent shift in  $D_e$  values and increased uncertainty in the accuracy of age estimates. A 20% disequilibrium marker is also shown.

**Fig. viii Age Range** The mean age range provides an estimate of sediment burial period based on mean  $D_e$  and  $D_e$  values with associated analytical uncertainties. The probability distribution indicates the inter-aliquot variability in age. The maximum influence of temporal variations in  $D_e$  forced by minima-maxima variation in moisture content and overburden thickness may prove instructive where there is uncertainty in these parameters, however the combined extremes represented should not be construed as preferred age estimates.

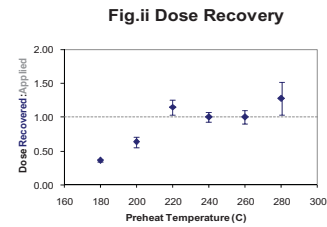


**Fig. iii Inter-aliquot  $D_e$  distribution**

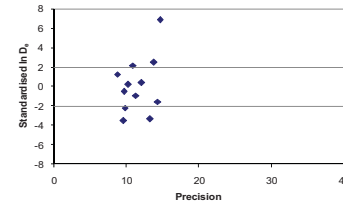


**Fig. iv Low and High Repeat Regenerative-dose Ratio**

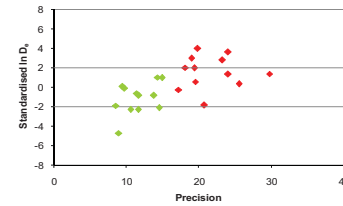


**Fig. v OSL to Post-IR OSL Ratio**

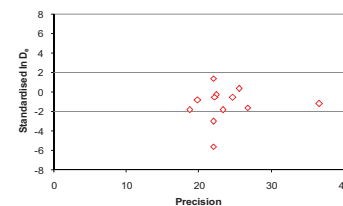


**Fig. vi Signal Analysis**

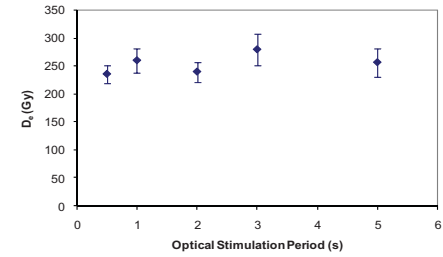


**Fig. vii U Decay Activity**

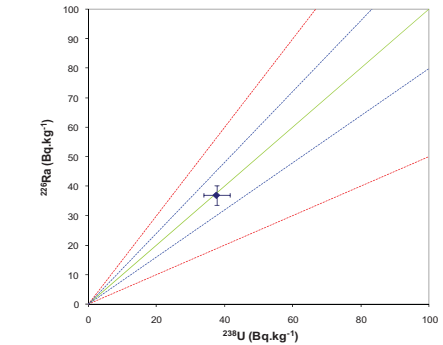
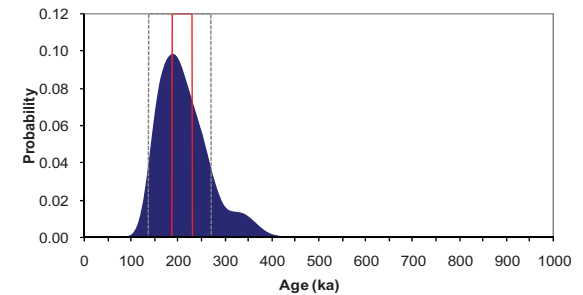


**Fig. viii Age Range**



## Appendix 16 Sample: GL10016

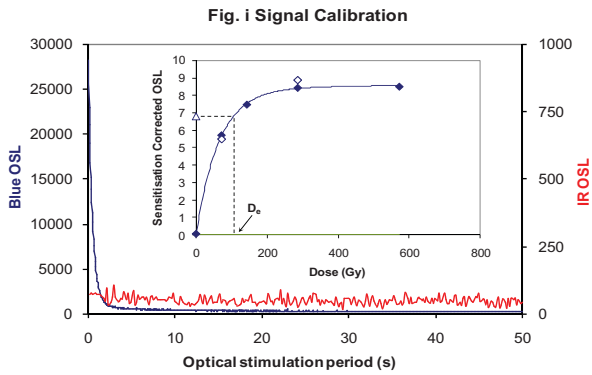


**Fig. i Signal Calibration** Natural blue and laboratory-induced infrared (IR) OSL signals. Detectable IR signal decays are diagnostic of feldspar contamination. Inset, the natural blue OSL signal (open triangle) of each aliquot is calibrated against known laboratory doses to yield equivalent dose ( $D_e$ ) values. Repeats of low and high doses (open diamonds) illustrate the success of sensitivity correction.

**Fig. ii Dose Recovery** The acquisition of  $D_e$  values is necessarily predicated upon thermal treatment of aliquots succeeding environmental and laboratory irradiation. The Dose Recovery test quantifies the combined effects of thermal transfer and sensitisation on the natural signal using a precise lab dose to simulate natural dose. Based on this an appropriate thermal treatment is selected to generate the final  $D_e$  value.

**Fig. iii Inter-aliquot  $D_e$  distribution** Provides a measure of inter-aliquot statistical concordance in  $D_e$  values derived from natural irradiation. Discordant data (those points lying beyond  $\pm 2$  standardised  $\ln D_e$ ) reflects heterogeneous dose absorption and/or inaccuracies in calibration.

**Fig. iv Low and High Repeat Regenerative-dose Ratio** Measures the statistical concordance of signals from repeated low and high regenerative-doses. Discordant data (those points lying beyond  $\pm 2$  standardised  $\ln D_e$ ) indicate inaccurate sensitivity correction.

**Fig. v OSL to Post-IR OSL Ratio** Measures the statistical concordance of OSL and post-IR OSL responses to the same regenerative-dose. Discordant, underestimating data (those points lying below -2 standardised  $\ln D_e$ ) highlight the presence of significant feldspar contamination.

**Fig. vi Signal Analysis** Statistically significant increase in natural  $D_e$  value with signal stimulation period is indicative of a partially-bleached signal, provided a significant increase in  $D_e$  results from simulated partial bleaching followed by insignificant adjustment in  $D_e$  for simulated zero and full bleach conditions. Ages from such samples are considered maximum estimates. In the absence of a significant rise in  $D_e$  with stimulation time, simulated partial bleaching and zero/full bleach tests are not assessed.

**Fig. vii U Activity** Statistical concordance (equilibrium) in the activities of the daughter radioisotope  $^{226}\text{Ra}$  with its parent  $^{238}\text{U}$  may signify the temporal stability of  $D_e$  emissions from these chains. Significant differences (disequilibrium;  $>50\%$ ) in activity indicate addition or removal of isotopes creating a time-dependent shift in  $D_e$  values and increased uncertainty in the accuracy of age estimates. A 20% disequilibrium marker is also shown.

**Fig. viii Age Range** The mean age range provides an estimate of sediment burial period based on mean  $D_e$  and  $D_e$  values with associated analytical uncertainties. The probability distribution indicates the inter-aliquot variability in age. The maximum influence of temporal variations in  $D_e$  forced by minima-maxima variation in moisture content and overburden thickness may prove instructive where there is uncertainty in these parameters, however the combined extremes represented should not be construed as preferred age estimates.

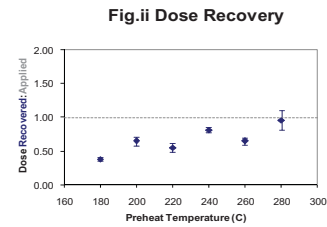


**Fig. iii Inter-aliquot  $D_e$  distribution**

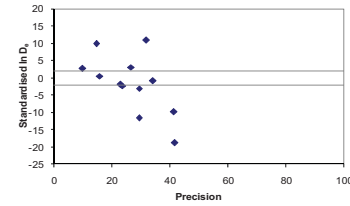


**Fig. iv Low and High Repeat Regenerative-dose Ratio**

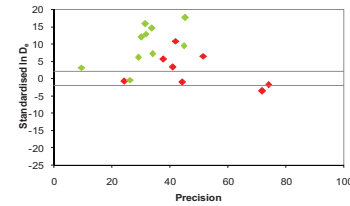


**Fig. v OSL to Post-IR OSL Ratio**

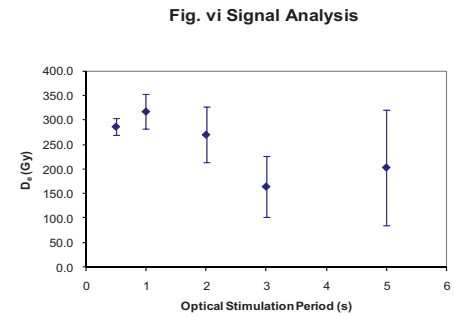
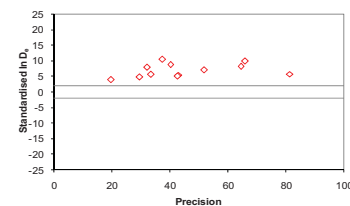


**Fig. vii U Decay Activity**

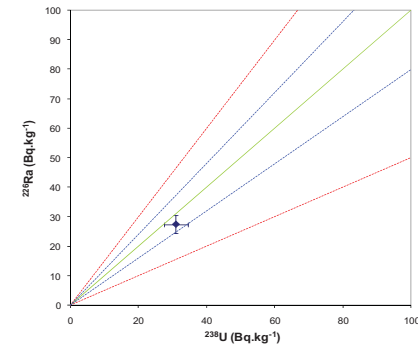
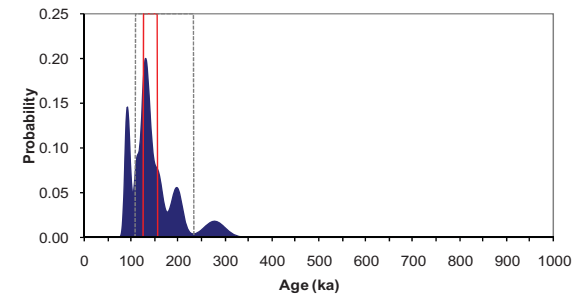


**Fig. viii Age Range**



**Appendix 17a  
Sample: GL1001  
Laboratory A**

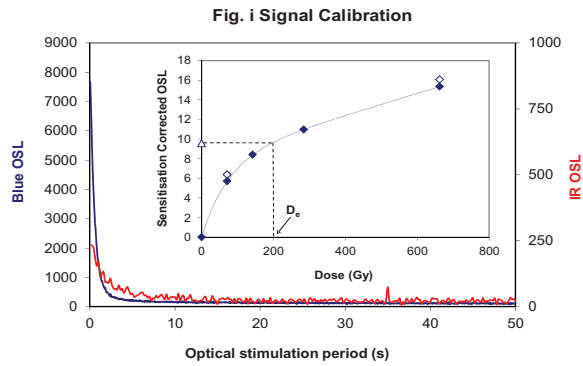


**Fig. i Signal Calibration** Natural blue and laboratory-induced infrared (IR) OSL signals. Detectable IR signal decays are diagnostic of feldspar contamination. Inset, the natural blue OSL signal (open triangle) of each aliquot is calibrated against known laboratory doses to yield equivalent dose ( $D_e$ ) values. Repeats of low and high doses (open diamonds) illustrate the success of sensitivity correction.

**Fig. ii Dose Recovery** The acquisition of  $D_e$  values is necessarily predicated upon thermal treatment of aliquots succeeding environmental and laboratory irradiation. The Dose Recovery test quantifies the combined effects of thermal transfer and sensitisation on the natural signal using a precise lab dose to simulate natural dose. Based on this an appropriate thermal treatment is selected to generate the final  $D_e$  value.

**Fig. iii Inter-aliquot  $D_e$  distribution** Provides a measure of inter-aliquot statistical concordance in  $D_e$  values derived from natural irradiation. Discordant data (those points lying beyond  $\pm 2$  standardised  $\ln D_e$ ) reflects heterogeneous dose absorption and/or inaccuracies in calibration.

**Fig. iv Low and High Repeat Regenerative-dose Ratio** Measures the statistical concordance of signals from repeated low and high regenerative-doses. Discordant data (those points lying beyond  $\pm 2$  standardised  $\ln D_e$ ) indicate inaccurate sensitivity correction.

**Fig. v OSL to Post-IR OSL Ratio** Measures the statistical concordance of OSL and post-IR OSL responses to the same regenerative-dose. Discordant, underestimating data (those points lying below -2 standardised  $\ln D_e$ ) highlight the presence of significant feldspar contamination.

**Fig. vi Signal Analysis** Statistically significant increase in natural  $D_e$  value with signal stimulation period is indicative of a partially-bleached signal, provided a significant increase in  $D_e$  results from simulated partial bleaching followed by insignificant adjustment in  $D_e$  for simulated zero and full bleach conditions. Ages from such samples are considered maximum estimates. In the absence of a significant rise in  $D_e$  with stimulation time, simulated partial bleaching and zero/full bleach tests are not assessed.

**Fig. vii U Activity** Statistical concordance (equilibrium) in the activities of the daughter radioisotope  $^{226}\text{Ra}$  with its parent  $^{238}\text{U}$  may signify the temporal stability of  $D_e$  emissions from these chains. Significant differences (disequilibrium;  $>50\%$ ) in activity indicate addition or removal of isotopes creating a time-dependent shift in  $D_e$  values and increased uncertainty in the accuracy of age estimates. A 20% disequilibrium marker is also shown.

**Fig. viii Age Range** The mean age range provides an estimate of sediment burial period based on mean  $D_e$  and  $D_e$  values with associated analytical uncertainties. The probability distribution indicates the inter-aliquot variability in age. The maximum influence of temporal variations in  $D_e$  forced by minima-maxima variation in moisture content and overburden thickness may prove instructive where there is uncertainty in these parameters, however the combined extremes represented should not be construed as preferred age estimates.

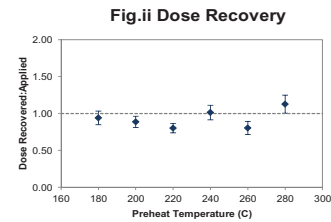


**Fig. ii Dose Recovery**

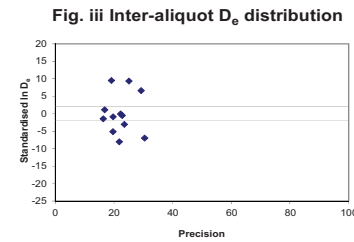


**Fig. iii Inter-aliquot  $D_e$  distribution**

**Fig. iv Low and High Repeat Regenerative-dose Ratio**

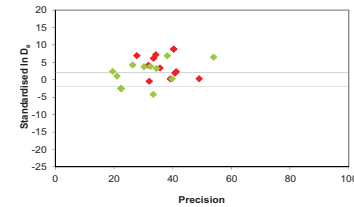


**Fig. v OSL to Post-IR OSL Ratio**

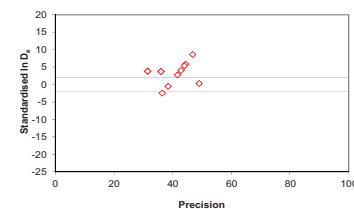


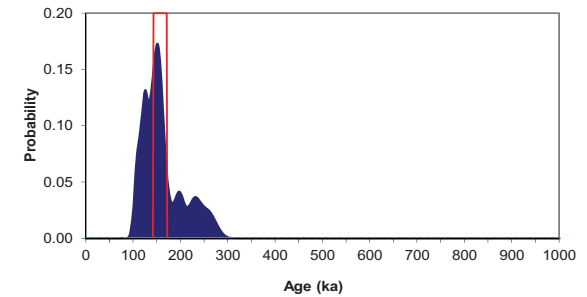
**Fig. vi Signal Analysis**

*Not applicable to inter-laboratory comparison*

**Fig. vii U Decay Activity**

*Not applicable to inter-laboratory comparison*

**Fig. viii Age Range**



**Appendix 17b  
Sample: GL1001  
Laboratory B**

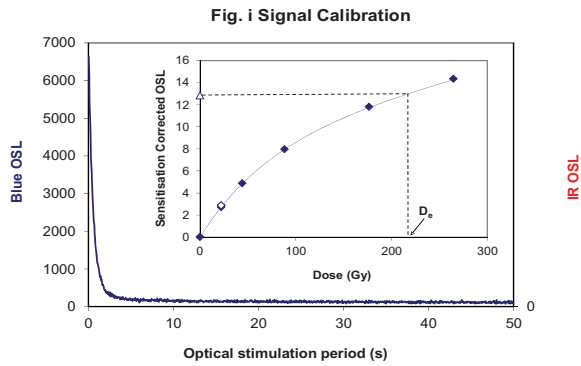


**Fig. i Signal Calibration** Natural blue and laboratory-induced infrared (IR) OSL signals. Detectable IR signal decays are diagnostic of feldspar contamination. Inset, the natural blue OSL signal (open triangle) of each aliquot is calibrated against known laboratory doses to yield equivalent dose ( $D_e$ ) values. Repeats of low and high doses (open diamonds) illustrate the success of sensitivity correction.

**Fig. ii Dose Recovery** The acquisition of  $D_e$  values is necessarily predicated upon thermal treatment of aliquots succeeding environmental and laboratory irradiation. The Dose Recovery test quantifies the combined effects of thermal transfer and sensitisation on the natural signal using a precise lab dose to simulate natural dose. Based on this an appropriate thermal treatment is selected to generate the final  $D_e$  value.

**Fig. iii Inter-aliquot  $D_e$  distribution** Provides a measure of inter-aliquot statistical concordance in  $D_e$  values derived from natural irradiation. Discordant data (those points lying beyond  $\pm 2$  standardised  $\ln D_e$ ) reflects heterogeneous dose absorption and/or inaccuracies in calibration.

**Fig. iv Low and High Repeat Regenerative-dose Ratio** Measures the statistical concordance of signals from repeated low and high regenerative-doses. Discordant data (those points lying beyond  $\pm 2$  standardised  $\ln D_e$ ) indicate inaccurate sensitivity correction.

**Fig. v OSL to Post-IR OSL Ratio** Measures the statistical concordance of OSL and post-IR OSL responses to the same regenerative-dose. Discordant, underestimating data (those points lying below -2 standardised  $\ln D_e$ ) highlight the presence of significant feldspar contamination.

**Fig. vi Signal Analysis** Statistically significant increase in natural  $D_e$  value with signal stimulation period is indicative of a partially-bleached signal, provided a significant increase in  $D_e$  results from simulated partial bleaching followed by insignificant adjustment in  $D_e$  for simulated zero and full bleach conditions. Ages from such samples are considered maximum estimates. In the absence of a significant rise in  $D_e$  with stimulation time, simulated partial bleaching and zero/full bleach tests are not assessed.

**Fig. vii U Activity** Statistical concordance (equilibrium) in the activities of the daughter radioisotope  $^{226}\text{Ra}$  with its parent  $^{238}\text{U}$  may signify the temporal stability of  $D_e$  emissions from these chains. Significant differences (disequilibrium;  $>50\%$ ) in activity indicate addition or removal of isotopes creating a time-dependent shift in  $D_e$  values and increased uncertainty in the accuracy of age estimates. A 20% disequilibrium marker is also shown.

**Fig. viii Age Range** The mean age range provides an estimate of sediment burial period based on mean  $D_e$  and  $D_e$  values with associated analytical uncertainties. The probability distribution indicates the inter-aliquot variability in age. The maximum influence of temporal variations in  $D_e$  forced by minima-maxima variation in moisture content and overburden thickness may prove instructive where there is uncertainty in these parameters, however the combined extremes represented should not be construed as preferred age estimates.

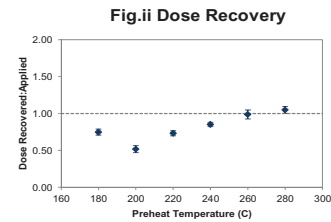


**Fig. ii Dose Recovery**

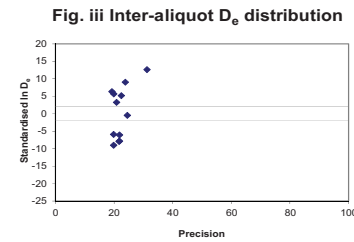


**Fig. iii Inter-aliquot  $D_e$  distribution**

**Fig. iv Low and High Repeat Regenerative-dose Ratio**

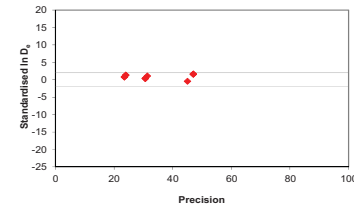


**Fig. v OSL to Post-IR OSL Ratio**

Not measured

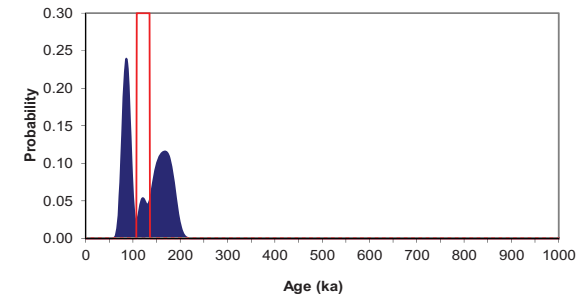
**Fig. vi Signal Analysis**

Not applicable to inter-laboratory comparison

**Fig. vii U Decay Activity**

Not applicable to inter-laboratory comparison

**Fig. viii Age Range**



Appendix 17c  
Sample: GL1001  
Laboratory C

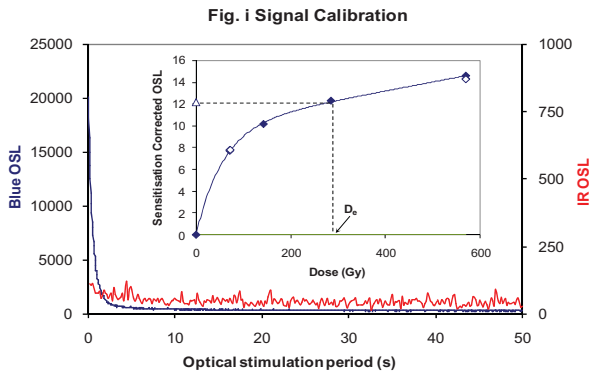


**Fig. i Signal Calibration** Natural blue and laboratory-induced infrared (IR) OSL signals. Detectable IR signal decays are diagnostic of feldspar contamination. Inset, the natural blue OSL signal (open triangle) of each aliquot is calibrated against known laboratory doses to yield equivalent dose ( $D_e$ ) values. Repeats of low and high doses (open diamonds) illustrate the success of sensitivity correction.

**Fig. ii Dose Recovery** The acquisition of  $D_e$  values is necessarily predicated upon thermal treatment of aliquots succeeding environmental and laboratory irradiation. The Dose Recovery test quantifies the combined effects of thermal transfer and sensitisation on the natural signal using a precise lab dose to simulate natural dose. Based on this an appropriate thermal treatment is selected to generate the final  $D_e$  value.

**Fig. iii Inter-aliquot  $D_e$  distribution** Provides a measure of inter-aliquot statistical concordance in  $D_e$  values derived from natural irradiation. Discordant data (those points lying beyond  $\pm 2$  standardised  $\ln D_e$ ) reflects heterogeneous dose absorption and/or inaccuracies in calibration.

**Fig. iv Low and High Repeat Regenerative-dose Ratio** Measures the statistical concordance of signals from repeated low and high regenerative-doses. Discordant data (those points lying beyond  $\pm 2$  standardised  $\ln D_e$ ) indicate inaccurate sensitivity correction.

**Fig. v OSL to Post-IR OSL Ratio** Measures the statistical concordance of OSL and post-IR OSL responses to the same regenerative-dose. Discordant, underestimating data (those points lying below -2 standardised  $\ln D_e$ ) highlight the presence of significant feldspar contamination.

**Fig. vi Signal Analysis** Statistically significant increase in natural  $D_e$  value with signal stimulation period is indicative of a partially-bleached signal, provided a significant increase in  $D_e$  results from simulated partial bleaching followed by insignificant adjustment in  $D_e$  for simulated zero and full bleach conditions. Ages from such samples are considered maximum estimates. In the absence of a significant rise in  $D_e$  with stimulation time, simulated partial bleaching and zero/full bleach tests are not assessed.

**Fig. vii U Activity** Statistical concordance (equilibrium) in the activities of the daughter radioisotope  $^{226}\text{Ra}$  with its parent  $^{238}\text{U}$  may signify the temporal stability of  $D_e$  emissions from these chains. Significant differences (disequilibrium;  $>50\%$ ) in activity indicate addition or removal of isotopes creating a time-dependent shift in  $D_e$  values and increased uncertainty in the accuracy of age estimates. A 20% disequilibrium marker is also shown.

**Fig. viii Age Range** The mean age range provides an estimate of sediment burial period based on mean  $D_e$  and  $D_e$  values with associated analytical uncertainties. The probability distribution indicates the inter-aliquot variability in age. The maximum influence of temporal variations in  $D_e$  forced by minima-maxima variation in moisture content and overburden thickness may prove instructive where there is uncertainty in these parameters, however the combined extremes represented should not be construed as preferred age estimates.

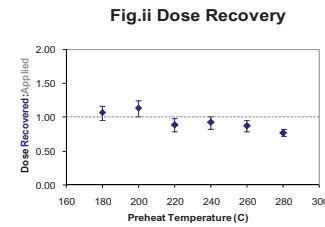


**Fig. iii Inter-aliquot  $D_e$  distribution**

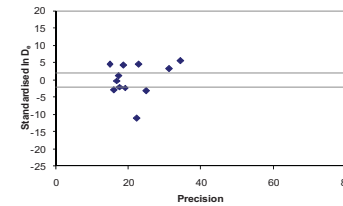


**Fig. iv Low and High Repeat Regenerative-dose Ratio**

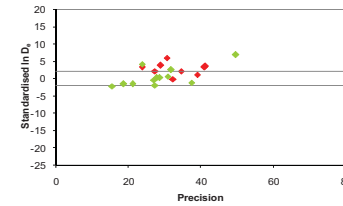


**Fig. v OSL to Post-IR OSL Ratio**

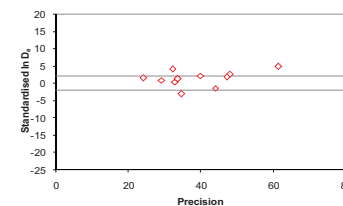


**Fig. vi Signal Analysis**

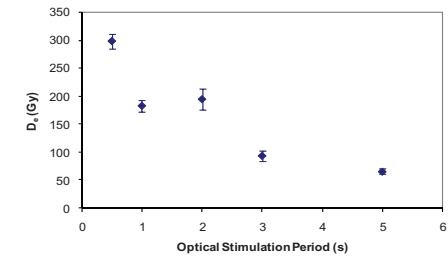


**Fig. vii U Decay Activity**

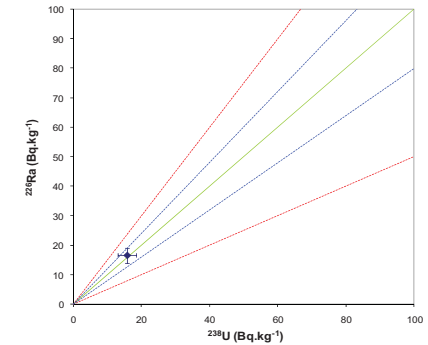
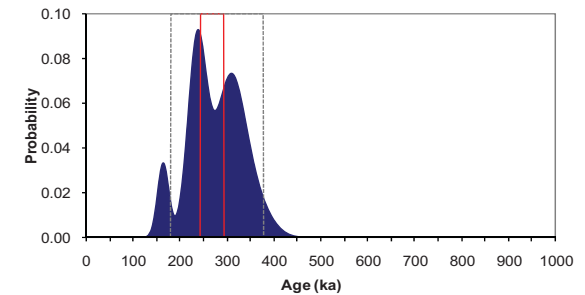


**Fig. viii Age Range**



**Appendix 18a  
Sample: GL1002  
Laboratory A**

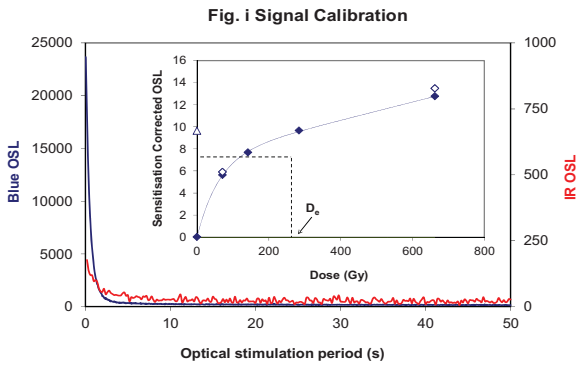


**Fig. i Signal Calibration** Natural blue and laboratory-induced infrared (IR) OSL signals. Detectable IR signal decays are diagnostic of feldspar contamination. Inset, the natural blue OSL signal (open triangle) of each aliquot is calibrated against known laboratory doses to yield equivalent dose ( $D_e$ ) values. Repeats of low and high doses (open diamonds) illustrate the success of sensitivity correction.

**Fig. ii Dose Recovery** The acquisition of  $D_e$  values is necessarily predicated upon thermal treatment of aliquots succeeding environmental and laboratory irradiation. The Dose Recovery test quantifies the combined effects of thermal transfer and sensitisation on the natural signal using a precise lab dose to simulate natural dose. Based on this an appropriate thermal treatment is selected to generate the final  $D_e$  value.

**Fig. iii Inter-aliquot  $D_e$  distribution** Provides a measure of inter-aliquot statistical concordance in  $D_e$  values derived from natural irradiation. Discordant data (those points lying beyond  $\pm 2$  standardised  $\ln D_e$ ) reflects heterogeneous dose absorption and/or inaccuracies in calibration.

**Fig. iv Low and High Repeat Regenerative-dose Ratio** Measures the statistical concordance of signals from repeated low and high regenerative-doses. Discordant data (those points lying beyond  $\pm 2$  standardised  $\ln D_e$ ) indicate inaccurate sensitivity correction.

**Fig. v OSL to Post-IR OSL Ratio** Measures the statistical concordance of OSL and post-IR OSL responses to the same regenerative-dose. Discordant, underestimating data (those points lying below -2 standardised  $\ln D_e$ ) highlight the presence of significant feldspar contamination.

**Fig. vi Signal Analysis** Statistically significant increase in natural  $D_e$  value with signal stimulation period is indicative of a partially-bleached signal, provided a significant increase in  $D_e$  results from simulated partial bleaching followed by insignificant adjustment in  $D_e$  for simulated zero and full bleach conditions. Ages from such samples are considered maximum estimates. In the absence of a significant rise in  $D_e$  with stimulation time, simulated partial bleaching and zero/full bleach tests are not assessed.

**Fig. vii U Activity** Statistical concordance (equilibrium) in the activities of the daughter radioisotope  $^{226}\text{Ra}$  with its parent  $^{238}\text{U}$  may signify the temporal stability of  $D_e$  emissions from these chains. Significant differences (disequilibrium;  $>50\%$ ) in activity indicate addition or removal of isotopes creating a time-dependent shift in  $D_e$  values and increased uncertainty in the accuracy of age estimates. A 20% disequilibrium marker is also shown.

**Fig. viii Age Range** The mean age range provides an estimate of sediment burial period based on mean  $D_e$  and  $D_e$  values with associated analytical uncertainties. The probability distribution indicates the inter-aliquot variability in age. The maximum influence of temporal variations in  $D_e$  forced by minima-maxima variation in moisture content and overburden thickness may prove instructive where there is uncertainty in these parameters, however the combined extremes represented should not be construed as preferred age estimates.

**Fig.ii Dose Recovery**

Extrapolated from GL10001  
Laboratory B data

**Fig. iii Inter-aliquot  $D_e$  distribution**

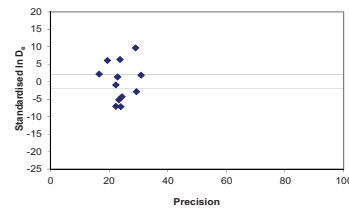


**Fig. iv Low and High Repeat Regenerative-dose Ratio**

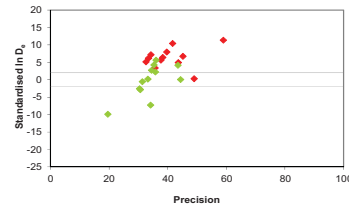


**Fig. v OSL to Post-IR OSL Ratio**

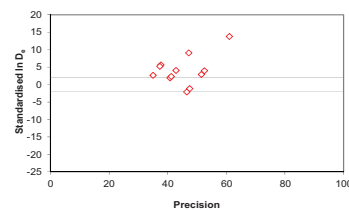


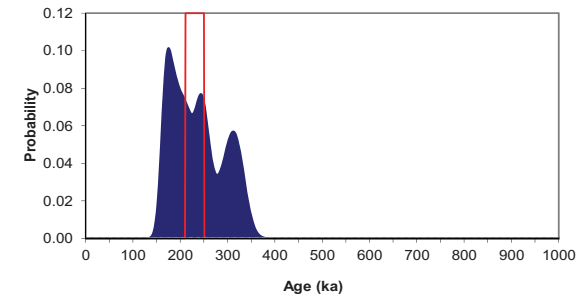
**Fig. vi Signal Analysis**

Not applicable to inter-laboratory comparison

**Fig. vii U Decay Activity**

Not applicable to inter-laboratory comparison

**Fig. viii Age Range**



Appendix 18b  
Sample: GL10002  
Laboratory B



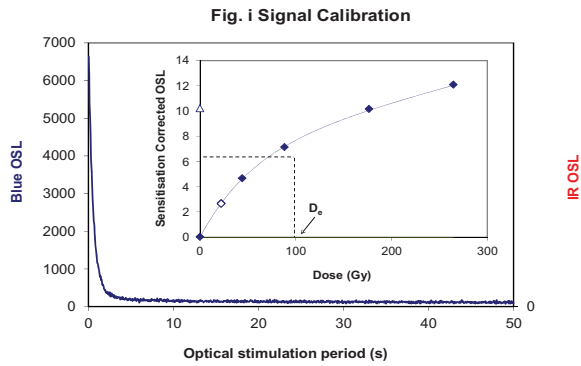


**Fig. i Signal Calibration** Natural blue and laboratory-induced infrared (IR) OSL signals. Detectable IR signal decays are diagnostic of feldspar contamination. Inset, the natural blue OSL signal (open triangle) of each aliquot is calibrated against known laboratory doses to yield equivalent dose ( $D_e$ ) values. Repeats of low and high doses (open diamonds) illustrate the success of sensitivity correction.

**Fig. ii Dose Recovery** The acquisition of  $D_e$  values is necessarily predicated upon thermal treatment of aliquots succeeding environmental and laboratory irradiation. The Dose Recovery test quantifies the combined effects of thermal transfer and sensitisation on the natural signal using a precise lab dose to simulate natural dose. Based on this an appropriate thermal treatment is selected to generate the final  $D_e$  value.

**Fig. iii Inter-aliquot  $D_e$  distribution** Provides a measure of inter-aliquot statistical concordance in  $D_e$  values derived from natural irradiation. Discordant data (those points lying beyond  $\pm 2$  standardised  $\ln D_e$ ) reflects heterogeneous dose absorption and/or inaccuracies in calibration.

**Fig. iv Low and High Repeat Regenerative-dose Ratio** Measures the statistical concordance of signals from repeated low and high regenerative-doses. Discordant data (those points lying beyond  $\pm 2$  standardised  $\ln D_e$ ) indicate inaccurate sensitivity correction.

**Fig. v OSL to Post-IR OSL Ratio** Measures the statistical concordance of OSL and post-IR OSL responses to the same regenerative-dose. Discordant, underestimating data (those points lying below -2 standardised  $\ln D_e$ ) highlight the presence of significant feldspar contamination.

**Fig. vi Signal Analysis** Statistically significant increase in natural  $D_e$  value with signal stimulation period is indicative of a partially-bleached signal, provided a significant increase in  $D_e$  results from simulated partial bleaching followed by insignificant adjustment in  $D_e$  for simulated zero and full bleach conditions. Ages from such samples are considered maximum estimates. In the absence of a significant rise in  $D_e$  with stimulation time, simulated partial bleaching and zero/full bleach tests are not assessed.

**Fig. vii U Activity** Statistical concordance (equilibrium) in the activities of the daughter radioisotope  $^{226}\text{Ra}$  with its parent  $^{238}\text{U}$  may signify the temporal stability of  $D_e$  emissions from these chains. Significant differences (disequilibrium;  $>50\%$ ) in activity indicate addition or removal of isotopes creating a time-dependent shift in  $D_e$  values and increased uncertainty in the accuracy of age estimates. A 20% disequilibrium marker is also shown.

**Fig. viii Age Range** The mean age range provides an estimate of sediment burial period based on mean  $D_e$  and  $D_e$  values with associated analytical uncertainties. The probability distribution indicates the inter-aliquot variability in age. The maximum influence of temporal variations in  $D_e$  forced by minima-maxima variation in moisture content and overburden thickness may prove instructive where there is uncertainty in these parameters, however the combined extremes represented should not be construed as preferred age estimates.

**Fig. ii Dose Recovery**

Extrapolated from GL10001 Laboratory C data

**Fig. iii Inter-aliquot  $D_e$  distribution**

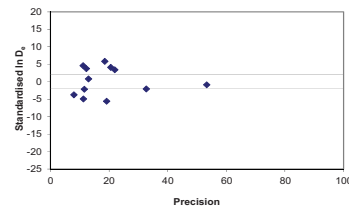


**Fig. iv Low and High Repeat Regenerative-dose Ratio**

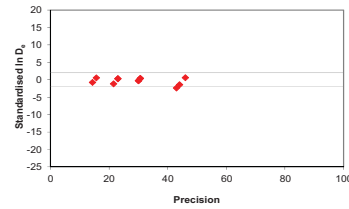


**Fig. v OSL to Post-IR OSL Ratio**

Not measured

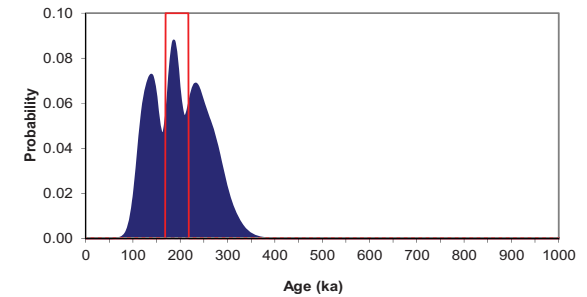
**Fig. vi Signal Analysis**

Not applicable to inter-laboratory comparison

**Fig. vii U Decay Activity**

Not applicable to inter-laboratory comparison

**Fig. viii Age Range**



Appendix 18c  
Sample: GL10002  
Laboratory C

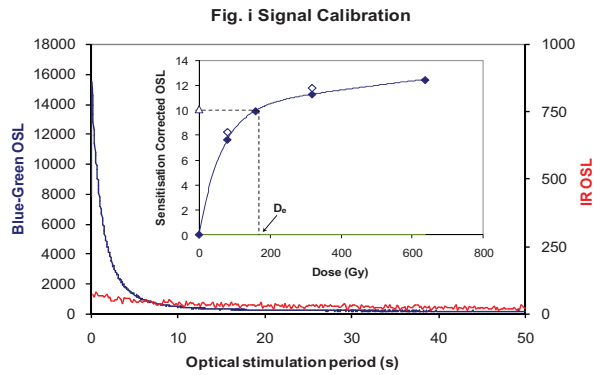


**Fig. i Signal Calibration** Natural blue and laboratory-induced infrared (IR) OSL signals. Detectable IR signal decays are diagnostic of feldspar contamination. Inset, the natural blue OSL signal (open triangle) of each aliquot is calibrated against known laboratory doses to yield equivalent dose ( $D_e$ ) values. Repeats of low and high doses (open diamonds) illustrate the success of sensitivity correction.

**Fig. ii Dose Recovery** The acquisition of  $D_e$  values is necessarily predicated upon thermal treatment of aliquots succeeding environmental and laboratory irradiation. The Dose Recovery test quantifies the combined effects of thermal transfer and sensitisation on the natural signal using a precise lab dose to simulate natural dose. Based on this an appropriate thermal treatment is selected to generate the final  $D_e$  value.

**Fig. iii Inter-aliquot  $D_e$  distribution** Provides a measure of inter-aliquot statistical concordance in  $D_e$  values derived from natural irradiation. Discordant data (those points lying beyond  $\pm 2$  standardised  $\ln D_e$ ) reflects heterogeneous dose absorption and/or inaccuracies in calibration.

**Fig. iv Low and High Repeat Regenerative-dose Ratio** Measures the statistical concordance of signals from repeated low and high regenerative-doses. Discordant data (those points lying beyond  $\pm 2$  standardised  $\ln D_e$ ) indicate inaccurate sensitivity correction.

**Fig. v OSL to Post-IR OSL Ratio** Measures the statistical concordance of OSL and post-IR OSL responses to the same regenerative-dose. Discordant, underestimating data (those points lying below -2 standardised  $\ln D_e$ ) highlight the presence of significant feldspar contamination.

**Fig. vi Signal Analysis** Statistically significant increase in natural  $D_e$  value with signal stimulation period is indicative of a partially-bleached signal, provided a significant increase in  $D_e$  results from simulated partial bleaching followed by insignificant adjustment in  $D_e$  for simulated zero and full bleach conditions. Ages from such samples are considered maximum estimates. In the absence of a significant rise in  $D_e$  with stimulation time, simulated partial bleaching and zero/full bleach tests are not assessed.

**Fig. vii U Activity** Statistical concordance (equilibrium) in the activities of the daughter radioisotope  $^{226}\text{Ra}$  with its parent  $^{238}\text{U}$  may signify the temporal stability of  $D_e$  emissions from these chains. Significant differences (disequilibrium;  $>50\%$ ) in activity indicate addition or removal of isotopes creating a time-dependent shift in  $D_e$  values and increased uncertainty in the accuracy of age estimates. A 20% disequilibrium marker is also shown.

**Fig. viii Age Range** The mean age range provides an estimate of sediment burial period based on mean  $D_e$  and  $D_e$  values with associated analytical uncertainties. The probability distribution indicates the inter-aliquot variability in age. The maximum influence of temporal variations in  $D_e$  forced by minima-maxima variation in moisture content and overburden thickness may prove instructive where there is uncertainty in these parameters, however the combined extremes represented should not be construed as preferred age estimates.

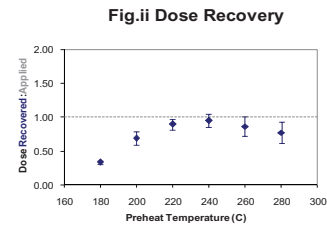


**Fig. ii Dose Recovery**

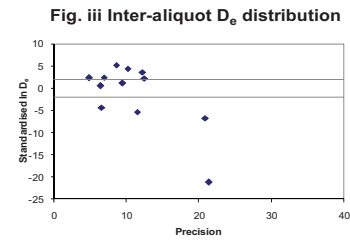


**Fig. iii Inter-aliquot  $D_e$  distribution**

**Fig. iv Low and High Repeat Regenerative-dose Ratio**

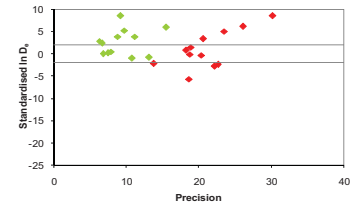


**Fig. v OSL to Post-IR OSL Ratio**

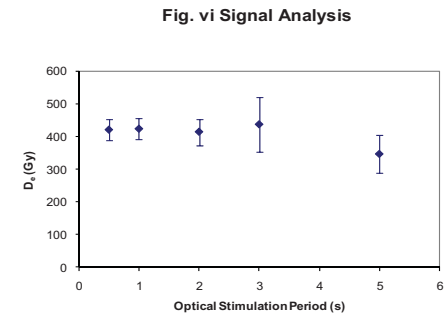
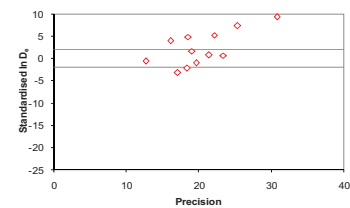


**Fig. vi Signal Analysis**

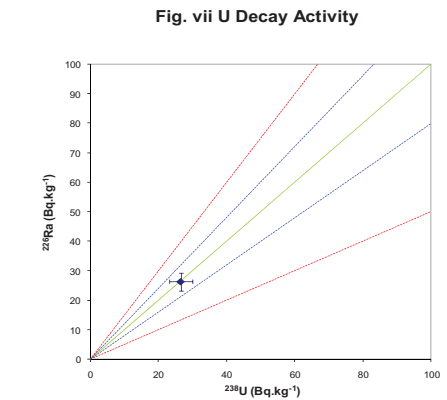


**Fig. vii U Decay Activity**

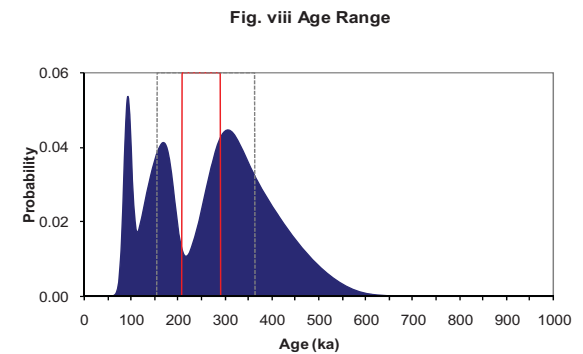


**Fig. viii Age Range**

## Appendix 19 Sample: GL10019

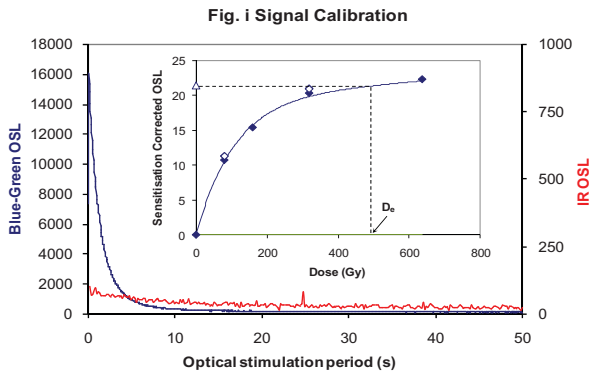


**Fig. i Signal Calibration** Natural blue and laboratory-induced infrared (IR) OSL signals. Detectable IR signal decays are diagnostic of feldspar contamination. Inset, the natural blue OSL signal (open triangle) of each aliquot is calibrated against known laboratory doses to yield equivalent dose ( $D_e$ ) values. Repeats of low and high doses (open diamonds) illustrate the success of sensitivity correction.

**Fig. ii Dose Recovery** The acquisition of  $D_e$  values is necessarily predicated upon thermal treatment of aliquots succeeding environmental and laboratory irradiation. The Dose Recovery test quantifies the combined effects of thermal transfer and sensitisation on the natural signal using a precise lab dose to simulate natural dose. Based on this an appropriate thermal treatment is selected to generate the final  $D_e$  value.

**Fig. iii Inter-aliquot  $D_e$  distribution** Provides a measure of inter-aliquot statistical concordance in  $D_e$  values derived from natural irradiation. Discordant data (those points lying beyond  $\pm 2$  standardised  $\ln D_e$ ) reflects heterogeneous dose absorption and/or inaccuracies in calibration.

**Fig. iv Low and High Repeat Regenerative-dose Ratio** Measures the statistical concordance of signals from repeated low and high regenerative-doses. Discordant data (those points lying beyond  $\pm 2$  standardised  $\ln D_e$ ) indicate inaccurate sensitivity correction.

**Fig. v OSL to Post-IR OSL Ratio** Measures the statistical concordance of OSL and post-IR OSL responses to the same regenerative-dose. Discordant, underestimating data (those points lying below -2 standardised  $\ln D_e$ ) highlight the presence of significant feldspar contamination.

**Fig. vi Signal Analysis** Statistically significant increase in natural  $D_e$  value with signal stimulation period is indicative of a partially-bleached signal, provided a significant increase in  $D_e$  results from simulated partial bleaching followed by insignificant adjustment in  $D_e$  for simulated zero and full bleach conditions. Ages from such samples are considered maximum estimates. In the absence of a significant rise in  $D_e$  with stimulation time, simulated partial bleaching and zero/full bleach tests are not assessed.

**Fig. vii U Activity** Statistical concordance (equilibrium) in the activities of the daughter radioisotope  $^{226}\text{Ra}$  with its parent  $^{238}\text{U}$  may signify the temporal stability of  $D_e$  emissions from these chains. Significant differences (disequilibrium;  $>50\%$ ) in activity indicate addition or removal of isotopes creating a time-dependent shift in  $D_e$  values and increased uncertainty in the accuracy of age estimates. A 20% disequilibrium marker is also shown.

**Fig. viii Age Range** The mean age range provides an estimate of sediment burial period based on mean  $D_e$  and  $D_e$  values with associated analytical uncertainties. The probability distribution indicates the inter-aliquot variability in age. The maximum influence of temporal variations in  $D_e$  forced by minima-maxima variation in moisture content and overburden thickness may prove instructive where there is uncertainty in these parameters, however the combined extremes represented should not be construed as preferred age estimates.

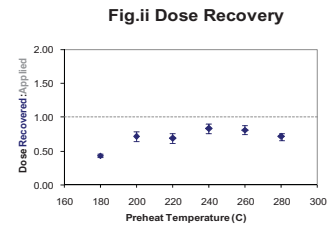


**Fig. iii Inter-aliquot  $D_e$  distribution**

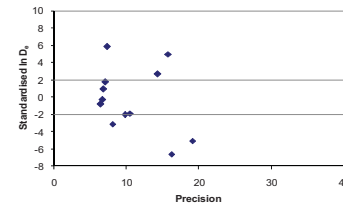


**Fig. iv Low and High Repeat Regenerative-dose Ratio**

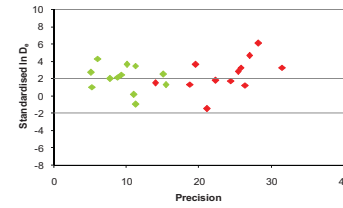


**Fig. v OSL to Post-IR OSL Ratio**

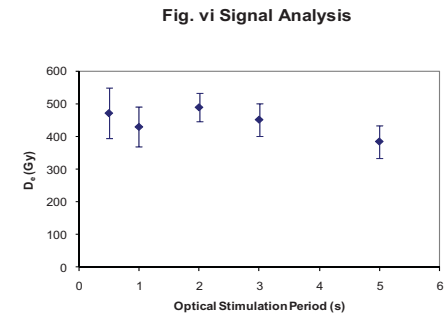
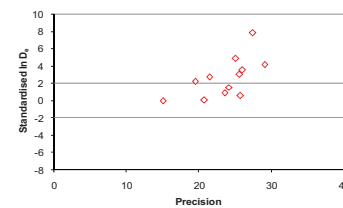


**Fig. vii U Decay Activity**

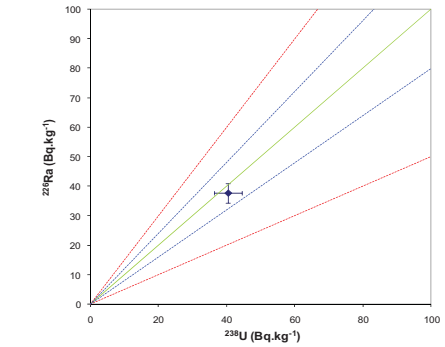
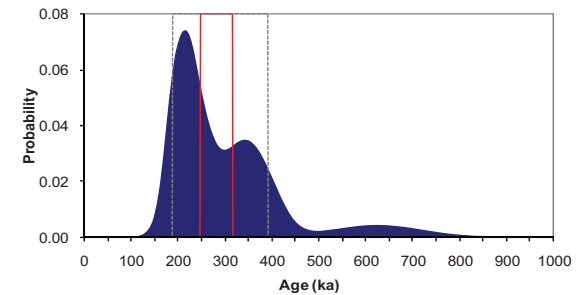


**Fig. viii Age Range**



## Appendix 20 Sample: GL10020

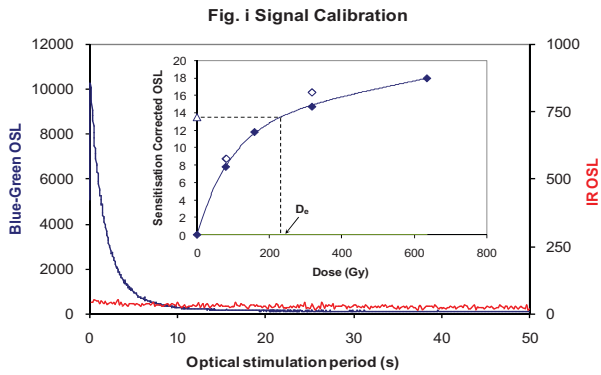


**Fig. i Signal Calibration** Natural blue and laboratory-induced infrared (IR) OSL signals. Detectable IR signal decays are diagnostic of feldspar contamination. Inset, the natural blue OSL signal (open triangle) of each aliquot is calibrated against known laboratory doses to yield equivalent dose ( $D_e$ ) values. Repeats of low and high doses (open diamonds) illustrate the success of sensitivity correction.

**Fig. ii Dose Recovery** The acquisition of  $D_e$  values is necessarily predicated upon thermal treatment of aliquots succeeding environmental and laboratory irradiation. The Dose Recovery test quantifies the combined effects of thermal transfer and sensitisation on the natural signal using a precise lab dose to simulate natural dose. Based on this an appropriate thermal treatment is selected to generate the final  $D_e$  value.

**Fig. iii Inter-aliquot  $D_e$  distribution** Provides a measure of inter-aliquot statistical concordance in  $D_e$  values derived from natural irradiation. Discordant data (those points lying beyond  $\pm 2$  standardised  $\ln D_e$ ) reflects heterogeneous dose absorption and/or inaccuracies in calibration.

**Fig. iv Low and High Repeat Regenerative-dose Ratio** Measures the statistical concordance of signals from repeated low and high regenerative-doses. Discordant data (those points lying beyond  $\pm 2$  standardised  $\ln D_e$ ) indicate inaccurate sensitivity correction.

**Fig. v OSL to Post-IR OSL Ratio** Measures the statistical concordance of OSL and post-IR OSL responses to the same regenerative-dose. Discordant, underestimating data (those points lying below -2 standardised  $\ln D_e$ ) highlight the presence of significant feldspar contamination.

**Fig. vi Signal Analysis** Statistically significant increase in natural  $D_e$  value with signal stimulation period is indicative of a partially-bleached signal, provided a significant increase in  $D_e$  results from simulated partial bleaching followed by insignificant adjustment in  $D_e$  for simulated zero and full bleach conditions. Ages from such samples are considered maximum estimates. In the absence of a significant rise in  $D_e$  with stimulation time, simulated partial bleaching and zero/full bleach tests are not assessed.

**Fig. vii U Activity** Statistical concordance (equilibrium) in the activities of the daughter radioisotope  $^{226}\text{Ra}$  with its parent  $^{238}\text{U}$  may signify the temporal stability of  $D_e$  emissions from these chains. Significant differences (disequilibrium;  $>50\%$ ) in activity indicate addition or removal of isotopes creating a time-dependent shift in  $D_e$  values and increased uncertainty in the accuracy of age estimates. A 20% disequilibrium marker is also shown.

**Fig. viii Age Range** The mean age range provides an estimate of sediment burial period based on mean  $D_e$  and  $D_e$  values with associated analytical uncertainties. The probability distribution indicates the inter-aliquot variability in age. The maximum influence of temporal variations in  $D_e$  forced by minima-maxima variation in moisture content and overburden thickness may prove instructive where there is uncertainty in these parameters, however the combined extremes represented should not be construed as preferred age estimates.

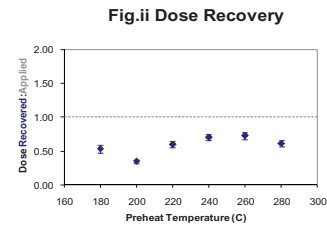


**Fig. ii Dose Recovery**

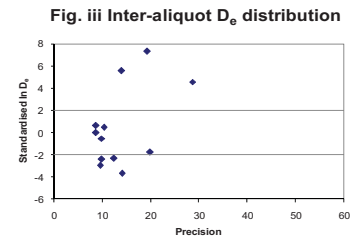


**Fig. iii Inter-aliquot  $D_e$  distribution**

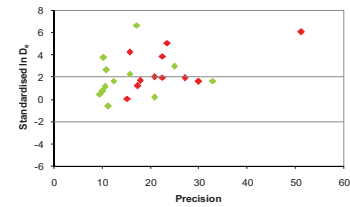


**Fig. iv Low and High Repeat Regenerative-dose Ratio**

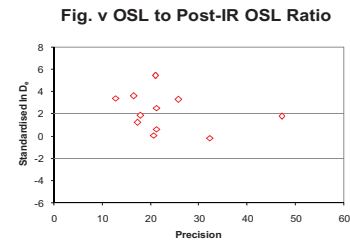


**Fig. v OSL to Post-IR OSL Ratio**

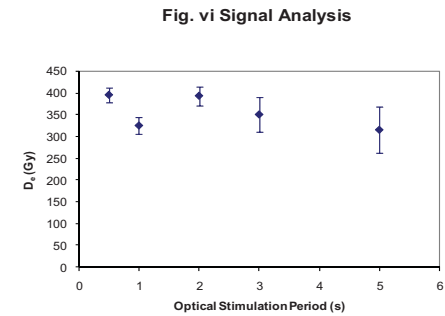


**Fig. vi Signal Analysis**

**Fig. vii U Decay Activity**

*$^{226}\text{Ra}$  peak beneath detection limits*

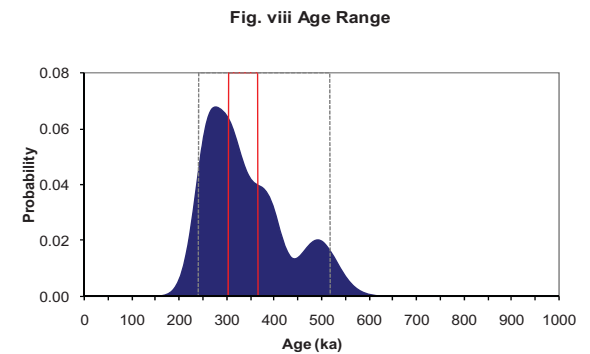


**Fig. viii Age Range**

## Appendix 21 Sample: GL10055

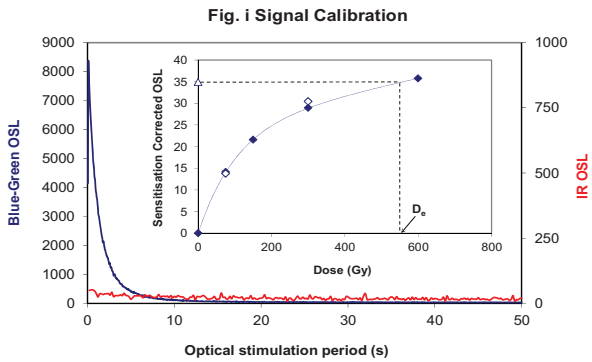


**Fig. i Signal Calibration** Natural blue and laboratory-induced infrared (IR) OSL signals. Detectable IR signal decays are diagnostic of feldspar contamination. Inset, the natural blue OSL signal (open triangle) of each aliquot is calibrated against known laboratory doses to yield equivalent dose ( $D_e$ ) values. Repeats of low and high doses (open diamonds) illustrate the success of sensitivity correction.

**Fig. ii Dose Recovery** The acquisition of  $D_e$  values is necessarily predicated upon thermal treatment of aliquots succeeding environmental and laboratory irradiation. The Dose Recovery test quantifies the combined effects of thermal transfer and sensitisation on the natural signal using a precise lab dose to simulate natural dose. Based on this an appropriate thermal treatment is selected to generate the final  $D_e$  value.

**Fig. iii Inter-aliquot  $D_e$  distribution** Provides a measure of inter-aliquot statistical concordance in  $D_e$  values derived from natural irradiation. Discordant data (those points lying beyond  $\pm 2$  standardised  $\ln D_e$ ) reflects heterogeneous dose absorption and/or inaccuracies in calibration.

**Fig. iv Low and High Repeat Regenerative-dose Ratio** Measures the statistical concordance of signals from repeated low and high regenerative-doses. Discordant data (those points lying beyond  $\pm 2$  standardised  $\ln D_e$ ) indicate inaccurate sensitivity correction.

**Fig. v OSL to Post-IR OSL Ratio** Measures the statistical concordance of OSL and post-IR OSL responses to the same regenerative-dose. Discordant, underestimating data (those points lying below -2 standardised  $\ln D_e$ ) highlight the presence of significant feldspar contamination.

**Fig. vi Signal Analysis** Statistically significant increase in natural  $D_e$  value with signal stimulation period is indicative of a partially-bleached signal, provided a significant increase in  $D_e$  results from simulated partial bleaching followed by insignificant adjustment in  $D_e$  for simulated zero and full bleach conditions. Ages from such samples are considered maximum estimates. In the absence of a significant rise in  $D_e$  with stimulation time, simulated partial bleaching and zero/full bleach tests are not assessed.

**Fig. vii U Activity** Statistical concordance (equilibrium) in the activities of the daughter radioisotope  $^{226}\text{Ra}$  with its parent  $^{238}\text{U}$  may signify the temporal stability of  $D_e$  emissions from these chains. Significant differences (disequilibrium;  $>50\%$ ) in activity indicate addition or removal of isotopes creating a time-dependent shift in  $D_e$  values and increased uncertainty in the accuracy of age estimates. A 20% disequilibrium marker is also shown.

**Fig. viii Age Range** The mean age range provides an estimate of sediment burial period based on mean  $D_e$  and  $D_e$  values with associated analytical uncertainties. The probability distribution indicates the inter-aliquot variability in age. The maximum influence of temporal variations in  $D_e$  forced by minima-maxima variation in moisture content and overburden thickness may prove instructive where there is uncertainty in these parameters, however the combined extremes represented should not be construed as preferred age estimates.

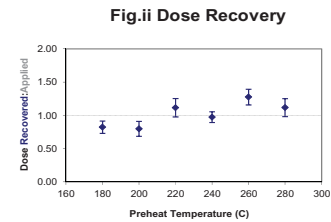


**Fig. ii Dose Recovery**

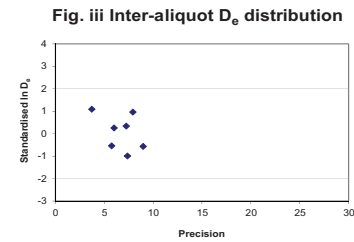


**Fig. iii Inter-aliquot  $D_e$  distribution**

**Fig. iv Low and High Repeat Regenerative-dose Ratio**

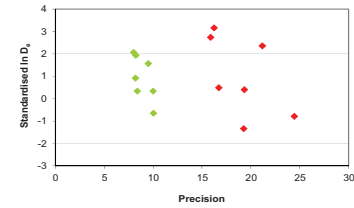


**Fig. v OSL to Post-IR OSL Ratio**

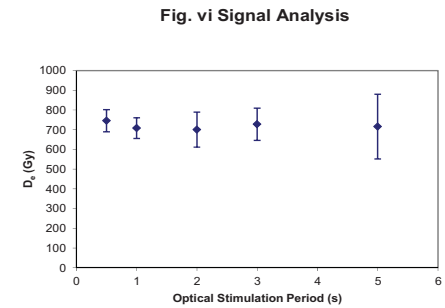
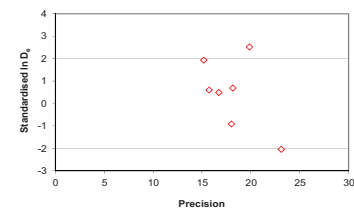


**Fig. vi Signal Analysis**

**Fig. vii U Decay Activity**

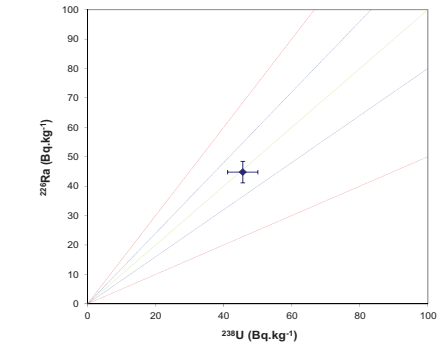
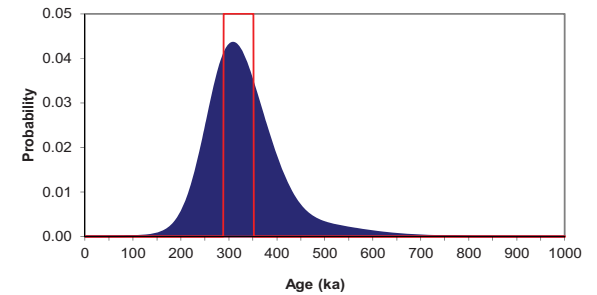


**Fig. viii Age Range**



## Appendix 22 Sample: GL10063

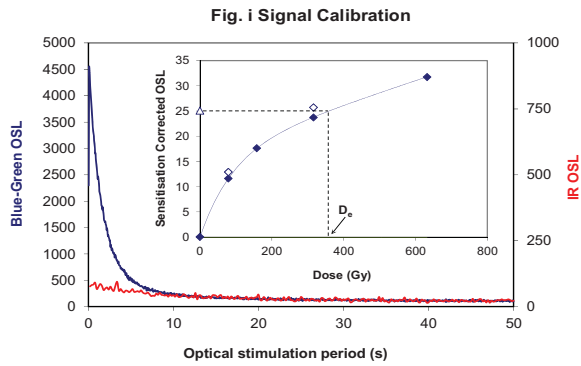


**Fig. i Signal Calibration** Natural blue and laboratory-induced infrared (IR) OSL signals. Detectable IR signal decays are diagnostic of feldspar contamination. Inset, the natural blue OSL signal (open triangle) of each aliquot is calibrated against known laboratory doses to yield equivalent dose ( $D_e$ ) values. Repeats of low and high doses (open diamonds) illustrate the success of sensitivity correction.

**Fig. ii Dose Recovery** The acquisition of  $D_e$  values is necessarily predicated upon thermal treatment of aliquots succeeding environmental and laboratory irradiation. The Dose Recovery test quantifies the combined effects of thermal transfer and sensitisation on the natural signal using a precise lab dose to simulate natural dose. Based on this an appropriate thermal treatment is selected to generate the final  $D_e$  value.

**Fig. iii Inter-aliquot  $D_e$  distribution** Provides a measure of inter-aliquot statistical concordance in  $D_e$  values derived from natural irradiation. Discordant data (those points lying beyond  $\pm 2$  standardised  $\ln D_e$ ) reflects heterogeneous dose absorption and/or inaccuracies in calibration.

**Fig. iv Low and High Repeat Regenerative-dose Ratio** Measures the statistical concordance of signals from repeated low and high regenerative-doses. Discordant data (those points lying beyond  $\pm 2$  standardised  $\ln D_e$ ) indicate inaccurate sensitivity correction.

**Fig. v OSL to Post-IR OSL Ratio** Measures the statistical concordance of OSL and post-IR OSL responses to the same regenerative-dose. Discordant, underestimating data (those points lying below -2 standardised  $\ln D_e$ ) highlight the presence of significant feldspar contamination.

**Fig. vi Signal Analysis** Statistically significant increase in natural  $D_e$  value with signal stimulation period is indicative of a partially-bleached signal, provided a significant increase in  $D_e$  results from simulated partial bleaching followed by insignificant adjustment in  $D_e$  for simulated zero and full bleach conditions. Ages from such samples are considered maximum estimates. In the absence of a significant rise in  $D_e$  with stimulation time, simulated partial bleaching and zero/full bleach tests are not assessed.

**Fig. vii U Activity** Statistical concordance (equilibrium) in the activities of the daughter radioisotope  $^{226}\text{Ra}$  with its parent  $^{238}\text{U}$  may signify the temporal stability of  $D_e$  emissions from these chains. Significant differences (disequilibrium;  $>50\%$ ) in activity indicate addition or removal of isotopes creating a time-dependent shift in  $D_e$  values and increased uncertainty in the accuracy of age estimates. A 20% disequilibrium marker is also shown.

**Fig. viii Age Range** The mean age range provides an estimate of sediment burial period based on mean  $D_e$  and  $D_e$  values with associated analytical uncertainties. The probability distribution indicates the inter-aliquot variability in age. The maximum influence of temporal variations in  $D_e$  forced by minima-maxima variation in moisture content and overburden thickness may prove instructive where there is uncertainty in these parameters, however the combined extremes represented should not be construed as preferred age estimates.

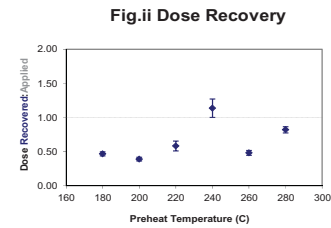


**Fig. iii Inter-aliquot  $D_e$  distribution**

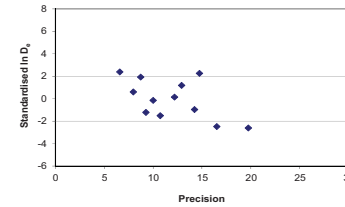


**Fig. iv Low and High Repeat Regenerative-dose Ratio**

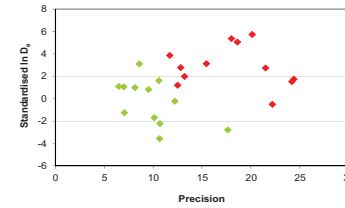


**Fig. v OSL to Post-IR OSL Ratio**

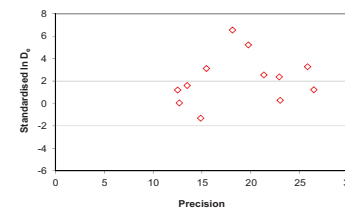


**Fig. vi Signal Analysis**

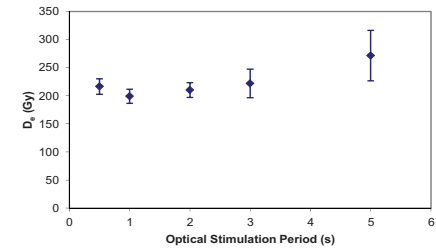


**Fig. vii U Decay Activity**

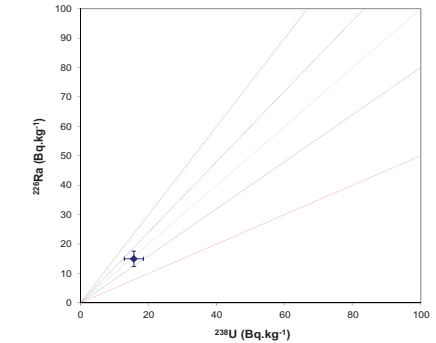
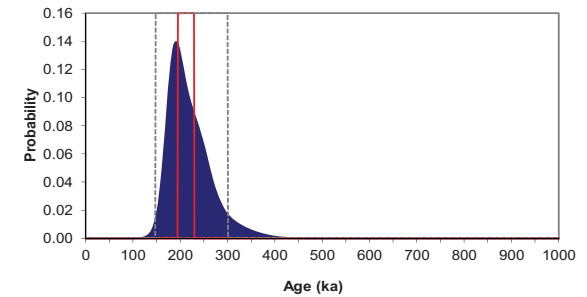


**Fig. viii Age Range**



## Appendix 23 Sample: GL10064

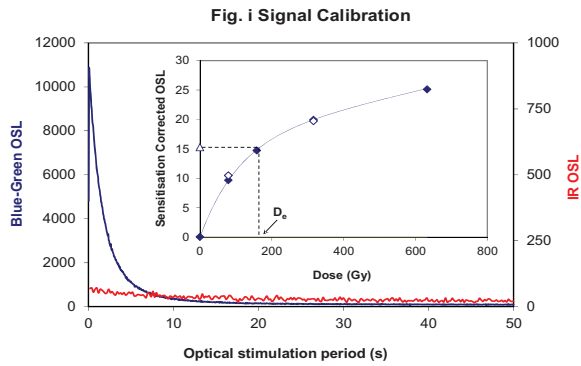


**Fig. i Signal Calibration** Natural blue and laboratory-induced infrared (IR) OSL signals. Detectable IR signal decays are diagnostic of feldspar contamination. Inset, the natural blue OSL signal (open triangle) of each aliquot is calibrated against known laboratory doses to yield equivalent dose ( $D_e$ ) values. Repeats of low and high doses (open diamonds) illustrate the success of sensitivity correction.

**Fig. ii Dose Recovery** The acquisition of  $D_e$  values is necessarily predicated upon thermal treatment of aliquots succeeding environmental and laboratory irradiation. The Dose Recovery test quantifies the combined effects of thermal transfer and sensitisation on the natural signal using a precise lab dose to simulate natural dose. Based on this an appropriate thermal treatment is selected to generate the final  $D_e$  value.

**Fig. iii Inter-aliquot  $D_e$  distribution** Provides a measure of inter-aliquot statistical concordance in  $D_e$  values derived from natural irradiation. Discordant data (those points lying beyond  $\pm 2$  standardised  $\ln D_e$ ) reflects heterogeneous dose absorption and/or inaccuracies in calibration.

**Fig. iv Low and High Repeat Regenerative-dose Ratio** Measures the statistical concordance of signals from repeated low and high regenerative-doses. Discordant data (those points lying beyond  $\pm 2$  standardised  $\ln D_e$ ) indicate inaccurate sensitivity correction.

**Fig. v OSL to Post-IR OSL Ratio** Measures the statistical concordance of OSL and post-IR OSL responses to the same regenerative-dose. Discordant, underestimating data (those points lying below -2 standardised  $\ln D_e$ ) highlight the presence of significant feldspar contamination.

**Fig. vi Signal Analysis** Statistically significant increase in natural  $D_e$  value with signal stimulation period is indicative of a partially-bleached signal, provided a significant increase in  $D_e$  results from simulated partial bleaching followed by insignificant adjustment in  $D_e$  for simulated zero and full bleach conditions. Ages from such samples are considered maximum estimates. In the absence of a significant rise in  $D_e$  with stimulation time, simulated partial bleaching and zero/full bleach tests are not assessed.

**Fig. vii U Activity** Statistical concordance (equilibrium) in the activities of the daughter radioisotope  $^{226}\text{Ra}$  with its parent  $^{238}\text{U}$  may signify the temporal stability of  $D_e$  emissions from these chains. Significant differences (disequilibrium;  $>50\%$ ) in activity indicate addition or removal of isotopes creating a time-dependent shift in  $D_e$  values and increased uncertainty in the accuracy of age estimates. A 20% disequilibrium marker is also shown.

**Fig. viii Age Range** The mean age range provides an estimate of sediment burial period based on mean  $D_e$  and  $D_e$  values with associated analytical uncertainties. The probability distribution indicates the inter-aliquot variability in age. The maximum influence of temporal variations in  $D_e$  forced by minima-maxima variation in moisture content and overburden thickness may prove instructive where there is uncertainty in these parameters, however the combined extremes represented should not be construed as preferred age estimates.

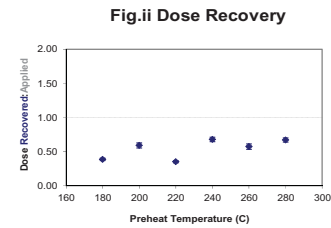


**Fig. iii Inter-aliquot  $D_e$  distribution**

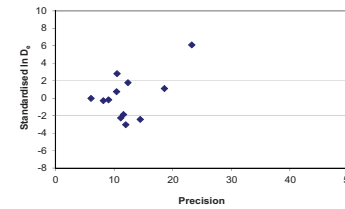


**Fig. iv Low and High Repeat Regenerative-dose Ratio**

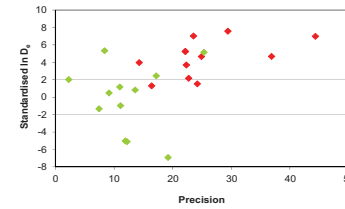


**Fig. v OSL to Post-IR OSL Ratio**

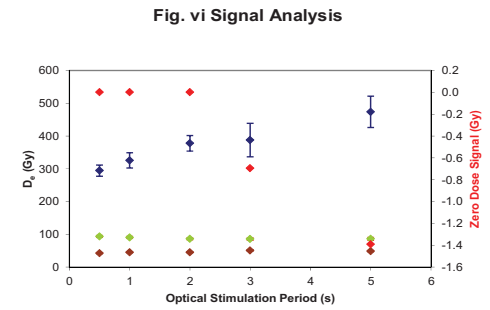
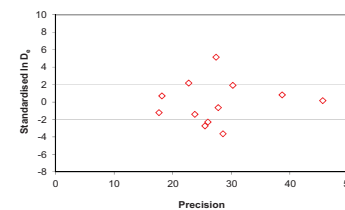


**Fig. vii U Decay Activity**

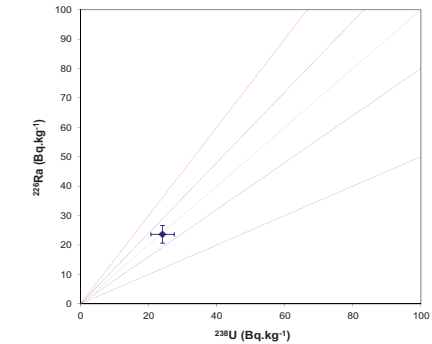
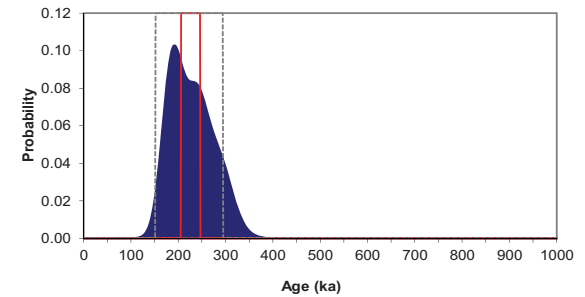


**Fig. viii Age Range**



## Appendix 24 Sample: GL10065

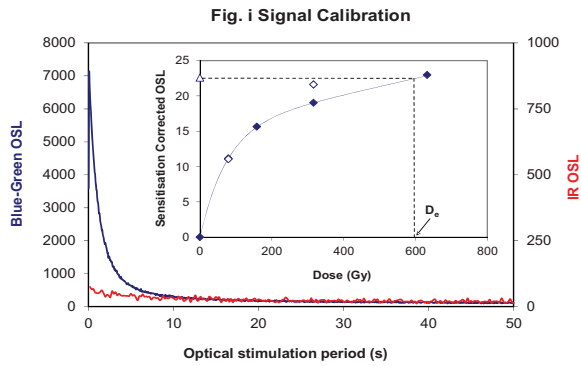


**Fig. i Signal Calibration** Natural blue and laboratory-induced infrared (IR) OSL signals. Detectable IR signal decays are diagnostic of feldspar contamination. Inset, the natural blue OSL signal (open triangle) of each aliquot is calibrated against known laboratory doses to yield equivalent dose ( $D_e$ ) values. Repeats of low and high doses (open diamonds) illustrate the success of sensitivity correction.

**Fig. ii Dose Recovery** The acquisition of  $D_e$  values is necessarily predicated upon thermal treatment of aliquots succeeding environmental and laboratory irradiation. The Dose Recovery test quantifies the combined effects of thermal transfer and sensitisation on the natural signal using a precise lab dose to simulate natural dose. Based on this an appropriate thermal treatment is selected to generate the final  $D_e$  value.

**Fig. iii Inter-aliquot  $D_e$  distribution** Provides a measure of inter-aliquot statistical concordance in  $D_e$  values derived from natural irradiation. Discordant data (those points lying beyond  $\pm 2$  standardised  $\ln D_e$ ) reflects heterogeneous dose absorption and/or inaccuracies in calibration.

**Fig. iv Low and High Repeat Regenerative-dose Ratio** Measures the statistical concordance of signals from repeated low and high regenerative-doses. Discordant data (those points lying beyond  $\pm 2$  standardised  $\ln D_e$ ) indicate inaccurate sensitivity correction.

**Fig. v OSL to Post-IR OSL Ratio** Measures the statistical concordance of OSL and post-IR OSL responses to the same regenerative-dose. Discordant, underestimating data (those points lying below -2 standardised  $\ln D_e$ ) highlight the presence of significant feldspar contamination.

**Fig. vi Signal Analysis** Statistically significant increase in natural  $D_e$  value with signal stimulation period is indicative of a partially-bleached signal, provided a significant increase in  $D_e$  results from simulated partial bleaching followed by insignificant adjustment in  $D_e$  for simulated zero and full bleach conditions. Ages from such samples are considered maximum estimates. In the absence of a significant rise in  $D_e$  with stimulation time, simulated partial bleaching and zero/full bleach tests are not assessed.

**Fig. vii U Activity** Statistical concordance (equilibrium) in the activities of the daughter radioisotope  $^{226}\text{Ra}$  with its parent  $^{238}\text{U}$  may signify the temporal stability of  $D_e$  emissions from these chains. Significant differences (disequilibrium;  $>50\%$ ) in activity indicate addition or removal of isotopes creating a time-dependent shift in  $D_e$  values and increased uncertainty in the accuracy of age estimates. A 20% disequilibrium marker is also shown.

**Fig. viii Age Range** The mean age range provides an estimate of sediment burial period based on mean  $D_e$  and  $D_e$  values with associated analytical uncertainties. The probability distribution indicates the inter-aliquot variability in age. The maximum influence of temporal variations in  $D_e$  forced by minima-maxima variation in moisture content and overburden thickness may prove instructive where there is uncertainty in these parameters, however the combined extremes represented should not be construed as preferred age estimates.

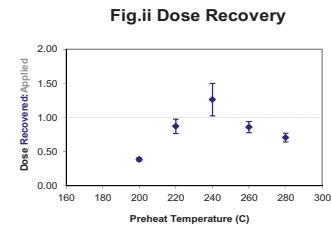


**Fig. ii Dose Recovery**

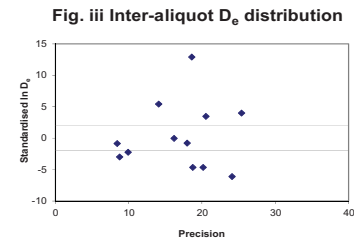


**Fig. iii Inter-aliquot  $D_e$  distribution**

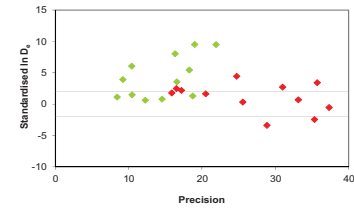


**Fig. iv Low and High Repeat Regenerative-dose Ratio**

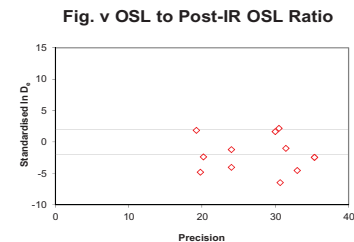


**Fig. v OSL to Post-IR OSL Ratio**

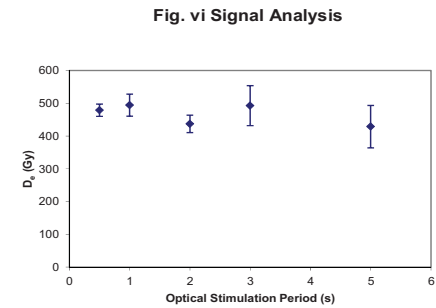


**Fig. vi Signal Analysis**

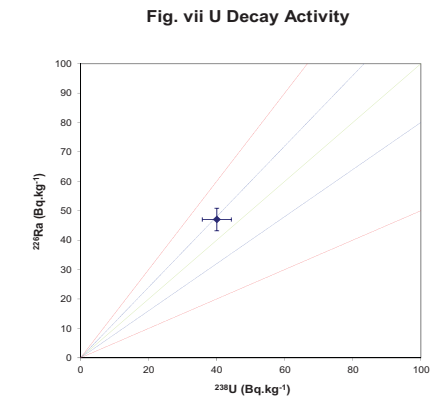


**Fig. vii U Decay Activity**

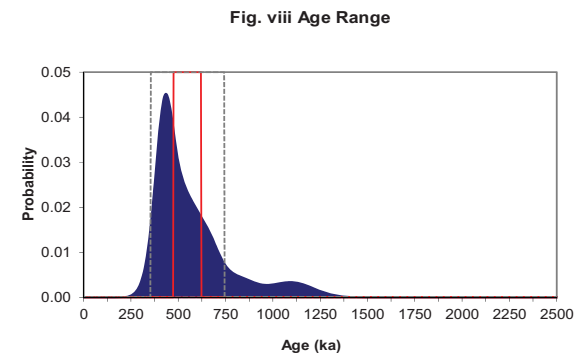


**Fig. viii Age Range**

**Appendix 25  
Sample: GL10066**



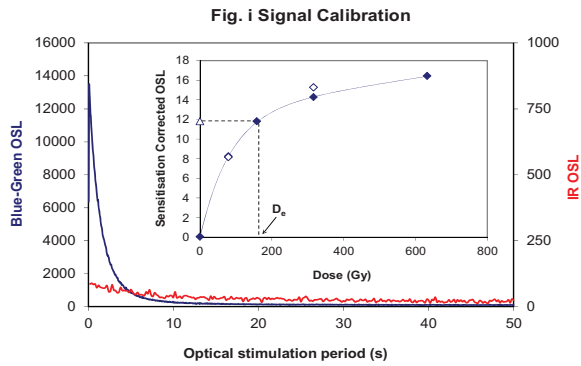


**Fig. i Signal Calibration** Natural blue and laboratory-induced infrared (IR) OSL signals. Detectable IR signal decays are diagnostic of feldspar contamination. Inset, the natural blue OSL signal (open triangle) of each aliquot is calibrated against known laboratory doses to yield equivalent dose ( $D_e$ ) values. Repeats of low and high doses (open diamonds) illustrate the success of sensitivity correction.

**Fig. ii Dose Recovery** The acquisition of  $D_e$  values is necessarily predicated upon thermal treatment of aliquots succeeding environmental and laboratory irradiation. The Dose Recovery test quantifies the combined effects of thermal transfer and sensitisation on the natural signal using a precise lab dose to simulate natural dose. Based on this an appropriate thermal treatment is selected to generate the final  $D_e$  value.

**Fig. iii Inter-aliquot  $D_e$  distribution** Provides a measure of inter-aliquot statistical concordance in  $D_e$  values derived from natural irradiation. Discordant data (those points lying beyond  $\pm 2$  standardised  $\ln D_e$ ) reflects heterogeneous dose absorption and/or inaccuracies in calibration.

**Fig. iv Low and High Repeat Regenerative-dose Ratio** Measures the statistical concordance of signals from repeated low and high regenerative-doses. Discordant data (those points lying beyond  $\pm 2$  standardised  $\ln D_e$ ) indicate inaccurate sensitivity correction.

**Fig. v OSL to Post-IR OSL Ratio** Measures the statistical concordance of OSL and post-IR OSL responses to the same regenerative-dose. Discordant, underestimating data (those points lying below -2 standardised  $\ln D_e$ ) highlight the presence of significant feldspar contamination.

**Fig. vi Signal Analysis** Statistically significant increase in natural  $D_e$  value with signal stimulation period is indicative of a partially-bleached signal, provided a significant increase in  $D_e$  results from simulated partial bleaching followed by insignificant adjustment in  $D_e$  for simulated zero and full bleach conditions. Ages from such samples are considered maximum estimates. In the absence of a significant rise in  $D_e$  with stimulation time, simulated partial bleaching and zero/full bleach tests are not assessed.

**Fig. vii U Activity** Statistical concordance (equilibrium) in the activities of the daughter radioisotope  $^{226}\text{Ra}$  with its parent  $^{238}\text{U}$  may signify the temporal stability of  $D_e$  emissions from these chains. Significant differences (disequilibrium;  $>50\%$ ) in activity indicate addition or removal of isotopes creating a time-dependent shift in  $D_e$  values and increased uncertainty in the accuracy of age estimates. A 20% disequilibrium marker is also shown.

**Fig. viii Age Range** The mean age range provides an estimate of sediment burial period based on mean  $D_e$  and  $D_e$  values with associated analytical uncertainties. The probability distribution indicates the inter-aliquot variability in age. The maximum influence of temporal variations in  $D_e$  forced by minima-maxima variation in moisture content and overburden thickness may prove instructive where there is uncertainty in these parameters, however the combined extremes represented should not be construed as preferred age estimates.

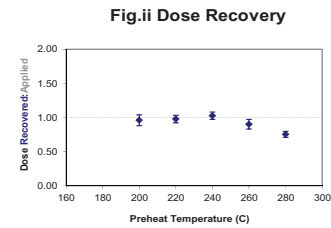


**Fig. ii Dose Recovery**

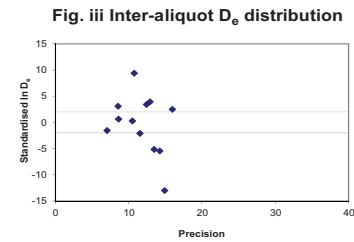


**Fig. iii Inter-aliquot  $D_e$  distribution**

**Fig. iv Low and High Repeat Regenerative-dose Ratio**

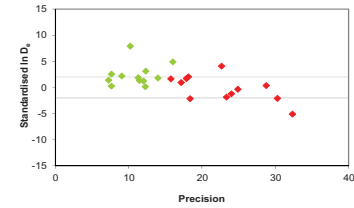


**Fig. v OSL to Post-IR OSL Ratio**

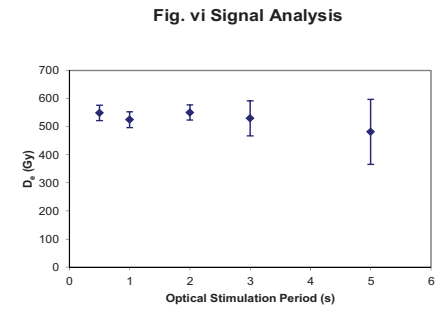
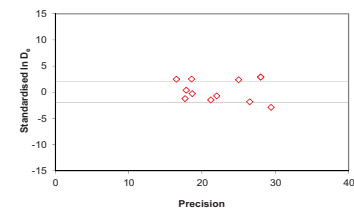


**Fig. vi Signal Analysis**

**Fig. vii U Decay Activity**

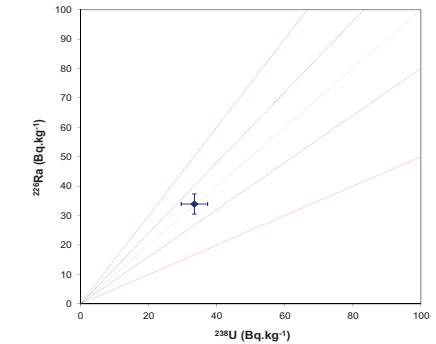
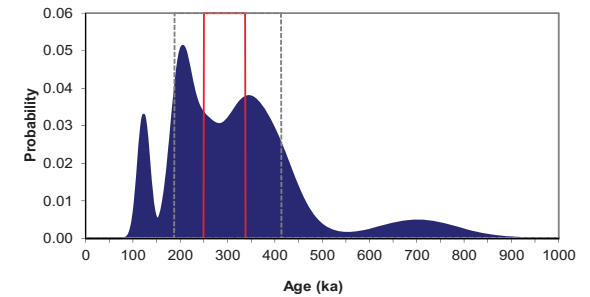


**Fig. viii Age Range**



## Appendix 26 Sample: GL10067

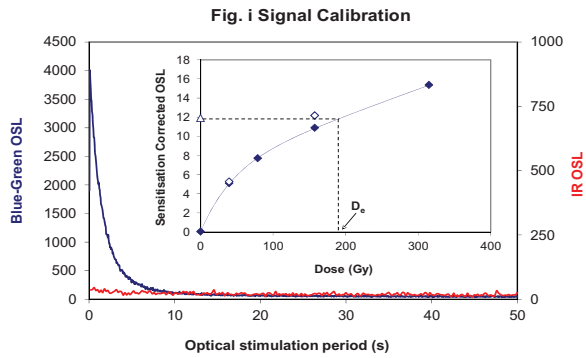


**Fig. i Signal Calibration** Natural blue and laboratory-induced infrared (IR) OSL signals. Detectable IR signal decays are diagnostic of feldspar contamination. Inset, the natural blue OSL signal (open triangle) of each aliquot is calibrated against known laboratory doses to yield equivalent dose ( $D_e$ ) values. Repeats of low and high doses (open diamonds) illustrate the success of sensitivity correction.

**Fig. ii Dose Recovery** The acquisition of  $D_e$  values is necessarily predicated upon thermal treatment of aliquots succeeding environmental and laboratory irradiation. The Dose Recovery test quantifies the combined effects of thermal transfer and sensitisation on the natural signal using a precise lab dose to simulate natural dose. Based on this an appropriate thermal treatment is selected to generate the final  $D_e$  value.

**Fig. iii Inter-aliquot  $D_e$  distribution** Provides a measure of inter-aliquot statistical concordance in  $D_e$  values derived from natural irradiation. Discordant data (those points lying beyond  $\pm 2$  standardised  $\ln D_e$ ) reflects heterogeneous dose absorption and/or inaccuracies in calibration.

**Fig. iv Low and High Repeat Regenerative-dose Ratio** Measures the statistical concordance of signals from repeated low and high regenerative-doses. Discordant data (those points lying beyond  $\pm 2$  standardised  $\ln D_e$ ) indicate inaccurate sensitivity correction.

**Fig. v OSL to Post-IR OSL Ratio** Measures the statistical concordance of OSL and post-IR OSL responses to the same regenerative-dose. Discordant, underestimating data (those points lying below -2 standardised  $\ln D_e$ ) highlight the presence of significant feldspar contamination.

**Fig. vi Signal Analysis** Statistically significant increase in natural  $D_e$  value with signal stimulation period is indicative of a partially-bleached signal, provided a significant increase in  $D_e$  results from simulated partial bleaching followed by insignificant adjustment in  $D_e$  for simulated zero and full bleach conditions. Ages from such samples are considered maximum estimates. In the absence of a significant rise in  $D_e$  with stimulation time, simulated partial bleaching and zero/full bleach tests are not assessed.

**Fig. vii U Activity** Statistical concordance (equilibrium) in the activities of the daughter radioisotope  $^{226}\text{Ra}$  with its parent  $^{238}\text{U}$  may signify the temporal stability of  $D_e$  emissions from these chains. Significant differences (disequilibrium;  $>50\%$ ) in activity indicate addition or removal of isotopes creating a time-dependent shift in  $D_e$  values and increased uncertainty in the accuracy of age estimates. A 20% disequilibrium marker is also shown.

**Fig. viii Age Range** The mean age range provides an estimate of sediment burial period based on mean  $D_e$  and  $D_e$  values with associated analytical uncertainties. The probability distribution indicates the inter-aliquot variability in age. The maximum influence of temporal variations in  $D_e$  forced by minima-maxima variation in moisture content and overburden thickness may prove instructive where there is uncertainty in these parameters, however the combined extremes represented should not be construed as preferred age estimates.

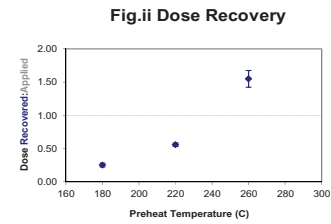


**Fig. iii Inter-aliquot  $D_e$  distribution**

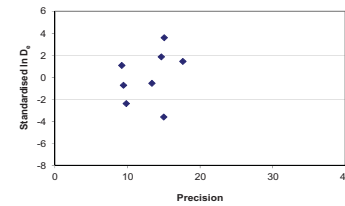


**Fig. iv Low and High Repeat Regenerative-dose Ratio**

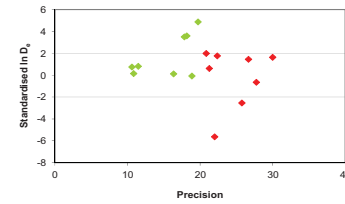


**Fig. v OSL to Post-IR OSL Ratio**

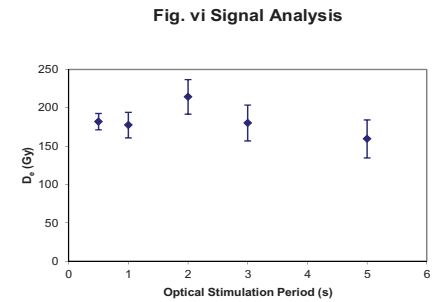
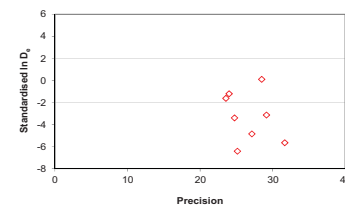


**Fig. vii U Decay Activity**

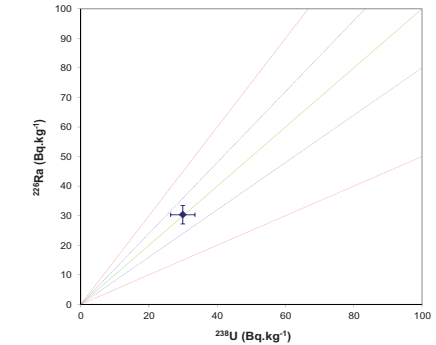
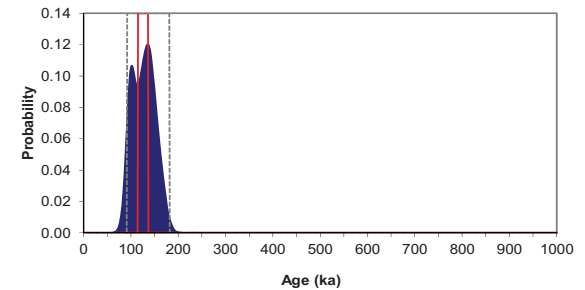


**Fig. viii Age Range**



## Appendix 27 Sample: GL10084



## ENGLISH HERITAGE RESEARCH AND THE HISTORIC ENVIRONMENT

English Heritage undertakes and commissions research into the historic environment, and the issues that affect its condition and survival, in order to provide the understanding necessary for informed policy and decision making, for the protection and sustainable management of the resource, and to promote the widest access, appreciation and enjoyment of our heritage. Much of this work is conceived and implemented in the context of the National Heritage Protection Plan. For more information on the NHPP please go to <http://www.english-heritage.org.uk/professional/protection/national-heritage-protection-plan/>.

The Heritage Protection Department provides English Heritage with this capacity in the fields of building history, archaeology, archaeological science, imaging and visualisation, landscape history, and remote sensing. It brings together four teams with complementary investigative, analytical and technical skills to provide integrated applied research expertise across the range of the historic environment. These are:

- \* Intervention and Analysis (including Archaeology Projects, Archives, Environmental Studies, Archaeological Conservation and Technology, and Scientific Dating)
- \* Assessment (including Archaeological and Architectural Investigation, the Blue Plaques Team and the Survey of London)
- \* Imaging and Visualisation (including Technical Survey, Graphics and Photography)
- \* Remote Sensing (including Mapping, Photogrammetry and Geophysics)

The Heritage Protection Department undertakes a wide range of investigative and analytical projects, and provides quality assurance and management support for externally-commissioned research. We aim for innovative work of the highest quality which will set agendas and standards for the historic environment sector. In support of this, and to build capacity and promote best practice in the sector, we also publish guidance and provide advice and training. We support community engagement and build this in to our projects and programmes wherever possible.

We make the results of our work available through the Research Report Series, and through journal publications and monographs. Our newsletter *Research News*, which appears twice a year, aims to keep our partners within and outside English Heritage up-to-date with our projects and activities.

A full list of Research Reports, with abstracts and information on how to obtain copies, may be found on [www.english-heritage.org.uk/researchreports](http://www.english-heritage.org.uk/researchreports)

*For further information visit [www.english-heritage.org.uk](http://www.english-heritage.org.uk)*

